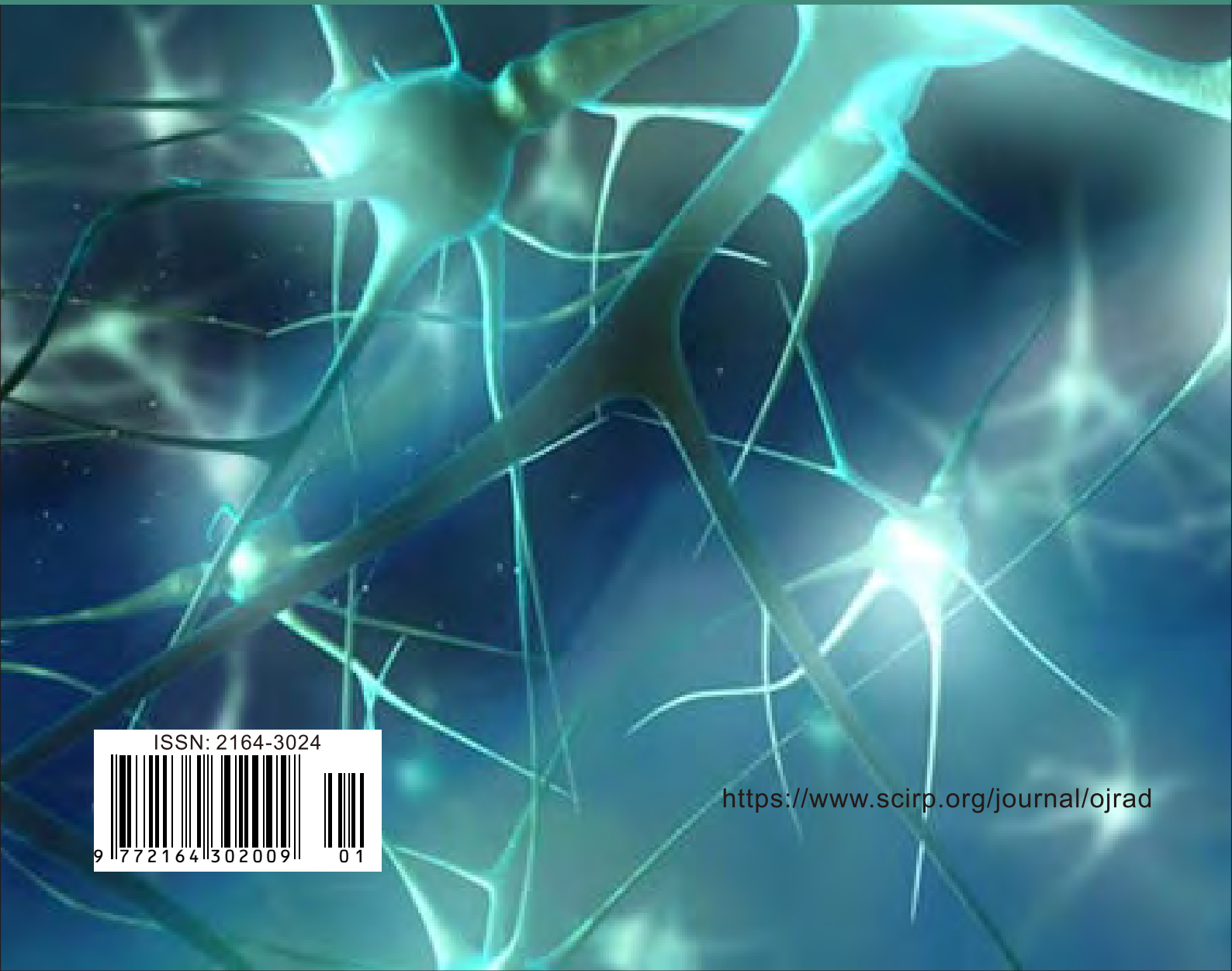


ISSN: 2164-3024 Volume 13, Number 1, March 2023



Open Journal of Radiology



ISSN: 2164-3024



9 772164 302009 01

<https://www.scirp.org/journal/ojrad>

Journal Editorial Board

ISSN Print: 2164-3024 ISSN Online: 2164-3032

<https://www.scirp.org/journal/ojrad>

Editor-in-Chief

Prof. Joseph Sekiguchi Yu The Ohio State University, USA

Editorial Board

Dr. Prachi Pragya Agarwal University of Michigan, USA
Prof. Kyung J. Cho University of Michigan Health System, USA
Dr. James Chow University of Toronto, Canada
Prof. Timothy Q. Duong UT Health Science Center San Antonio, USA
Dr. Natia Esiashvili Emory University, USA
Dr. Merja Laitinen University of Helsinki, Finland
Prof. Jing-Huei Lee University of Cincinnati, USA
Prof. Sang Kun Lee Seoul National University College of Medicine, South Korea
Dr. Jianfei Liu Duke University Medical Center, USA
Prof. Mustafa Zuhair Mahmoud Prince Sattam bin Abdulaziz University, Saudi Arabia
Dr. Christina Malamateniou King's College London, UK
Dr. Robert J. Min Weill Cornell Medical College, USA
Dr. Saeed Mirsadraee University of Edinburgh, UK
Prof. Mark D. Morasch Northwestern University, USA
Dr. Dongfeng Pan University of Virginia, USA
Dr. Hyunjin Park Sungkyunkwan University, South Korea
Prof. Suliman G. Salih Taibah University, Saudi Arabia
Dr. Paul Eduard Sijens University Medical Center Groningen, The Netherlands
Dr. Hyo-Chun Yoon University of Utah School of Medicine, USA
Prof. Ramzi Tamer Younis University of Miami, USA

Table of Contents

Volume 13 Number 1

March 2023

Role of Lung Ultrasound in the Assessment of Hydration Status of Chronic Haemodialysis Patients

S. F. Dongmo, J.-R. T. Moulion, D. G. Teuwafeu, S. G. Chuanguieu, F. J. F. Kaze, B. Moifo.....1

Contribution of Cardiac MRI in the Diagnosis of Acute Myocarditis

A. S. Keita, M. Camara, M. Diallo, A. Dembele, M. Cisse.....17

Evaluation of Entrance Skin Dose from Paediatric Diagnostic X-Ray Examination

M. O. Adelayi, O. S. Ajayi.....26

Radiation Doses in Diagnostic Radiology and Method for Dose Reduction

T. M. Taha, H. A. Ahmed, F. A. Shaheen.....34

A Validated Model for the Imaging Diagnosis of Cystic Lung Disease

W. T. Miller, K. C. Patterson, S. Sood, J. E. Schmitt, A. A. Wani, R. Borden, M. Galperin-Aisenberg,
M. K. Porteus, M. L. Hershman, M. Hewitt, J. Levy, V. D. Babatunde, T. Glushko, T. J. Niesen,
S. Leshchinskiy, K. Sahakyan, K. Desai, J. A. Gillman, S. Reddy, M. Shriver, N. B. Linna, A. M. Noor,
A. Buz, M. E. Biron, S. Simpson.....42

Compliance of Magnetic Resonance Imaging Examination Requests at the Diagnostic Center of the National Social Security Fund of Conakry

O. A. Bah, A. Sakho, A. A. Balde, A. I. Barry, K. M. Douty, A. Toure.....58

Burden of Congenital Defects Diagnosed through Ultrasonography in Soba Fetomaternal Unit, Khartoum, Sudan

M. A. M. A. Osman, I. A. A. Elhassan, F. N. Khan, A. Alimam, M. Noma, A. Fazari.....67

Place of Selective Tubal Catheterization in the Management of Female Infertility in Togo

K. E. V. Adjénou, H. Sabi Couscous, N. Saha, K. Kafupi, E. Wallace, S. Lantam, A. Abdoulatif, A. Kokou,
L. K. Agoda-Koussema.....77

Open Journal of Radiology (OJRad)

Journal Information

SUBSCRIPTIONS

The *Open Journal of Radiology* (Online at Scientific Research Publishing, <https://www.scirp.org/>) is published quarterly by Scientific Research Publishing, Inc., USA.

Subscription rates:

Print: \$79 per issue.

To subscribe, please contact Journals Subscriptions Department, E-mail: sub@scirp.org

SERVICES

Advertisements

Advertisement Sales Department, E-mail: service@scirp.org

Reprints (minimum quantity 100 copies)

Reprints Co-ordinator, Scientific Research Publishing, Inc., USA.

E-mail: sub@scirp.org

COPYRIGHT

Copyright and reuse rights for the front matter of the journal:

Copyright © 2023 by Scientific Research Publishing Inc.

This work is licensed under the Creative Commons Attribution International License (CC BY).

<http://creativecommons.org/licenses/by/4.0/>

Copyright for individual papers of the journal:

Copyright © 2023 by author(s) and Scientific Research Publishing Inc.

Reuse rights for individual papers:

Note: At SCIRP authors can choose between CC BY and CC BY-NC. Please consult each paper for its reuse rights.

Disclaimer of liability

Statements and opinions expressed in the articles and communications are those of the individual contributors and not the statements and opinion of Scientific Research Publishing, Inc. We assume no responsibility or liability for any damage or injury to persons or property arising out of the use of any materials, instructions, methods or ideas contained herein. We expressly disclaim any implied warranties of merchantability or fitness for a particular purpose. If expert assistance is required, the services of a competent professional person should be sought.

PRODUCTION INFORMATION

For manuscripts that have been accepted for publication, please contact:

E-mail: ojrad@scirp.org

Role of Lung Ultrasound in the Assessment of Hydration Status of Chronic Haemodialysis Patients

Sylviane Fomekong Dongmo^{1*}, Jean-Roger Tapouh Moulion², Denis Georges Teuwafeu¹, Samory Guedje Chuangueu³, François Jérôme Folefack Kaze³, Boniface Moifo⁴

¹Department of Internal Medicine and Paediatrics, Faculty of Health Sciences, University of Buea, Buea, Cameroon

²Department of Radiology, Faculty of Medicine and Pharmaceutical Sciences, University of Dschang, Dschang, Cameroon

³Department of Internal Medicine and Specialties, Faculty of Medicine and Biomedical Sciences, University of Yaoundé 1, Yaoundé, Cameroon

⁴Department of Radiology and Medical Imaging, Faculty of Medicine and Biomedical Sciences, University of Yaoundé 1, Yaoundé, Cameroon

Email: *dongfosyl@yahoo.fr

How to cite this paper: Dongmo, S.F., Moulion, J.-R.T., Teuwafeu, D.G., Chuangueu, S.G., Kaze, F.J.F. and Moifo, B. (2023) Role of Lung Ultrasound in the Assessment of Hydration Status of Chronic Haemodialysis Patients. *Open Journal of Radiology*, 13, 1-16.

<https://doi.org/10.4236/ojrad.2023.131001>

Received: December 18, 2022

Accepted: February 7, 2023

Published: February 10, 2023

Copyright © 2023 by author(s) and Scientific Research Publishing Inc. This work is licensed under the Creative Commons Attribution International License (CC BY 4.0).

<http://creativecommons.org/licenses/by/4.0/>



Open Access

Abstract

Background: Fluid overload is frequent in Haemodialysis (HD) and is one of the major factors of cardiovascular morbidity and mortality for chronic HD patients. The main challenge with chronic haemodialysis patients is indeed the maintenance of a normal extracellular volume through dry weight determination. Our study aimed at assessing the role of lung ultrasound in the detection of B-lines for the determination of hydration status in chronic HD patients. **Methods:** We conducted a cross-sectional study including 31 patients undergoing chronic HD treatment for at least 3 months, in the Yaounde University Teaching Hospital dialysis unit. Lung ultrasonography and clinical examinations were performed immediately before dialysis, and 30 minutes after dialysis. Differences between clinical and ultrasound variables before and after dialysis were measured to assess the effects of dialysis. Association between categorical variables was assessed with the Chi-squared test or Fischer test, and Rho's Spearman coefficient for quantitative variables. **Results:** There was a reduction in the median of B-lines score after dialysis [12 (7 - 26) versus 8 (5 - 13)], clinical score [2 (1 - 3) versus 0 (-1 - 2)], mean of systolic blood pressure (164.74 ± 26.50 versus 158.48 ± 27.89), frequency of dyspnoea in patients (32.3% versus 6.5%); and raising of the frequency of cramps in patients (0% versus 19.4%) and all statistically significant ($p \leq 0.031$). B-lines score before and after dialysis was associated with dyspnoea and raised jugular venous pressure ($p < 0.05$). B-lines score before dialysis was correlated with B-lines score after dialysis ($r = 0.805$; $p < 0.001$), B-lines reduction ($r = 0.862$; $p <$

0.001), and clinical score ($r = 0.49$; $p = 0.005$). Reduction of B-lines score was not correlated with weight loss. **Conclusion:** Lung ultrasound for the detection of B-lines reflects the variation of extracellular volume during dialysis and can even capture pulmonary oedema at a pre-clinical stage. It is then a reliable and sensible method for assessing extravascular lung water and thus hydration status of haemodialysis patients. It could constitute a better alternative for an objective and accurate definition of dry weight, specifically in the African and Cameroonian context, with its assets being low cost, availability, and easiness to perform in a large population of HD patients. We, therefore, recommend further multicentric studies in order to design a standardized protocol of ultrasound follow-up for all chronic HD patients' hydration status assessments.

Keywords

Haemodialysis, Lung Ultrasound, B-Lines, Hydration Status, Clinical Score

1. Background

Haemodialysis (HD) is the most common technique of Renal Replacement Therapy (RRT) used in the treatment of End-Stage Renal Disease (ESRD) over the world, representing 75% of the methods for the treatment of patients in Europe and in Central Asia [1] and 95% of patients in North-Africa [2]. It is the only RRT available in Cameroon where the mortality rate is high with a mean survival time of 8 months after initiation [3]. The main comorbidities of chronic HD patients in Cameroon are: high blood pressure, diabetes, and other cardiovascular diseases [1] [4].

Chronic fluid overload is frequent in HD and is a major factor for the high cardiovascular morbidity and mortality observed in chronic HD patients [5] [6]. It is directly associated with high blood pressure, arterial wall rigidity, left ventricular hypertrophy, and heart failure [7] [8]. One of the main challenges faced in HD is the maintenance of a normal extracellular volume through the determination of patients' dry weight [9].

The precise assessment of hydration status is very important for the optimal treatment of HD patients, as it enables a reliable determination of patients' dry weight. There are many methods used in assessing patients' hydration status: clinical examination, ultrasound measurement of inferior vena cava diameter and its collapsibility index, biomarkers (Atrial natriuretic peptide, Brain and Pro-brain natriuretic peptide), and bioimpedance methods [10].

Clinical methods are subjective and less efficient for the precise assessment of chronic HD patients' hydration status [5], and require time and precise skills from the clinician to reach the dry weight upon many consecutive dialysis sessions [11].

The clinical examination aims at detecting signs of fluid overload and those of

dehydration and vascular instability [6]. According to many scholars [6] [7] [12] [13] [14] [15] [16], this classical clinical and empirical approach is less reliable, does not always help detect patients' hydration status, and could even be contradictory. The continuous removal of water during dialysis up to symptomatic hypotension [7] could help to obtain the dry weight upon several consecutive dialysis sessions. However, there is a risk of overestimation of patients' dry weight, which could cause chronic fluid overload, or underestimation of dry weight leading to immediate intra- or post-dialysis complications [17].

In many studies, multifrequency bioimpedance (BIS) has been described as a reliable dry weight determination method in chronic HD patients [15] [18] giving room to a precise assessment of patients' hydration status [15] [19].

In low-income countries, like Cameroon, the clinical approach remains the only method used in determining HD patients' hydration status given the lack of technologies such as bioimpedance. Moreover, the use of clinical methods is compromised; on one hand, the reduction of dialysis sessions from 3 to 2 sessions per week and patients' poor observance of medical instructions. On the other hand, the irregularity of dialysis sessions because of short-term challenges observed in dialysis centres, and financial difficulties faced by patients prevents continuous weight loss monitoring. Such clinical estimate is achieved by means of trial and is therefore prone to imprecision.

These difficulties observed in the prevention of chronic fluid overload highlight the need to acquire a tool that could be used for a precise, rapid, and objective assessment of hydration status and a rapid determination of HD patients' dry weight in Cameroon.

Lung ultrasound through the detection of B-lines has been described as an assessment method of HD patients' hydration status and is much more used in determining lung extravascular fluid volume [9] [10] [20]. Lung ultrasound can evaluate extravascular lung water by identifying B-lines, which are vertical artifacts arising from the pleural line, extending to the edge of the screen, and which move synchronously with respiratory. Such artifacts, in reference to Kerley B lines on chest X-ray, are described in lung ultrasound as comet-tail artifacts formed as the ultrasound beam meets thickened interlobular septa filled with water in case of interstitial lung oedema [21] [22]. This method is easy, fast, cheap, and non-invasive, requiring just an ultrasound machine with a linear, convex, or sectoral transducer [21].

This study aims at assessing the benefits of lung ultrasound in common clinical practices to determine chronic HD patients' hydration status.

2. Methods

This was a cross-sectional 07 months study (November 2016-May 2017) including 31 HD patients, aged 18 and above who have been on dialysis for more than 3 months at the Yaoundé University and Teaching Hospital (CHUY). It is one of the reference hospitals in Cameroon where patients suffering from end-stage chron-

ic kidney disease undergo 4 hours of dialysis twice weekly.

Exclusion criteria include the presence of acute diseases or diseases that require hospital admissions such as decompensated cirrhosis, end-stage cancer, and systemic infections, patients on vacation or tourists, pregnant women, and patients who refused to sign informed consent forms.

Each patient was assessed clinically and administered lung ultrasound immediately before and 30 minutes after the second dialysis session of the week.

2.1. Lung Ultrasound

Lung ultrasounds were performed by one operator, specially trained to recognize and interpret B-lines. Lung ultrasound was performed on patient in a supine position using a Doppler portable ultrasound tool with a vascular probe of 6 - 12 MHz (BK Medical Mini Focus[®]) for the detection of B-lines. Comet-tails or “B-lines” are defined as hyperechoic reflections which originate only from and travel roughly perpendicular to the pleural line of the lung. They have a narrow base and form a ray spreading away from the transducer towards the bottom of the screen (similar to a rocket at lift-up) and synchronously move with lung respiration [23] [24]. Areas explored included anterior and lateral regions of the two hemithorax, from 2nd to 4th intercostal space, and from 1st to 5th intercostal space in the right side of the chest. For each intercostal space, B-lines were detected in 4 different sites: para-sternal, midclavicular, anterior axillary and mid axillary areas, giving 28 positions per test [25] [26]. For all the explored sites, B-lines ranged from 0 to 10. Number 0 indicated the absence of B-lines whereas number 10 stood for complete blank screen. All the B-lines detected on various sites explored produced a score, the score of B-lines, indicating the severity of lung congestion [25] [26]. Patients were grouped according to these scores and to the following levels of lung congestion as previously described in other studies: No congestion ≤ 5 B-lines, mild congestion: 6 - 15, moderate congestion: 16 - 30, severe congestion: >30 [9] [22] [26] [27]. **Figure 1** shows examples of B-lines.

2.2. Clinical Examination

Clinical examination was performed before the dialysis and 30 minutes after the session. All patients were evaluated during the second dialysis session of the week. Hemodynamic and anthropometric parameters such as blood pressure, heart rate, weight and height were taken. Clinical examination substantially consisted in identifying symptoms and signs of hyperhydration or fluid overload and of dehydration or hypovolemia. Each functional or physical sign related to hyperhydration such as peripheral oedema, dyspnea, high blood pressure, jugular veins turgor, ascites [6] [24] [28] [29] [30] was given a positive figure whereas negative figures were attributed to signs indicating hypovolemia such as dizziness, asthenia, cramps, low blood pressure [6] [24] [28], resulting to a clinical score as interpreted in **Table 1**.

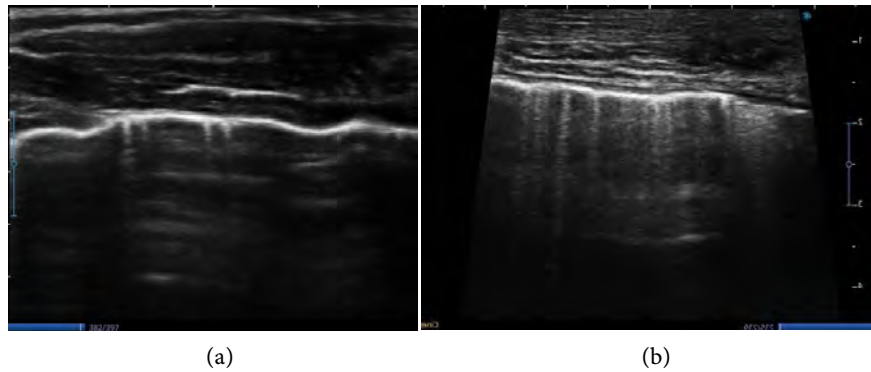


Figure 1. Lung ultrasound, 2 different patients. (a) 4 B-lines; (b) 10 B-lines.

Table 1. Description of the clinical score assessing the hydration status.

Hydration Status	Score	Description
Hypovolemia	≤ -3	Patent Hypovolemia
	-2	Latent Hypovolemia
	-1	Undefined
Normal	0	Normal
Hyperhydration	1	Undefined
	2	Latent Fluid Overload
	≥ 3	Patent Fluid Overload

This clinical score before and after dialysis were compared, to determine the impact of dialysis on clinical signs assessing the hydration status.

2.3. Data Analysis

Data were recorded and treated with Excel 2013, then exported to BM-Statistical Package for Social Sciences (IBM-SPSS) 22.0 for statistical analysis. Tables and figures were obtained using Excel 2013.

Data were presented as mean and standard deviation, median and interquartile range, or frequency and percentage, as appropriate. We used the Shapiro Wilk test to determine the normality of our quantitative variables' distribution.

For qualitative variables, we used the Chi-square test to compare groups of patients or the Fischer test when the expected number of patients was below 5, and the Mc Nemar test was used to compare variables.

For quantitative variables, the student *test-t* was used for independent samples and the Wilcoxon signed-rank test, where appropriate. Correlations between variables were assessed using Spearman's rank correlation coefficient. The relationship between the B-lines before and after dialysis was measured using the intra-class correlation coefficient. The significance threshold was established for $p < 0.05$.

3. Results

31 patients were registered, aged between 27 to 70 years with an average age of

49 years \pm 11.4. The first cause of kidney disease was hypertensive nephropathy (32.3%) followed by chronic glomerulonephritis (25.8%) and diabetic nephropathy (19.4%). The major comorbidities of these patients were high blood pressure (83.9%), diabetes (29%), heart failure (16%) and left ventricular hypertrophy (16%).

3.1. Variations in Clinical and Ultrasonographic Signs after Dialysis

After dialysis, it was observed that the number of dyspnoeic patients significantly reduced but more patients complained of cramps (Table 2). Up to 42.5% of patients proved to have fluid overload before dialysis; whereas 16.1% showed a normal clinical hydration status (Table 3).

Levels of systolic blood pressure and weight decreased considerably after dialysis. Blood pressure decreased from 164.74 (\pm 26.50) to 158.48 (\pm 27.89) mmHg and weight loss from 74.76 (\pm 11.4) to 71.38 (\pm 11.34) kg. It was also observed that their clinical score significantly dropped after dialysis ($p < 0.001$).

B-lines number median reduced considerably after dialysis ($p < 0.001$), as described in Table 4.

Table 2. Changes in clinical signs after dialysis.

Variables	Number N (%)			P-value
	Clinical Signs	Before Dialysis	After Dialysis	
Signs of Congestion	Peripheral Edema	6 (19.4)	3 (9.7)	0.25
	Dyspnea	10 (32.3)	2 (6.5)	0.008
	AP \geq 140/90 mmHg	27 (87.1)	22 (71)	0.125
	Jugular Veins Turgor	16 (51.6)	12 (38.7)	0.125
	Ascites	3 (9.7)	2 (6.5)	1
Signs of Hypovolemia	Low Blood Pressure	0.	1 (3.2)	1
	Dizziness	1 (3.2)	6 (19.4)	0.063
	Cramps	0.	6 (19.4)	0.031
	Asthenia	0.	2 (6.5)	0.5

Values are given in frequency and percentage in brackets; significant p values are in bold.

Table 3. Hydration status according to clinical score.

Clinical Score	Clinical Hydration Status	Before Dialysis N (%)	After Dialysis N (%)
≤ -3	Patent Hypovolemia	0.	1 (3.2)
-2	Latent Hypovolemia	1 (3.2)	2 (6.5)
-1	Undefined	0.	5 (16.1)
0	Normal	0.	5 (16.1)
1	Undefined	11 (35.5)	8 (25.8)
2	Latent Fluid Overload	5 (16.1)	5 (16.1)
≥ 3	Patent Fluid Overload	14 (45.2)	5 (16.1)

Values are given in frequency and percentages in brackets.

Table 4. Changes in the number of B-lines after dialysis.

Number of B-lines	N (%) before Dialysis	N (%) after Dialysis
<6 = No Congestion	4 (12.9)	8 (25.8)
[6 - 15] = Mild Congestion	15 (48.4)	17 (54.8)
[16 - 30] = Moderate Congestion	8 (25.8)	6 (19.4)
>30 = Severe Congestion	4 (12.9)	0

Values are given in frequency and percentage in brackets; lung congestion < 6 B-lines = no congestion, [6 - 15] = mild congestion, [16 - 30] = moderate congestion, >30 = severe congestion.

3.2. Factors Associated with the Number of B-Lines

The clinical factors associated with the presence of B-lines before dialysis were dyspnoea and jugular veins turgor. This association decreased after dialysis. Indeed the number of dyspnoeic patients increased with the severity of lung congestion assessed by the number of B-lines (**Figure 2**). It was the same observation with the jugular vein's turgor (**Figure 3**). This number was very low after dialysis.

3.3. Correlation between Measured Parameters and the Number of B-Lines

We assessed the number of B lines before and after dialysis, the decrease in the number of B lines after dialysis and the various measured clinical parameters.

Clinical parameters associated with the number of B-lines before dialysis:

There was a big correlation between the number of B lines before and after dialysis ($r = 0.805$, $p < 0.001$), measured by the interclass correlation coefficient. The number of B-lines was also associated with the clinical score before dialysis ($r = 0.549$; $p = 0.001$).

Clinical and ultrasonographic parameters associated with the decrease in the number of B lines:

Table 5 shows that the decrease in the number of B-lines after dialysis was strongly associated with the number of B lines before dialysis ($r = 0.862$; $p < 0.001$).

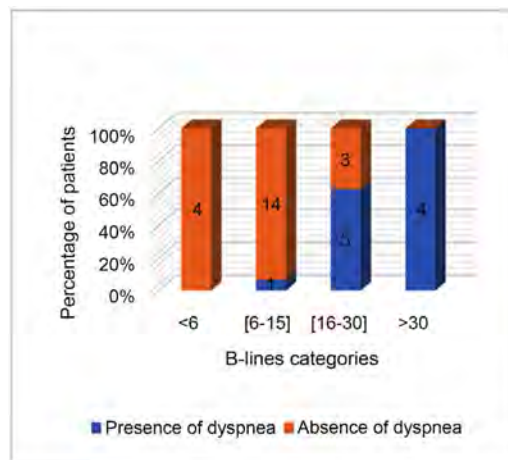
Clinical and sonographical parameters associated with the number of B-lines before dialysis:

Findings in **Table 6** show that the number of B-lines after dialysis was strongly correlated with that of the presence of B-lines before dialysis ($r = 0.935$; $p < 0.001$) and with the reduction of B-lines after dialysis ($r = 0.672$; $p < 0.001$).

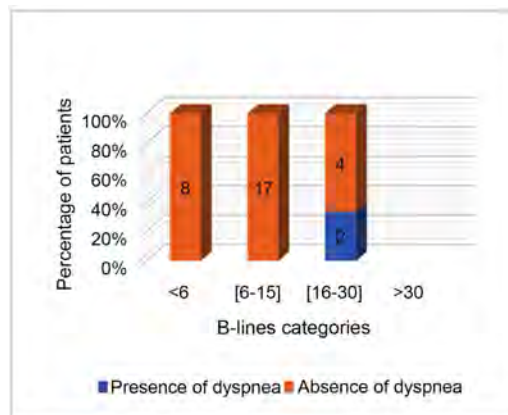
4. Discussion

There is a correlation between hyperhydration and the high mortality rate of HD patients following quantitative assessment of hydration status [6]. The main aim of RRT in HD patients with ESRD is the adequate control of extravascular fluid level. Hyperhydration has a significant impact on high blood pressure, the de-

velopment of arteriosclerosis and on the high prevalence of left ventricular hypertrophy observed in chronic HD patients [8] [16]. Despite the various methods used to assess the HD patients' hydration status, dry weight assessment remains a big challenge, notably for developing countries where there is lack of appropriate technical facilities. This study aimed at determining the contribution of lung ultrasound techniques in the assessment of the chronic HD patients' hydration status.



(a)



(b)

Figure 2. Repartition of dyspnea according to B-lines. (a) = in pre-dialysis, (b) = in post-dialysis; lung congestion: absent < 6, mild = [6 - 15], moderate = [16 - 30], severe > 30.

Table 5. Correlation with the reduction of the number of B-lines.

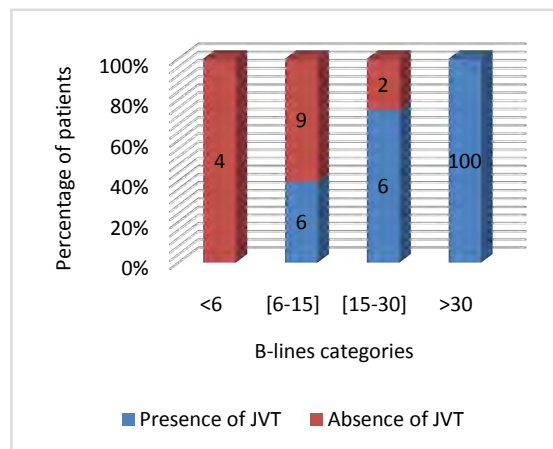
Variables	Spearman's Rank Correlation Coefficient	P-value
B1-lines	0.862	0.000
Δweight	0.061	0.746

B1-lines = number of B-lines before dialysis; Δweight = change of weight before and after dialysis; significant p-values are in bold.

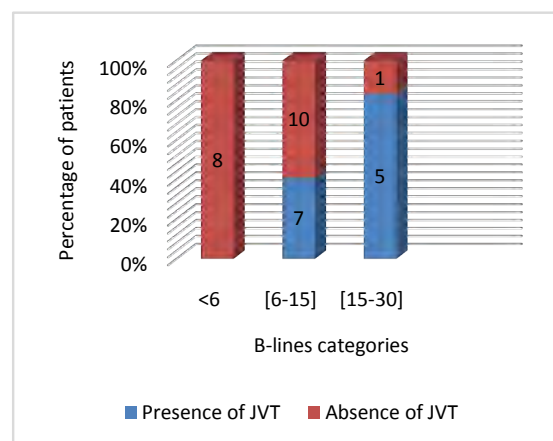
Table 6. Correlation with the number of B-lines after dialysis.

Variables	Spearman's Rank Correlation Coefficient	P-value
B1-lines	0.935	0.000
ΔB-lines	0.672	0.000
Systolic Blood Pressure	0.121	0.515
Diastolic Blood Pressure	-0.084	0.653
Pulses	0.157	0.400
SaO₂	-0.166	0.371
Clinical Score 2	0.211	0.255

B1-lines = number of B-lines before dialysis; Δ B-lines = decrease in the number of B-lines after dialysis; clinical score 2 = clinical score after dialysis; SaO₂ = oxygen saturation; significant p-values are in bold.



(a)



(b)

Figure 3. Repartition of jugular veins turgor according to B-lines. (a) = in pre-dialysis, (b) = in post-dialysis; lung congestion: absent < 6, mild = [6 - 15], moderate = [16 - 30], severe > 30.

4.1. Analysis of the Variation in Clinical and Sonographical Signs after Dialysis

In this study, we observed that there is a significant decrease in the number of B-lines after dialysis, as described in many previous studies [9] [20] [24] [31]. B-lines are associated with the accumulation of water during the interdialytic period and reflect the variation in the level of extravascular lung water which occurs during dialysis [32]. In their study, Khamis *et al.* also showed a significant decrease of number of B-lines post-dialysis, especially for the group of patient with interdialytic hypertension (from 10 to 4 B-lines) [20]. Noble *et al.* [33] and Mallamaci *et al.* [22] proved that the number of B-lines rapidly and in a reliable manner reflects the extracellular fluid variation, with an average duration of 4 minutes for the change on the screen [22]. Whereas inferior vena cava ultrasound can only be performed two hours after dialysis because of the equilibration time between interstitial and intravascular compartments [22] [34] [35]. Equally, multifrequency bioimpedance should be done 30 minutes to two hours after dialysis [36] [37].

After dialysis, we observed a significant drop in the systolic blood pressure, though it was low compared to studies carried out in Europe [9] [22] [31] [38]. This could be explained by the fact that the patients described within this study presented with a higher blood pressure probably related to the reduction of weekly dialysis sessions and the irregular intake of antihypertensive drugs. There was also a significant drop in the clinical score showing that it could reflect the variation in hydration status after dialysis.

4.2. Analysis of Factors Associated with the Presence of Sonographical B-Lines

A correlation between dyspnea and the presence of B-lines was observed before dialysis; a similar correlation was also observed by Siriopol *et al.* [9] and Mallamaci *et al.* [22]. The role of fluid overload in the development of pulmonary oedema was highlighted by the significant decrease in the number of dyspnoeic patients after dialysis [9] [22].

We also observed a correlation between the presence of B-lines in pre- and post-dialysis and jugular veins turgor ($p = 0.005$). This correlation reduced after dialysis ($p = 0.022$). Furthermore, jugular veins turgor was more sensitive than dyspnoea in predicting pulmonary oedema. Indeed, jugular veins turgor could be felt with mild lung congestion (**Figure 2**). This correlation with jugular veins turgidity was not found in the literature, thus the specificity of our study. Moreover, dyspnea and jugular veins turgor were observed only after a minimum of 6 B-lines, indicating that lung ultrasound could help detect the formation of pulmonary oedema at the preclinical stage, also shown by Mallamaci *et al.* [22] and Allinovi *et al.* [28]. Therefore, it is a sensitive indicator of the efficiency of ultrafiltration given the regression of dyspnea post-dialysis (**Figure 3**).

We did not find any significant difference in peripheral oedema at pre- and

post-dialysis. This explains the non-specificity of this clinical sign in the assessment of hyperhydration as described by Torino *et al.* [39].

We could also establish a clinical score based on patients' physical and functional signs, and this score was positively correlated with the number of B-lines before dialysis ($r = 0.49$, $p = 0.005$). These findings are similar to those presented by Allinovi *et al.* [28] who found a linear correlation between B-lines number and the clinical assessed level of fluid overload.

4.3. Analysis of the Correlation of Measured Parameters and B-Lines

Despite significant weight loss post-dialysis (-3.38 kg, $p < 0.001$), there was no correlation between the number of B-lines after dialysis and weight variation. This is similar to findings by Siriopol *et al.* [9], Khamis *et al.* [20] and Mallamaci *et al.* [22]. Whereas Vitturi *et al.* [24] obtained a relatively low number of B-lines, and they described a high correlation between the decrease in the number of B-lines and weight loss after dialysis. However, their target population was made up only of asymptomatic patients with clinically determined dry weight [24]. Therefore, the absence of a correlation between weight variation and the reduction of the number of B-lines in our study could probably be due to the fact that patients were not at their dry weight, thus the relatively high number of B-lines; and secondly from the high number of dyspnoeic patients.

Studies carried out by Mallamaci *et al.* [22] showed a high correlation between the number of B-lines, the reduction of the number of B-lines and the cardiographic parameters, particularly the ejection fraction of left ventricle. According to them, the presence of B-lines essentially depends on the fraction of systolic ejection rather than on the fluid overload. In the same light, Siriopol *et al.* [38] found that lung ultrasound could produce the same information as echocardiography; and so, could improve treatment and prognosis of chronic HD patients, since it's easier, more accessible and cheaper than echocardiography.

In the light of these analyses, lung ultrasound could be a good alternative for an objective and precise assessment of HD patients' hydration status. It could contribute to a reliable weight loss determination, as described by other researchers [24] [30] [34]. It is a non-invasive test, easy to perform by non-specialists [22] [28], and could easily be used in Africa and in Cameroon, particularly given the availability of ultrasound machines in our hospitals and in some nephrology units. Compared to BIS or inferior vena cava diameter measurement which are costly, this test simply requires standard equipment [23] [31]. Its intra- and inter-observer reproducibility is good and higher than that of inferior vena cava ultrasound measurement [22] [24] and with a good inter probe reproducibility [22], making it easy to perform this test even with a probe for kidney evaluation (3.5 MHz). Moreover, studies have shown that determination of extravascular lung water using a lung ultrasound machine was highly associated with the mortality and the occurrence of cardiovascular difficulties in chronic HD patients [9]

[27], thus indicating its role in assessing haemodialysis prognosis. This ultrasound technique has the advantage that it can be performed immediately after a dialysis session on different categories of HD patients (young children, patients with metallic implants, amputees, etc.). One of the major benefits of lung ultrasound is its superior correlation with every other hydration status assessment techniques (bioimpedance, sonographic measurement of inferior vena cava, clinical methods) [24] [28] [31].

From the analysis above, the integration of lung ultrasound in the follow up of chronic HD patients is recommended for an objective assessment of their hydration status and the precise determination of their dry weight.

5. Limitations

Our study is limited by the small sample population obtained from just one dialysis centre, because of the unavailability of ultrasound machines.

Ultrasound measurements of the inferior vena cava and multifrequency bioimpedance were not available to enable a direct comparison with our findings.

Most of the chronic HD patients from our centre had no clinically determined dry weight because of the difficulties faced by the centre during our study period.

6. Conclusions

The findings of our study show that lung ultrasound could be efficient in the rapid evaluation of fluid overload in chronic HD patients through the detection of lung oedema in the preclinical stage. It, therefore, contributes to the optimisation of ultrafiltration and the improvement in prognosis.

It could be a good alternative for the objective and precise determinations of chronic HD patients' dry weight in Africa and in Cameroon, particularly because it is easy to perform, available, cheaper, and can apply to the majority of chronic HD populations. It would be interesting to carry out a study with a larger sample population (multicentric study) in order to design a standardised protocol of ultrasound follow-up for all chronic HD patients' hydration status assessments.

Acknowledgements

We wish to thank Dr. Fokou for the portable ultrasound machine that served in performing lung ultrasounds.

Availability of Data and Materials

The data (in French) analyzed during the current study are available from the corresponding author upon reasonable request.

Authors' Contributions

All authors contributed to the study conception and study design and were responsible for ethical approval. SFD and JRTM supervised data collection. SGC,

JRTM, and SFD conducted the interviews, the clinical exams, and the lung ultrasounds. SFD performed the data analysis and data interpretation in collaboration with SGC, JRTM, DGT, and BM. SFD and JRTM participate in drafting the manuscript. DGT, FJFK, and MB made critical revisions for important intellectual content. The final version of the manuscript was read and approved by all authors.

Ethics Approval and Consent to Participate

This study was performed in accordance with Helsinki Declaration, and has been approved by the ethics committee of the Faculty of Medicine and Biomedical Sciences of the University of Yaoundé I. The ethical clearance reference number is 162/UYY/FMSB/VDRC/CSD. Written informed consent was obtained from each participant prior to the data collection.

Consent for Publication

Not applicable, since all the data was de-identified and presented on a group level to protect the providers' anonymity.

Conflicts of Interest

The authors declare no conflicts of interest regarding the publication of this paper.

References

- [1] Anand, S., Bitton, A. and Gaziano, T. (2013) The Gap between Estimated Incidence of End-Stage Renal Disease and Use of Therapy. *PLOS ONE*, **8**, e72860. <https://doi.org/10.1371/journal.pone.0072860>
- [2] Barsoum, R.S. (2013) Burden of Chronic Kidney Disease: North Africa. *Kidney International Supplements*, **3**, 164-166. <https://doi.org/10.1038/kisup.2013.5>
- [3] Fouda, H., Ashuntantang, G., Kaze, F. and Halle, M.-P. (2017) La survie en hémodialyse chronique au Cameroun. *The Pan African Medical Journal*, **26**, Article 97. <https://doi.org/10.11604/pamj.2017.26.97.9658>
- [4] Aseneh, J.B., Kemah, B.L., Mabouna, S., *et al.* (2020) Chronic Kidney Disease in Cameroon: A Scoping Review. *BMC Nephrology*, **21**, Article No. 409. <https://doi.org/10.1186/s12882-020-02072-5>
- [5] Raimann, J., Liu, L., Ulloa, D., Kotanko, P. and Levin, N.W. (2008) Consequences of Overhydration and the Need for Dry Weight Assessment. *Contributions to Nephrology*, **161**, 99-107. <https://doi.org/10.1159/000130414>
- [6] Wizemann, V., Wabel, P., Chamney, P., *et al.* (2009) The Mortality Risk of Overhydration in Haemodialysis Patients. *Nephrology Dialysis Transplantation*, **24**, 1574-1579. <https://doi.org/10.1093/ndt/gfn707>
- [7] Onofriescu, M., Hogas, S., Voroneanu, L., *et al.* (2014) Bioimpedance-Guided Fluid Management in Maintenance Hemodialysis: A Pilot Randomized Controlled Trial. *American Journal of Kidney Diseases*, **64**, 111-118. <https://doi.org/10.1053/j.ajkd.2014.01.420>
- [8] Tonelli, M., Wiebe, N., Culeton, B., *et al.* (2006) Chronic Kidney Disease and Mor-

- tality Risk: A Systematic Review. *Journal of the American Society of Nephrology*, **17**, 2034-2047. <https://doi.org/10.1681/ASN.2005101085>
- [9] Siriopol, D., Hogas, S., Voroneanu, L., *et al.* (2013) Predicting Mortality in Haemodialysis Patients: A Comparison between Lung Ultrasonography, Bioimpedance Data and Echocardiography Parameters. *Nephrology Dialysis Transplantation*, **28**, 2851-2859. <https://doi.org/10.1093/ndt/gft260>
- [10] Ekinci, C., Karabork, M., Siriopol, D., *et al.* (2018) Effects of Volume Overload and Current Techniques for the Assessment of Fluid Status in Patients with Renal Disease. *Blood Purification*, **46**, 34-47. <https://doi.org/10.1159/000487702>
- [11] Alijanian, N., Naini, A.E., Shahidi, S., Liaghat, L. and Samani, R.R. (2012) The Comparative Evaluation of Patients' Body Dry Weight under Hemodialysis Using Two Methods: Bioelectrical Impedance Analysis and Conventional Method. *Journal of Research in Medical Sciences*, **17**, 923-927.
- [12] Kouw, P.M., Kooman, J.P., Cheriex, E.C., *et al.* (1993) Assessment of Postdialysis Dry Weight: A Comparison of Techniques. *Journal of the American Society of Nephrology*, **4**, 98-104. <https://doi.org/10.1681/ASN.V4198>
- [13] Leunissen, K.M., Kouw, P., Kooman, J.P., *et al.* (1993) New Techniques to Determine Fluid Status in Hemodialyzed Patients. *Kidney International Supplements*, **41**, S50-S56.
- [14] Wabel, P., Chamney, P., Moissl, U. and Jirka, T. (2009) Importance of Whole-Body Bioimpedance Spectroscopy for the Management of Fluid Balance. *Blood Purification*, **27**, 75-80. <https://doi.org/10.1159/000167013>
- [15] Moissl, U., Arias-Guillén, M., Wabel, P., *et al.* (2013) Bioimpedance-Guided Fluid Management in Hemodialysis Patients. *Clinical Journal of the American Society of Nephrology*, **8**, 1575-1582. <https://doi.org/10.2215/CJN.12411212>
- [16] Passauer, J., Petrov, H., Schleser, A., Leicht, J. and Pucalka, K. (2010) Evaluation of Clinical Dry Weight Assessment in Haemodialysis Patients Using Bioimpedance Spectroscopy: A Cross-Sectional Study. *Nephrology Dialysis Transplantation*, **25**, 545-551. <https://doi.org/10.1093/ndt/gfp517>
- [17] Jaeger, J.Q. and Mehta, R.L. (1999) Assessment of Dry Weight in Hemodialysis an Overview. *Journal of the American Society of Nephrology*, **10**, 392-403. <https://doi.org/10.1681/ASN.V102392>
- [18] Vujčić, B., Mikolasević, I., Racki, S., *et al.* (2013) BCM—Body Composition Monitor: A New Tool for the Assessment of Volume-Dependent Hypertension in Patients on Maintenance Haemodialysis. *Collegium Antropologicum*, **37**, 815-819.
- [19] Onofriescu, M., Siriopol, D., Voroneanu, L., *et al.* (2015) Overhydration, Cardiac Function and Survival in Hemodialysis Patients. *PLOS ONE*, **10**, e0135691. <http://www.ncbi.nlm.nih.gov/pmc/articles/PMC4537261> <https://doi.org/10.1371/journal.pone.0135691>
- [20] Khamis, S.S.A., Yassein, Y.S., El Zorkany, K.M.A., Mousa, W.A., Kora, A.S.A. and Ragheb, A. (2020) Study the Role of Lung Ultrasound in Assessment of Subclinical Fluid Overload in Maintenance Hemodialysis Patients with Intra-Dialytic Hypertension. *Open Journal of Nephrology*, **10**, 199-211. <https://doi.org/10.4236/ojneph.2020.103019>
- [21] Ivanov, I., *et al.* (2020) Lung Ultrasound for Volume Status Assessment in Chronic Hemodialysis Patients. *Vojnosanitetski Pregled*, **77**, 943-949. <https://doi.org/10.2298/VSP180622167I>
- [22] Mallamaci, F., Benedetto, F.A., Tripepi, R., *et al.* (2010) Detection of Pulmonary Congestion by Chest Ultrasound in Dialysis Patients. *JACC: Cardiovascular Imag-*

- ing*, **3**, 586-594. <https://doi.org/10.1016/j.jcmg.2010.02.005>
- [23] Lichtenstein, D.A. (2003) Échographie pleuro-pulmonaire. *Réanimation*, **11**, 19-29. [https://doi.org/10.1016/S1624-0693\(02\)00005-1](https://doi.org/10.1016/S1624-0693(02)00005-1)
- [24] Vitturi, N., Dugo, M., Soattin, M., et al. (2014) Lung Ultrasound during Hemodialysis: The Role in the Assessment of Volume Status. *International Urology and Nephrology*, **46**, 169-174. <https://doi.org/10.1007/s11255-013-0500-5>
- [25] Picano, E., Frassi, F., Agricola, E., Gligorova, S., Gargani, L. and Mottola, G. (2006) Ultrasound Lung Comets: A Clinically Useful Sign of Extravascular Lung Water. *Journal of the American Society of Echocardiography*, **19**, 356-363. <https://doi.org/10.1016/j.echo.2005.05.019>
- [26] Summerfield, D.T. and Johnson, B.D. (2013) Lung Ultrasound Comet Tails—Technique and Clinical Significance. In: Squeri, A., Ed., *Hot Topics in Echocardiography*, IntechOpen, London, 51-64.
- [27] Zoccali, C., Torino, C., Tripepi, R., et al. (2013) Pulmonary Congestion Predicts Cardiac Events and Mortality in ESRD. *Journal of the American Society of Nephrology*, **24**, 639-646. <https://doi.org/10.1681/ASN.2012100990>
- [28] Allinovi, M., Saleem, M.A., Burgess, O., Armstrong, C. and Hayes, W. (2016) Finding Covert Fluid: Methods for Detecting Volume Overload in Children on Dialysis. *Pediatric Nephrology*, **31**, 2327-2335. <https://doi.org/10.1007/s00467-016-3431-4>
- [29] Srisuwan, K., Hongsawong, N., Lumpaopong, A., Thirakhupt, P. and Chulamokha, Y. (2015) Blood Volume Monitoring to Assess Dry Weight in Pediatric Chronic Hemodialysis Patients. *Journal of the Medical Association of Thailand*, **98**, 1089-1096.
- [30] Viazzi, F., Leoncini, G., Ratto, E., et al. (2017) Peripheral Artery Disease and Blood Pressure Profile Abnormalities in Hemodialysis Patients. *Journal of Nephrology*, **30**, 427-433. <https://doi.org/10.1007/s40620-016-0322-5>
- [31] Alexiadis, G., Panagoutsos, S., Roumeliotis, S., et al. (2017) Comparison of Multiple Fluid Status Assessment Methods in Patients on Chronic Hemodialysis. *International Urology and Nephrology*, **49**, 525-532. <https://doi.org/10.1007/s11255-016-1473-y>
- [32] Allinovi, M., Saleem, M., Romagnani, P., Nazerian, P. and Hayes, W. (2017) Lung Ultrasound: A Novel Technique for Detecting Fluid Overload in Children on Dialysis. *Nephrology Dialysis Transplantation*, **32**, 541-547. <https://doi.org/10.1093/ndt/gfw037>
- [33] Noble, V.E., Murray, A.F., Capp, R., et al. (2009) Ultrasound Assessment for Extravascular Lung Water in Patients Undergoing Hemodialysis. Time Course for Resolution. *Chest*, **135**, 1433-1439. <https://doi.org/10.1378/chest.08-1811>
- [34] Feissel, M., Michard, F., Faller, J.-P. and Teboul, J.-L. (2004) The Respiratory Variation in Inferior Vena Cava Diameter as a Guide to Fluid Therapy. *Intensive Care Medicine*, **30**, 1834-1837. <https://doi.org/10.1007/s00134-004-2233-5>
- [35] Katzarski, K.S., Nisell, J., Randmaa, I., et al. (1997) A Critical Evaluation of Ultrasound Measurement of Inferior Vena Cava Diameter in Assessing Dry Weight in Normotensive and Hypertensive Hemodialysis Patients. *American Journal of Kidney Diseases*, **30**, 459-465. [https://doi.org/10.1016/S0272-6386\(97\)90302-4](https://doi.org/10.1016/S0272-6386(97)90302-4)
- [36] Iorio, B.R.D., Scalfi, L., Terracciano, V. and Bellizzi, V. (2004) A Systematic Evaluation of Bioelectrical Impedance Measurement after Hemodialysis Session. *Kidney International*, **65**, 2435-2440. <https://doi.org/10.1111/j.1523-1755.2004.00660.x>
- [37] Wabel, P., Rode, C., Moissl, U., et al. (2007) Accuracy of Bioimpedance Spectroscopy (BIS) to Detect Fluid Status Changes in Hemodialysis Patients. *Nephrology Dialysis Transplantation*, **22**, VI129.

<https://www.researchgate.net/publication/267996959>

- [38] Siriopol, D., Voroneanu, L., Hogas, S., *et al.* (2016) Bioimpedance Analysis versus Lung Ultrasonography for Optimal Risk Prediction in Hemodialysis Patients. *The International Journal of Cardiovascular Imaging*, **32**, 263-270.
<https://doi.org/10.1007/s10554-015-0768-x>
- [39] Torino, C., Gargani, L., Sicari, R., *et al.* (2016) The Agreement between Auscultation and Lung Ultrasound in Hemodialysis Patients: The LUST Study. *Clinical Journal of the American Society of Nephrology*, **11**, 2005-2011.
<https://doi.org/10.2215/CJN.03890416>

Abbreviations

BIS: Bioimpedance Spectroscopy;

CHUY: Yaoundé University and Teaching Hospital;

HD: Haemodialysis;

JVT: Jugular Vein Turgor.

Contribution of Cardiac MRI in the Diagnosis of Acute Myocarditis

Aboubacar Sidiki Keita^{1*}, Mamoudou Camara², Mamadou Diallo², Adama Dembele³, Mamadou Cisse⁴

¹Medical Imaging Department, North Franche-Comte Hospital, Trevenans, France

²Faculty of Health Sciences and Techniques, Gamal Abdel Nasser University of Conakry, Conakry, Guinea

³Medical Imaging Department, Elbeuf Louviers Intercommunal Hospital Center, Elbeuf, France

⁴Medical Imaging Department, Blois Hospital Center, Blois, France

Email: *keitadoct@gmail.com

How to cite this paper: Keita, A.S., Camara, M., Diallo, M., Dembele, A. and Cisse, M. (2023) Contribution of Cardiac MRI in the Diagnosis of Acute Myocarditis. *Open Journal of Radiology*, 13, 17-25.

<https://doi.org/10.4236/ojrad.2023.131002>

Received: November 17, 2022

Accepted: February 25, 2023

Published: February 28, 2023

Copyright © 2023 by author(s) and Scientific Research Publishing Inc. This work is licensed under the Creative Commons Attribution International License (CC BY 4.0).

<http://creativecommons.org/licenses/by/4.0/>



Open Access

Abstract

Objective: To describe the MRI abnormalities observed in acute myocarditis.

Materials and Methods: Retrospective cross-sectional study with a descriptive aim, carried out at the North Franche-Comte Hospital, over a period of 12 months, from January 2021 to December 2021. It covered all patients who received an MRI of heart disease and were diagnosed with myocarditis. The diagnosis of myocarditis was retained in all patients on the basis of two arguments: a T2 PSIR hyper signal and a late enhancement at 15 min in T1 PSIR with gadolinium. **Results:** Myocarditis was diagnosed in 20 patients out of a total of 214 who performed cardiac MRI, *i.e.* 10.30% of cases. The average age was 33.7 ± 14.3 with extremes of 17 and 69 years. We observed a male predominance with 11 men (55%) for 9 women (45%) or a sex ratio of 1.2. Clinical suspicion of myocarditis and acute coronary syndrome were the main indications for MRI. The lesion sites were subepicardial (95%) and/or intramural (30%), respecting the subendocardium, interesting for the majority, segments 12 (anterolateral) in 50% and/or 11 (inferolateral) in 43% of cases. Global hypokinesia was observed in 30% of patients associated with a decrease in LVEF. There was no cardiac volume abnormality or valvular abnormality. **Conclusion:** Cardiac MRI is nowadays the most efficient non-invasive imaging in the diagnosis of acute myocarditis. The diagnosis of myocarditis was made on 2 pathognomonic signs, namely a T2 STIR hyper signal and late enhancement at 15 min in T1 PSIR after injection of gadolinium. The morphology and lesion locations were in agreement with those described in previous studies. Global hypokinesia and pericardial effusion were observed in some patients. On the other hand, there was neither valvular anomaly, nor cardiac volume anomaly.

Keywords

Cardiac MRI, Acute Myocarditis, Acute Coronary Syndrome

1. Introduction

Acute myocarditis is an inflammatory pathology of the myocardium, frequently of viral origin. When symptomatic, it is often difficult to diagnose, and the gold standard remains myocardial biopsy [1]. Myocarditis is a serious pathology, involved in the appearance of chronic dilated heart disease, but also in 8.6% to 12% of sudden deaths in young adults [2]. Faced with chest pain, electrocardiogram abnormalities and elevated blood levels of cardiac enzymes, myocarditis can be suspected in a young subject without cardiovascular risk factors, or at any age when coronary angiography is normal. However, first-line examinations do not provide the diagnosis of myocarditis with certainty, and do not make it possible to eliminate other etiologies, and in particular, an infarction with healthy coronary arteries [3]. There is, therefore, a need for a non-invasive diagnostic tool to confirm a diagnosis in these patients for whom the exit diagnosis is often a probability diagnosis. MRI is, therefore, the non-invasive diagnostic examination of reference, based on the semiological criteria of Lake-Louise, based on the identification of edema and capillary hyperemia, necrosis or myocardial fibrosis [4]. Initially, established in 2009, they were revised in 2018 based on developments in cardiac MRI acquisition techniques, in particular T1 and T2 mapping sequences and estimation of the Extracellular Volume (ECV) fraction of the myocardium [5]. Some authors have also shown that MRI with the injection of gadolinium, in this clinical situation, makes it possible to make the differential diagnosis between ischemic and non-ischemic pathologies [6]. By applying this semiology, we sought to confirm in our study the contribution of cardiac MRI in the face of a clinical picture suggestive of myocarditis, for which the first-line examinations cannot formally conclude.

2. Materials and Methods

We conducted a retrospective descriptive study. It took place in the Radiology Department of the North Franche-Comte Hospital (France). It covered a period of 12 months, from January 2021 to December 2021. The study population consisted of all patients seen for cardiac MRI. Were included in the study, patients in whom the diagnosis of myocarditis was retained in the presence of at least 2 of the 3 Lake Louise criteria, namely myocardial hyperemia, highlighted by an early global enhancement of the myocardium on T1-weighted sequences with the injection of gadolinium, regional or global myocardial edema, demonstrated by a hyper signal in T2-weighted STIR sequence and myocardial necrosis or fibrosis, most often multifocal, of subepicardial location (as opposed to scars under endo-heart attacks of ischemic origin), highlighted by late enhancement on T1-weighted se-

quences with the injection of gadolinium. Patients with a doubtful diagnosis with the presence of a single Lake Louise criterion associated or not with pericardial effusion and those with a strong clinical and biological suspicion but without signs on the MRI were not retained. The examinations were carried out with a Phillips brand 1.5 T MRI machine commissioned in 2017. The absence of major absolute contraindications, including the presence of a stent or a metal valve, was verified at prior. The patients were installed in the supine position with the knees supported in half flexion by a foam wedge; a phased array coil (dedicated cardiac coil) was used. The myocardium study protocol included: cine-MRI in short axis, long axis and 4 chambers with determination of LVEF, T2-weighted morphological sequence, 3D viability sequence at 6 min in short axis, long axis and four chambers and PSIR short axis to study late enhancement 15 min after injection of gadolinium.

The analysis was done by a senior radiologist, in two stages. First, a morphological analysis of the signal anomalies (shape and topography) according to the segmentation of the heart into 17 segments. Then, a functional analysis was done for the quantification of the systolic ejection fraction. We also looked for the presence of other signs such as valvular involvement. The parameters studied were recorded in the patient's file. These parameters were the sex and age of the patients, the indications and the protocol of the MRI examination, then the morphological lesions (late enhancement under endocardial, intramural, under endocardial or transmural) and functional anomalies observed (akinesia, hypokinesia or dyskinesia). Data entry and analysis were performed using Stata version 14 software. We performed a simple descriptive analysis of the different variables.

3. Results

Over a period of 12 months, 20 patients met our inclusion criteria out of a total of 214, *i.e.* 10.30% of patients who underwent cardiac MRI during the study period. We found a male predominance with 11 men (55%) for 9 women (45%) or a sex ratio of 1.2. The mean age of the patients was 33.7 ± 14.3 with extremes of 17 and 69 years. The majority age group (55%) was between 15 and 30 years old (**Table 1**).

The reasons for consultation were dominated by clinical suspicion of myocarditis and acute coronary syndrome respectively in 39% and 34% followed by chest pain in 27%.

A morphological abnormality such as slight dilation of the left ventricle was observed in two patients, *i.e.* 10%.

Regarding functional abnormalities, global hypokinesia of the left ventricle was observed in six patients, *i.e.* 30% associated with a drop in Left Ventricular Ejection Fraction (LVEF). There was no cardiac volume abnormality or valvular abnormality detected.

For the diagnosis of myocarditis, all the patients presented a T2 STIR hyper signal and a late enhancement on the T1 PSIR sequences with injection of gado-

linium (**Figure 1** and **Figure 2**).

The lesions were multisegmental and the majority were located in segments 12 (anterolateral) in 50% and/or 11 (inferolateral) in 43%.

There was a predominance of subepicardial lesions in 90% followed by intramural lesions in 30%. The morphology of the lesions was mainly linear 90% and/or nodular 25%. Pericardial effusion was observed in four 20% patients. There was no transmural involvement or isolated subendocardial involvement (**Table 2**).

Table 1. Distribution of patients according to age.

Age	Frequency	Percentage
15 - 30	11	55
30 - 45	4	20
45 - 60	4	20
≥60	1	5
Total	20	100

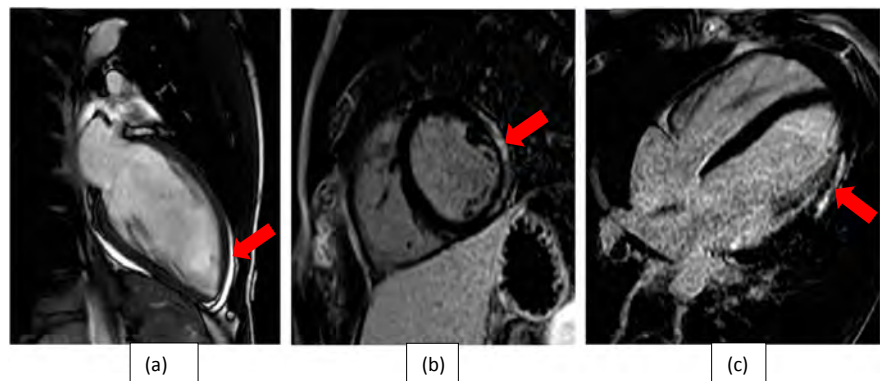


Figure 1. Cardiac MRI: (a) (long axis 2 chambers): pericardial effusion (red arrow); (b) and (c) late PSIR enhancement sequence 15 min after Gadolinium injection (2-cavity and 4-cavity minor axis incidence): late enhancement with subepicardial distribution (red arrows) in the median and apical, lateral and inferolateral wall.



Figure 2. Cardiac MRI (short axis 2 chambers T2 STIR), edema in T2 hyper signal (red arrow) of the infero-lateral wall of the left ventricle.

Table 2. Distribution of patients according to the site of the lesion.

Site	Frequency	Percentage
Subepicardial	19	95
Intramural	6	30
Subendocardial	0	0
Transmural	0	0

4. Discussion

Our study aimed to describe the MRI aspects of acute myocarditis.

4.1. Limitations of the Study

First of all, our workforce was, in fact during our study period we only listed 20 cases of myocarditis. Cardiac MRI is a long and restrictive examination; it requires in particular apneas and prolonged decubitus, as well as good cooperation from the patient. It is sometimes impossible to perform in arrhythmic or claustrophobic patients. There may therefore be a recruitment bias.

No myocardial biopsy was performed, which currently remains the gold standard for the diagnosis of myocarditis [1]. It is invasive and often unprofitable [3], and is currently not indicated as first-line treatment in the absence of signs of severity [7] [8]. Our diagnoses were therefore established according to the MRI semiology already described [4] [9]. The concordance of our results with these studies contributes to the validation of this semiology and the diagnostic capacities of MRI, as a non-invasive method.

4.2. Epidemioclinical Characteristics

Our patients were young, with an average age of 33.7 ± 14.3 and extremes of 17 and 69 years. Our result is close to that noted by Dubois (39.3 years) [10]. In our study, the patients were predominantly male (55%). This male predominance was observed in almost all of the available studies. Touré and Augier [11] [12] had observed it between 100% and 69%. In our series, the indication for MRI was dominated by clinical suspicion of myocarditis and acute coronary syndrome respectively in 39% and 34% followed by chest pain in 27%. In a study by OLOUDÉ *et al.*, coronary syndrome was the main indication for MRI 76% followed by suspicion of myocarditis 24% [13].

4.3. Examination Protocols

The myocardium study protocol included for all patients: cine-MRI sequence in the short axis, long axis and 4 cavities with determination of the LVEF, T2-weighted morphological sequence, 3D viability sequence at 6 min in the short axis, long axis and four chambers and short-axis PSIR to study late enhancement 10 min after gadolinium injection.

T1 and T2 maps of the myocardium, with quantification of the Extracellular

Volume (ECV), have recently been proposed for the tissue characterization of the myocardium. In patients with myocarditis, these techniques overcome certain limits of the Lake Louise criteria [14]. Mapping techniques provide quantitative data on tissue magnetic properties, including myocardial T1 and T2 relaxation times, and are therefore less sensitive to the limitations of the often subjective or visual assessment of signal intensity. They were not carried out in our service given the unavailability on our device. The T2-weighted morphological sequences made it possible to visualize in the patients edematous segments which appear in hyper signal within the myocardium. The dynamic sequences provided functional arguments concerning the systolic function of the LV (ejection fraction), the segmental kinetics, the measurements of diameters, thicknesses and volumes of the cardiac chambers. The sequences after injection confirmed the existence of a normal perfusion during the first pass. Late enhancement sequences were able to highlight contrast-enhancing segments in patients. Delayed enhancement after injection of contrast product would therefore constitute a sensitive and effective method for detecting the presence, distribution and extent of myocardial fibrosis or necrosis, and therefore myocarditis [15]. Several studies had correlated the presence of late enhancement and myocarditis proven by myocardial biopsy; with a specificity of 91.4% but a variable sensitivity of 73.8% on average. It would be possible that the sensitivity of this technique is dependent on the duration of the symptoms, with a higher sensitivity in the acute phase [16].

4.4. Morphological Lesions

All the patients in our study had presented a linear and/or nodular hyper signal, independent of the vascular territories, not reaching the subendocardium, on the T2 STIR sequence and an enhancement at 15 min after injection of Gadolinium on the T1 PSIR sequence. Our results were in agreement with those of Paule and Feldman [1] [12] who had reported that the majority of patients presented hyper signals suggestive of acute myocarditis in 91% in T2 STIR and 97% on late enhancement in T1 PSIR at 15 min. after gadolinium injection. The most important study concerning the analysis of myocarditis by MRI is that of Mahrholdt *et al.* [9], who evaluated 128 patients (87 of whom presented with myocarditis) by 1.5 T MRI (cine MRI, late enhancement analysis), MRI-guided endomyocardial biopsies, histological and virological analyses. In this study, late enhancement was present in 95% of patients with active myocarditis, 40% of patients with healing myocarditis, and none of the patients with no histopathological criteria for myocarditis (except for a patient with cardiac amyloidosis).

4.5. Topography of Lesions

In our study, lesions predominated in segments 11 and 12 in 43% and 50%. Our results were slightly superior to those of Augier [17] who had shown a predominance of lesions with contrast price at the level of segments 11 and 12 in 37%

for each of the sites. Other authors had also observed that generally, the preferential involvement would be the anterolateral wall, with or without thickening of the latter [18]. Mahroldt and Liu [8] [9] had also shown that the affected areas were in the early stage of the disease, the lateral wall (segment 11). At the level of the myocardium, the lesions were preferentially located subepicardial 90% and/or intramural 30%, never subendocardial. Our result was identical to that of Paule *et al.* who reported one or more foci of late subepicardial and/or intramyocardial enhancement in 90% of patients [12]. These results are in line with the data in the literature by constituting a reliable argument in favor of the diagnosis of acute myocarditis and helping to rule out an Acute Coronary Syndrome (ACS) [9]. In infarcts, the attack of the subendocardium is systematic and of more “brilliant” aspect because containing less viable myocytes between the areas of necroses [9].

4.6. Associated Lesions

In our study, pericardial effusion was associated in 4 out of 20 patients, *i.e.* 20%. This result is consistent with that of Laissy who reported pericardial effusion in 20% of patients [18]. Regarding functional abnormalities, we found global hypokinesia associated with a decrease in LVEF in 30% of patients. Roditi *et al.* [7], on 12 MRIs of patients presenting with myocarditis, noting kinetic disorders at the level of the zones marked by late enhancement in ten patients, and normal kinetics at the level of the marked zones in two patients. Not all authors agree on the correspondence between areas with kinetic disturbance and areas of late enhancement: most publications report late enhancements located outside dyskinetic areas [4] [18] [19].

5. Conclusion

The results of our study are in agreement with those of previous studies. The diagnosis of myocarditis was made in all patients on 2 pathognomonic signs, namely a T2 STIR hyper signal and late enhancement at 15 min in T1 PSIR after injection of gadolinium. As described in the literature, our patients were young with a male predominance, consulting mostly for acute coronary syndrome and/or for clinical suspicion of myocarditis. Lesion locations were voluntarily subepicardial and/or intramural, never subendocardial. Global hypokinesia and pericardial effusion were noted in some patients. On the other hand, there was neither valvular anomaly, nor anomaly of the cardiac volumes.

Authors' Contribution

All authors contributed to the acquisition of data, analysis and interpretation of the data and writing of the article.

Conflicts of Interest

The authors declare no conflicts of interest regarding the publication of this paper.

References

- [1] Feldman, A.M. and McNamara, D. (2000) Myocarditis. *The New England Journal of Medicine*, **343**, 1388-1398. <https://doi.org/10.1056/NEJM200011093431908>
- [2] Soumah, M.M., Kanikomo, D., Ndiaye, M. and Sow, M.L. (2013) The Sudden Death of Adult, Particularities in Africa: About 476 Cases. *The Pan African Medical Journal*, **16**, Article 125. <https://doi.org/10.11604/pamj.2013.16.125.2490>
- [3] Hombach, V., Merkle, N., Kestler, H.A., *et al.* (2010) Characterization of Patients with Acute Chest Pain Using Cardiac Magnetic Resonance Imaging. *Clinical Research in Cardiology Supplements*, **5**, 63-69. <https://doi.org/10.1007/s11789-010-0003-1>
- [4] Friedrich, M.G., Sechtem, U., Schulz-Menger, J., *et al.* (2009) Cardiovascular Magnetic Resonance in Myocarditis: A JACC White Paper. *Journal of the American College of Cardiology*, **53**, 1475-1487. <https://doi.org/10.1016/j.jacc.2009.02.007>
- [5] Ferreira, V.M., Schulz-Menger, J., Holmvang, G., *et al.* (2018) Cardiovascular Magnetic Resonance in Nonischemic Myocardial Inflammation: Expert Recommendations. *Journal of the American College of Cardiology*, **72**, 3158-3176. <https://doi.org/10.1016/j.jacc.2018.09.072>
- [6] Hunold, P., Schlosser, T., Vogt, F.M., *et al.* (2005) Myocardial Late Enhancement in Contrast-Enhanced Cardiac MRI: Distinction between Infarction Scar and Non-Infarction-Related Disease. *American Journal of Roentgenology* **184**, 1420-1426. <https://doi.org/10.2214/ajr.184.5.01841420>
- [7] Roditi, G.H., Hartnell, G.G. and Cohen, M.C. (2000) MRI Changes in Myocarditis—Evaluation with Spin Echo, Cine MR Angiography and Contrast Enhanced Spin Echo Imaging. *Clinical Radiology*, **55**, 752-758. <https://doi.org/10.1053/crad.2000.0519>
- [8] Liu, P.P. and Yan, A.T. (2005) Cardiovascular Magnetic Resonance for the Diagnosis of Acute Myocarditis: Prospects for Detecting Myocardial Inflammation. *Journal of the American College of Cardiology*, **45**, 1823-1825. <https://doi.org/10.1016/j.jacc.2005.03.002>
- [9] Mahrholdt, H., Wagner, A., Deluigi, C.C., *et al.* (2006) Presentation, Patterns of Myocardial Damage, and Clinical Course of Viral Myocarditis. *Circulation*, **114**, 1581-1590. <https://doi.org/10.1161/CIRCULATIONAHA.105.606509>
- [10] Gillaume, D. (2009) Place de l'IRM Cardiaque devant un tableau clinique évocateur de myocardite. Thèse de Médecine, Université de Limoges, Limoges, 82 p.
- [11] Toure, A., Konan, A., N'dja, A.P., *et al.* (2022) Aspects IRM des Myocardites en Afrique Subsaharienne: Étude Préliminaire. *Health Sciences and Diseases*, **23**, 12-16. <https://www.hsd-fmsb.org/index.php/hsd/article/view/3860>
- [12] Paule, P., Roche, N.C., Chabrilat, Y., *et al.* (2014) Apport de l'IRM cardiaque dans l'évaluation initiale et le suivi des myocardites mimant un syndrome coronaire aigu: À propos d'une série de 43 patients. *Annales de Cardiologie et d'Angéiologie*, **63**, 331-338. <https://doi.org/10.1016/j.ancard.2014.08.006>
- [13] Oloude, N., Hounkpatin, B., Tixier, V., *et al.* (2014) Apport de l'IRM dans le diagnostic des myocardites aiguës. *Annales de Cardiologie et d'Angéiologie*, **63**, 404. <https://doi.org/10.1016/j.ancard.2014.09.020>
- [14] Kotanidis, C.P., Bazmpiani, M.-A., Haidich, A.-B., *et al.* (2018) Diagnostic Accuracy of Cardiovascular Magnetic Resonance in Acute Myocarditis: A Systematic Review and Meta-Analysis. *JACC: Cardiovascular Imaging*, **11**, 1583-1590. <https://doi.org/10.1016/j.jcmg.2017.12.008>
- [15] Kim, R.J., Wu, E., Rafael, A., *et al.* (2000) The Use of Contrast Enhanced Magnetic

Resonance Imaging to Identify Reversible Myocardial Dysfunction. *The New England Journal of Medicine*, **343**, 1445-1453.

<https://doi.org/10.1056/NEJM200011163432003>

- [16] Monney, P., Locca, D., Muzzarelli, S., *et al.* (2012) IRM cardiaque: Imagerie de référence dans le diagnostic des myocardites aiguës? *Revue Médicale Suisse*, **8**, 1177-1183.
- [17] Augier, C. (2011) Valeur pronostique de l'IRM cardiaque dans la myocardite aiguë: Mise au point d'un score de quantification de la prise de contraste tardive du gadolinium. Thèse d'Médecine, Université de Grenoble Alpes, Saint-Martin-d'Hères, 21 p.
- [18] Laissy, J.P. (2006) Imagerie par résonance magnétique des myocardites. *MT Cardio*, **2**, 616-621.
- [19] Abdel-Aty, H., Boye, P., Zagrosek, A., *et al.* (2005) Diagnostic Performance of Cardiovascular Magnetic Resonance in Patients with Suspected Acute Myocarditis: Comparison of Different Approaches. *Journal of the American College of Cardiology*, **45**, 1815. <https://doi.org/10.1016/j.jacc.2004.11.069>

Evaluation of Entrance Skin Dose from Paediatric Diagnostic X-Ray Examination

Moromoke Oluwayemisi Adelayi* , Oladele Samuel Ajayi

Department of Physics, Federal University of Technology, Akure, Nigeria

Email: *moromokeadelayi@gmail.com

How to cite this paper: Adelayi, M.O. and Ajayi, O.S. (2023) Evaluation of Entrance Skin Dose from Paediatric Diagnostic X-Ray Examination. *Open Journal of Radiology*, 13, 26-33.

<https://doi.org/10.4236/ojrad.2023.131003>

Received: October 23, 2022

Accepted: February 25, 2023

Published: February 28, 2023

Copyright © 2023 by author(s) and Scientific Research Publishing Inc.

This work is licensed under the Creative Commons Attribution International License (CC BY 4.0).

<http://creativecommons.org/licenses/by/4.0/>



Open Access

Abstract

As children are prone to be more radiosensitive than adults, it is imperative to assess the Entrance Skin Doses (ESDs) for patients being examined by X-rays, in order to ensure the optimization of dose while considering a number of other factors. The ESD received by 50 paediatrics (aged 1 - 13 years) undergoing 8 types of X-ray examinations were measured at Federal Teaching Hospital, Ido-Ekiti, Ekiti, Nigeria, within a period of February 2019 to March 2020 using thermoluminescent dosimeters. The mean \pm SD of ESDs were 0.85 ± 0.32 , 2.04 ± 0.75 , 0.60 ± 0.07 , 0.62 ± 0.22 , 0.57 ± 0.24 , 1.75 ± 0.76 , 0.93 ± 0.31 and 0.63 ± 0.06 mGy for Chest, Skull, Hand, Forearm, Knee, Abdomen, Leg and Feet, respectively. The mean ESDs were found to be within the recommended reference dose in all examinations, except for the Chest examination which was higher. The data obtained in this study will serve as existing data in Nigeria for future research works, as it would assist in optimizing dose to patients, especially the paediatrics.

Keywords

Entrance Skin Dose, Paediatrics, X-Rays

1. Introduction

In the diagnosis of pathological conditions, both in children and in adults, diagnostic radiology (otherwise known as X-rays) is an accepted imaging procedure that is typically used to diagnose bone degeneration, fractures, dislocations and infections in patients. However, it is important to understand the level of patient dose and corresponding factors that affect them [1] in order to achieve a good image quality production while minimizing the amount of dose a patient is being exposed to, most especially in paediatrics [2] [3]. This is because children live longer than adults, have growing organs and are prone to be more sensitive

to radiation effects than adults [4]. Thus, radiation protection of paediatric patients becomes important, as a result of the increased radiation risks to children.

It is worthy of note that the major focus of medical concerns is to produce a good quality image while limiting the levels of radiation exposure to patients. This becomes more essential while handling children; unfortunately, the same cannot be said about the medical concerns in Nigeria. Substantial dose reduction during the X-ray examination is possible without detriment to the image quality [2] through proper justification, optimization and application of dose limits in the examination procedures used.

The patient dose is often described by the Entrance Skin Dose (ESD), which is defined as the absorbed dose to air on the X-ray beam axis at the point where the X-ray beam enters the patient skin. Due to the fact that most diagnostic X-ray centres in Nigeria do not have a designated X-ray unit for paediatrics, such that the practice of radiographers in such units is basically for adults and inconsiderate of children. Hence, there is a possibility of children being exposed to higher levels of radiation while undergoing X-ray examinations, which is why optimization of dose and X-ray imaging parameters must be guided by the ALARA (As Low As Reasonably Achievable) principle [3]. Research work conducted in Nigeria on radiation dose to children in routine X-ray examination attributed the high ESD received by paediatric patients to a lack of dedicated X-ray units and personnel [5].

A large number of examinations are being carried out in Nigeria; however, the available dose information for paediatric patients is grossly inadequate. On this note, this research aims to measure the Entrance Skin Dose (ESD) of paediatric patients undergoing diagnostic X-ray examinations in Federal Teaching Hospital, Ido-Ekiti, Ekiti State.

2. Materials and Methods

This study was carried out at the radiology centre of Federal Teaching Hospital, Ido-Ekiti, Ekiti State, Nigeria in the period from February 2019 to March 2020. Due clearance was obtained from the ethical committee of the hospitals before commencing the research work, after which consent was obtained from parents or guardians of the patients. The sample size of 50 paediatric patients (male and female) between the ages of 1 - 13 years, who were referred to the X-ray unit of this hospital for diagnosis within the stated period, was considered.

The specification of the X-ray machine in this facility is as follows: Neusoft XG-CS-R-N Model; manufactured in year 2011, Installed in year 2013 with a Filtration of 2.0 mm Al/24 kV; 3600 W.

Different X-ray examinations including Chest PA, Skull AP, Hand AP, Forearm AP, Knee AP, Abdomen AP, Leg AP and Feet AP at a focus range of 70 - 100. Abdomen AP was done at 100 cm while Chest PA was at 120 cm. The age, weight, height, gender and BMI, type of X-ray examination, exposure projection (AP/PA) and X-ray tube details (kVp and mAs) for each patient were duly recorded.

Entrance Skin Dose (ESD) was measured using calibrated Thermo Luminescent Dosimeters (TLDs), affixed to the skin of patient along the path of the primary X-ray beam to measure doses to the chest, skull, hand, forearm, knee, abdomen, leg and feet. The weight of the patients were recorded using the hospital weighing scale, with a measuring tape held against a vertical pole to measure the height of the patient. The Body Mass Index (BMI) of the patient was calculated by dividing the weight (kg) of the patient by the square of the patient's height (m). Data obtained were transferred to Microsoft Excel spreadsheet, presented as mean \pm SD and afterwards analysed using statistical Package for Social Sciences (SPSS Inc., Chicago, IL, USA) version 23.0. Correlation between ESD and patient characteristics/exposure parameters was statistically significant at the $p < 0.05$.

3. Results

Table 1 shows the mean \pm SD values of all paediatric patients examined in this study. The sample size consists of 50 patients (30 males, 20 females) within the age range of 1 - 13 years with a mean age of 5.99 ± 3.80 years; weight ranged from 10 to 35 kg with a mean value of 22.56 ± 8.18 kg; the height ranged from 79 to 128 cm (99.92 ± 20.30 cm) and the Body Mass Index (BMI) of 22.17 ± 3.03 kg/m² which ranged from 17.72 to 36.22 kg/m².

The mean \pm SD values of the X-ray tube exposure parameters are presented in **Table 2**. The tube voltage (kVp) of 55.14 ± 15.05 ranged from 25 to 80, the tube current (mAs) of 9.60 ± 8.80 ranged from 2 to 30, the mean Focus to Skin Distance (FSD) ranged from 62 to 110 with a mean value of 87.98 ± 15.56 and the Entrance Skin Dose (ESD) had a mean value of 0.91 ± 0.49 mGy ranging from 0.23 to 2.90 mGy.

Table 3 shows a comparison of mean ESDs for different examinations observed in this study with other published works. The maximum ESD was observed in Skull AP (2.04 ± 0.75 mGy) while the minimum ESD was observed in Knee AP (0.57 ± 0.24 mGy).

Table 1. Mean and standard deviation of patient demographic data.

	Age (years)	Weight (kg)	Height (cm)	BMI (kg/m ²)
Mean \pm SD	5.99 ± 3.80	22.56 ± 8.18	99.92 ± 20.30	22.17 ± 3.03
Min	2	10	79	17.72
Max	13	35	128	36.22

Table 2. Mean and standard deviation of radiography X-ray machine.

	kVp	mAs	FSD	ESD
Mean \pm SD	55.14 ± 15.05	9.60 ± 8.80	87.98 ± 15.56	0.91 ± 0.49
Min	25	2	62	0.23
Max	80	30	110	2.90

In **Table 4** and **Table 5**, it was observed that age and type of exposure projection had no significant relationship with ESD. However, the age group of 5 - <10 years had the maximum number (21) of paediatric patients presenting for X-ray examinations and received the maximum ESD as seen in **Table 6**.

The weight and height of the patients had significant impact on the ESDs while there was no correlation between the patients' BMI and ESD (**Table 7**). A correlation between the exposure parameters in **Table 8** shows that there is a significant relationship between the ESDs and kVp/mAs, however, there is no correlation between FSD and ESD. A published work has earlier stated that dose absorbed by the skin is directly proportional to the square of the peak voltage, the tube current and the duration of exposure [1].

Table 3. Mean and standard deviation of ESDs for different X-ray examinations.

	N	ESD			<i>p-value</i>	Recommended Standards	
		Mean	Min	Max		EC, 1996 mGy	NRPB, 2000 mGy
Chest PA	8	0.85 ± 0.32	0.46	1.47		0.3	0.2
Skull AP	3	2.04 ± 0.75	1.59	2.90		5	3
Hand AP	11	0.60 ± 0.07	0.48	0.71		-	-
Forearm AP	5	0.62 ± 0.22	0.42	0.95	0.001	-	-
Knee AP	9	0.57 ± 0.24	0.29	1.10		-	-
Abdomen AP	2	1.75 ± 0.76	1.22	2.29		10	-
Leg AP	10	0.93 ± 0.31	0.60	1.44		-	-
Feet AP	2	0.63 ± 0.06	0.58	0.67		-	-
Total	50	1.00 ± 0.57	0.71	1.44			

Table 4. Mean and standard deviation of ESDs according to gender.

Gender	N	ESDs			
		Mean ± SD	Min	Max	<i>p-value</i>
Male	30	1.01 ± 0.55	0.23	2.90	
Female	20	0.75 ± 0.34	0.29	2.06	0.658
Total	50	0.88 ± 0.45	0.26	2.48	

Table 5. Mean and standard deviation of examination projections.

Projection	N	ESDs			
		Mean ± SD	Min	Max	<i>p-value</i>
AP	39	0.81 ± 0.48	0.29	2.90	
PA	11	0.96 ± 0.34	0.46	1.47	0.445
Total	50	0.89 ± 0.41	0.28	2.19	

Table 6. Mean and standard deviation of ESDs according to age group.

Age (Years)	N	ESDs			<i>p-value</i>
		Mean \pm SD	Min	Max	
1 - <5	17	0.68 \pm 0.20	0.32	1.29	0.807
5 - <10	21	1.10 \pm 0.62	0.29	2.90	
10 - 15	12	1.00 \pm 0.43	0.23	2.06	
Total	50	0.93 \pm 0.42	0.28	2.08	

Table 7. Correlation between the Entrance Skin Dose (ESD) and the patient characteristics.

Correlation between ESD and the Patient Characteristics		
Weight (kg)	Pearson Correlation (r)	0.266**
	R ²	0.071
	Significant Difference (p)	0.007
Height (cm)	Pearson Correlation (r)	0.253*
	R ²	0.064
	Significant Difference (p)	0.011
BMI (kg/m²)	Pearson Correlation (r)	-0.054
	R ²	0.003
	Significant Difference (p)	0.593
Age (years)	Pearson Correlation (r)	0.263**
	R ²	0.069
	Significant Difference (p)	0.008

*significant at 0.05 level (2-tailed), **significant at 0.01 level (2-tailed).

Table 8. Correlation between the Entrance Skin Dose (ESD) and exposure parameters.

Correlation between ESD and Exposure parameters		
Tube Voltage (kVp)	Pearson Correlation (r)	0.663**
	R ²	0.440
	Significant Difference (p)	0.000
Tube Current (mAs)	Pearson Correlation (r)	0.735**
	R ²	0.540
	Significant Difference (p)	0.000
FSD (cm)	Pearson Correlation (r)	0.108
	R ²	0.012
	Significant Difference (p)	0.286

*significant at 0.05 level (2-tailed), **significant at 0.01 level (2-tailed).

4. Discussion

The ESD of 50 patients (30 male; 20 female) were measured. In **Table 3**, it was observed that the measured ESDs in this study were lower than what was recorded in other studies; although the measured ESD for chest (0.85 \pm 0.32 mGy) in this study is higher than the recommended values [6] [7]. Also, the measured ESD for Skull AP (2.04 \pm 0.75 mGy) in this study is close to what was recorded by the NRPB report [7] by 0.96 mGy, but lower than the value recorded by the

European Commission [6].

Similar examinations carried out in Sudan showed the measured ESDs for Chest PA, Skull AP and Abdomen AP to be 0.16, 0.55 and 0.46 mGy respectively [8]. A study in Iran recorded 0.09 mGy for Chest PA and 0.10 mGy for Abdomen AP [9] while a similar study in Saudi Arabia recorded 0.32, 0.40 and 0.35 mGy for Chest PA, Skull AP and Abdomen AP respectively [10].

The type of equipment and radiographic technique used determines the quantity of radiation dose received by a patient; however, this procedure differs from one hospital to another. For example, a study conducted in Korea used a focus range of 180 cm [11], a similar study conducted in Zimbabwe maintained a focus range of 100 cm [12] while this study used a focus range of 70 - 100 cm. The use of different focus range by different authors has an effect on reported patient doses and may explain the reason for having varying entrance skin dose as reported by the authors. A report of a study conducted in year 2003 stated that an increase in film focus reduces, to some extent, the radiation dose for X-ray examinations by about 33% - 44% [13].

Furthermore, the use of low kVp and high mAs contribute to the dose a patient receives. It was observed for all types of examinations and projections in this study, that the tube current (mAs) comprises of low tube voltage (25 - 80 kVp) and high tube load (2 - 30 mAs) which is lower than the value [high voltage (60 - 79 kVp) and low tube load (2 - 7 mAs)] recommended by the European Commission [6]. As a result, this study recorded a significant correlation ($p < 0.01$) between the ESDs and kVp/mAs ($r = 0.663/r = 0.735$ respectively). A similar study carried out in three Nigerian Eastern hospitals recorded high doses of about 44.7% difference when compared with a similar study conducted in three Nigerian western hospitals; which was traceable to the use of low kVp and high mAs, as well as lack of standardization in procedures [14].

It is expected that the ESD should increase as the patients' weight increases. A correlation between ESD and patient weight in this study showed that the weight of the patients had significant impact on the ESDs ($r = 0.266$, $p = 0.007$). In addition to this, the age of patients is expected to affect the ESD value, however, it did not significantly contribute to the patient dose in this study ($r = 0.263$, $p = 0.008$). This is similar to the findings reported by Atalabi *et al.*, where age had no significant effect on the patient dose [5].

However, it is expected that exposure factors should be selected carefully to ensure dose optimization while examining paediatric patients. Thus, the higher dose observed in this study for Chest PA is unhealthy for the paediatric population. It was also observed in the course of the study that there is no designated X-ray department for children, such that the same X-ray exposure parameters are being used for both adult and paediatric populations.

The major limitation of this study was that the number of paediatric patients coming for X-ray examination is very small, compared to adults...thus, took more time to get the desired number of patients.

5. Conclusion

This study which was conducted at Federal Teaching Hospital Ido-Ekiti, Ekiti is considered to take a run at evaluating doses received by paediatric population between the ages of 1 - 13 years undergoing different X-ray examination procedures; taking into account, there is a wide variation in patient sizes as children grow in body sizes and in age. The mean ESDs were found to be within the recommended reference dose in all examinations, except for the Chest PA which was higher than the recommended dose reference. The data obtained in this study will serve as existing data in Nigeria for future research works, as it would assist in optimizing dose to patients, especially the paediatric population.

Acknowledgements

The authors appreciate the management and staff of Federal Teaching Hospital, Ido-Ekiti, Ekiti for giving research approval and rendering necessary assistance in the course of the study. Special thanks to Radiation Technology Institute, Lagos, Lagos State for making available their TLD facilities.

Conflicts of Interest

The authors declare no conflicts of interest regarding the publication of this paper.

References

- [1] Parry, R.A., Sharon, A., Glaze, M.S. and Benjamin, R.A. (1999) The AAPM/RSNA Physics Tutorial for Residents: Typical Patient Radiation Doses in Diagnostic Radiology. *Radiographics*, **19**, 1289-1302. <https://doi.org/10.1148/radiographics.19.5.g99se211289>
- [2] Charnock, P., Moores, B.M. and Wilde, R. (2013) Establishing Local and Regional DRLs by Means of Electronic Radiographical X-Ray Examination Records. *Radiation Protection Dosimetry*, **157**, 62-721. <https://doi.org/10.1093/rpd/nct125>
- [3] Willis, C.E. and Slovis, T.L. (2004) The ALARA Concept in Pediatric CR and DR: Dose Reduction in Pediatric Radiographic Exams—A White Paper Conference Executive Summary. *Pediatric Radiology*, **34**, S162-S164. <https://doi.org/10.1007/s00247-004-1264-y>
- [4] International Commission for Radiological Protection (ICRP) (2011) Radiation Protection in Paediatric Diagnostic and Interventional Radiology. *Annals of the ICRP*, **48**, 3982-4649.
- [5] Atalabi, O.M., Akinlade, B.I., Adekanmi, A.J. and Samuel, O.A. (2013) Entrance Surface Dose from Paediatric Diagnostic X-Ray Examinations in a Developing World Setting: Are We “ALARA Principle” Compliant? *British Journal of Medicine & Medical Research*, **3**, 2288-2298. <https://doi.org/10.9734/BJMMR/2013/4119>
- [6] (1996) European Guidelines on Quality Criteria for Diagnostic Radiographic Images in Paediatrics. EUR 16261.
- [7] National Radiology Protection Board (NRPB) (2002) Reference Doses and Patient Size in Paediatric Radiology. NRPB-R318.
- [8] Eljak, S.N.A., Ayad, C.E. and Abdalla, E.A. (2015) Evaluation of Entrance Skin Rad-

- iation Exposure Dose for Pediatrics Examined by Digital Radiography at Asser Central Hospital-KSA. *Open Journal of Radiology*, **5**, 125-130.
<https://doi.org/10.4236/ojrad.2015.53019>
- [9] Toossi, M.T.B. and Malekzadeh, M. (2012) Radiation Dose to Newborns in Neonatal Intensive Care Units. *Iranian Journal of Radiology*, **9**, 145-149.
<https://doi.org/10.5812/iranjradiol.8065>
- [10] Osman, H. (2013) Pediatric Radiation Dose from Routine X-Ray Examination Hospital Based Study, Taif Paediatric Hospital. *Scholars Journal of Applied Medical Sciences*, **5**, 511-515.
- [11] Kim, H.B., Do, K.H., Goo, W.H., Yang, H.D., Oh, Y.S., *et al.* (2012) National Survey of Radiation Doses of Pediatric Chest Radiography in Korea: Analysis of the Factors Affecting Radiation Doses. *Korean Journal Radiology*, **13**, 610-617.
<https://doi.org/10.3348/kjr.2012.13.5.610>
- [12] Beremauro, W., Kahari, C., Kowo, F. and Banhwa, J. (2015) Radiation Doses by Paediatric Patients during Chest X-Ray Examinations at a Central Hospital in Zimbabwe. *International Journal of Sciences: Basic and Applied Research (IJSBAR)*, **24**, 361-372.
- [13] Brennan, P.C., McDonnell, S. and O'Leary (2003) Increasing Film-Focus Distance Reduces Radiation Dose for X-Ray Examinations. *Radiation Protection*, **108**, 263-268.
<https://doi.org/10.1093/rpd/nch029>
- [14] Egbe, N.O., Inyang, S.O., Ibeagwu, O.B. and Chiaghanam, N.O. (2008) Paediatric Radiography Entrance Doses for Some Procedures in Three Hospitals within Eastern Nigeria. *Journal of Medical Physics*, **339**, 29-34.
<https://doi.org/10.4103/0971-6203.39422>

Radiation Doses in Diagnostic Radiology and Method for Dose Reduction

Taha M. Taha^{1*} , Hoda A. Ahmed², Fathy A. Shaheen²

¹Radiation Protection Department, Nuclear Research Center, Egyptian Atomic Energy Authority, Cairo, Egypt

²Radiology Unit, Medical Administration, Nuclear Research Center, Egyptian Atomic Energy Authority, Cairo, Egypt

Email: *tahaalfawwal@hotmail.com

How to cite this paper: Taha, T.M., Ahmed, H.A. and Shaheen, F.A. (2023) Radiation Doses in Diagnostic Radiology and Method for Dose Reduction. *Open Journal of Radiology*, 13, 34-41.

<https://doi.org/10.4236/ojrad.2023.131004>

Received: December 15, 2022

Accepted: February 25, 2023

Published: February 28, 2023

Copyright © 2023 by author(s) and Scientific Research Publishing Inc.

This work is licensed under the Creative Commons Attribution International License (CC BY 4.0).

<http://creativecommons.org/licenses/by/4.0/>



Open Access

Abstract

Objective: The current research study aims to calculate entrance surface air kerma for skull, chest, cervical spine, lumbar spine, and pelvic X-ray examinations in interior posterior and posterior interior positions and generate a method for chest dose reduction to decrease radiation risk. **Materials and Methods:** The indirect dose measurement was used in the current research. The X-ray tube output was measured using RAD-CHECK Plus ionization chamber and the indirect entrance surface air kerma was calculated via applying physical acquisition parameters such as a focus on skin distance, tube current times exposure time (mAs), and applied tube voltage (kV), and applying a mathematical model. **Results:** The main findings were obtained from comparing the radiation doses with the reference levels of International organizations such as the American College of Radiology and the International Atomic Energy Authority. The mean entrance skin dose for the skull (AP), skull (PA), skull (LAT), cervical spine (PA), cervical spine (LAT), lumbar spine (AP), lumbar spine (LAT), pelvis (AP), and pelvis (LAT) of adult X-ray examinations was within the diagnostic reference dose level values obtained by ACR (2018) except for the ESD for chest (AP) which was 0.88 mGy. **Conclusions:** The results of the study concluded that by adjusting the applied tube voltage, kV, and tube current product time, mAs decreased the radiation dose to the chest X-ray by 58%.

Keywords

Radiology, Entrance Skin Dose, Chest X-Ray, Dose Minimization

1. Introduction

Optimization of radiation dose delivered to patients is the main objective of radia-

tion protection principles. The shortage in the entrance skin dose database and the probability of delivering an excess dose to patients lead to calculating the Entrance Skin Dose (ESD) for patients undergoing diagnostic X-ray examinations and optimizing the dose delivered to the chest. Studying some factors affecting on patient doses should be made as a means to ensure the accuracy of the operating physical parameters and minimize a dose to a certain organ. Ionizing radiation in the medical field contributes significantly to the source of exposure of the population [1]. Dose measurements are required to comply with some international guidelines and regulations. The need for radiation dose assessment of patients during diagnostic X-ray examinations has been highlighted by the increasing knowledge of the hazards of ionizing radiation. In today's diagnostic radiology, there is a growing concern about radiation exposure. This can be seen in the recommendations of the International Commission on Radiation Protection. The guiding principles for setting a Diagnostic Reference Level (DRL) are: 1) the regional, national, or local objective is clearly defined, including the degree of specification of clinical and technical conditions for the medical imaging task; 2) the selected value of the DRL is based on relevant regional, national, or local data; 3) the quantity used for the DRL can be obtained practically; 4) the quantity used for the DRL is a suitable measure of the relative change in patient tissue doses and, therefore, of the relative change in patient risk for the given medical imaging task; and 5) how the DRL is to be applied in practice is clearly illustrated. All these recommendations advise that X-ray examinations should be conducted using techniques that keep patients' doses as low as compatible with the medical purposes of the examinations [1]. The ESD is a measure of the radiation dose absorbed by the skin where the X-ray beam enters the patient. The application of radiation physics in medicine includes three medical practices: diagnostic X-ray, nuclear medicine, and radiotherapy. Diagnostic X-ray practice is one of the medical applications of radiation in medicine [2]. Ofori *et al.* (2014) calculated the mean ESD and effective dose of seven different examinations using Cal Dose software [3]. The results showed that the mean patient Entrance Surface Doses (ESDs) were 0.27 mGy, 0.43 mGy, 1.31 mGy, 1.05 mGy, 0.45 mGy, 2.10 mGy, 3.25 mGy and the mean effective doses were 0.02 mSv, 0.01 mSv, 0.09 mSv, 0.05 mSv, 0.03 mSv, 0.13 mSv, 0.41 mSv for thorax (PA), thorax/chest (RLAT), pelvis (AP), cervical spine (AP), cervical spine (LAT), thoracic spine (AP) and lumbar spine (AP) respectively. Mor *et al.* (2018) estimated doses for chest X-ray examinations for adult patients using the indirect method and compared them with the Diagnostic Reference Levels (DRLs) [4]. Abubaker *et al.* (2017) estimated the Entrance Surface Dose (ESD) for adult patients who underwent diagnosis via X-ray examinations in one of the radiographic centers in Sebha city. The ESD has been estimated indirectly using exposure factors for patients. The results showed that the mean patient Entrance Surface Doses (ESDs) were 41.73 ± 5.84 mGy, 7.43 ± 2.58 mGy, 103.7 ± 125.53 mGy, 7.25 ± 4.32 mGy and 11.24 ± 16.18 mGy respectively for pelvis (AP), chest (AP), lumbar spine (AP), cervical spine (AP) and

skull (AP). In the present investigation, the authors conducted a study to assess the entrance skin dose for ten types of X-ray examinations: skull, chest (PA), chest (AP), skull and pelvic of patients (adult) Radiology Unit in the Nuclear Research Center (NRC) using the indirect method and created a new method for dose reduction [5]. Mohamadain *et al.* (2013) estimated the effective doses and body organ doses due to chest examinations in infants and pediatrics. Two examination incidences, AP and PA for chest X-ray exposures were evaluated and compared with respect to the radiographic technique employed [6]. Komarskiy *et al.* (2014) reduced Pulse X-ray diagnostics is capable of reducing radiation exposure considerably [7]. Njiki *et al.* (2019) investigated how accurate are TASMICS and TASMIP models in predicting the X-ray output of some Conventional Radiology X-ray Units with high-frequency generators [8]. Bope *et al.* (2022) studied the knowledge and practices of health professionals on the optimization of radiation protection in diagnostic radiology in children and adults in the general referral hospitals of Bukavu in South Kivu, DRC [9].

2. Materials and Methods

The current X-ray Toshiba model delta ray (E7239X) has the following features: Specially processed Rhenium-tungsten faced molybdenum target of 74 mm diameter. The tubes have foci 1.0 mm and 2.0 mm and are available for a maximum tube voltage of 125 kV with a single phase or three-phases accommodated with IEC 60526 type high voltage cable receptacles. Questionnaires were distributed to radiographers in charge of diagnostic facilities. Each radiographer was asked to provide information with respect to his X-ray Radiography Unit, including manufacturer, model, year of installation, physical half-value layer and X-ray exposure parameters such as kVp, mA, mAs, and Focus on Skin Distance (FSD). The ESD was assessed by the indirect method, using the data on the radiation output of the X-ray tubes and exposure factors (kVp and mAs). The detector was placed at a one-meter focus detector distance on the top of the table at 80 kVp setting. For minimizing the influence of the heel effect, the detector should be placed as close to the central axis as possible. The Focus Film Distance (FFD) and radiographic exposure factors (kVp and mAs) used for X-ray examinations were recorded on a self-designed questionnaire sheet. Datasheets were collected on a weekly basis, and the exposure factors recorded were cross-checked against actual practice with the radiographers who recorded exposure factors. The ESD was calculated in the present work via entering parameters which are focal to skin distance, FSD, mAs, and kV in mathematical Equation (1) used by Davies *et al.* (1997) [10].

$$ESD = O/P \times \left(\frac{100}{80}\right)^2 \times \left(\frac{100}{FSD}\right)^2 \times mAs \times BSF \quad (1)$$

where: O/P is the output in mGy/mAs of the X-ray tube at 80 KV at a distance 100 cm normalized to 10 mAs. BSF is backscatter factor for a particular examination at the required potential and was taken (IAEA, 2014) mAs. The Output

was measured using RAD-CHECK Plus ionization chamber, Nuclear Associates Division of Victoreen, Inc., USA with serial number 103008 and model 06-526.

3. Results

Ten routine types of X-ray examinations were studied: skull (AP), skull (PA), skull (LAT), chest (PA), cervical spine (AP), cervical spine (LAT), lumbar spine (AP), lumbar spine (LAT), pelvis (AP) and pelvis (LAT). The X-ray tube potential (kVp) and tube loadings (mAs) selected for the adult patients focused on skin distance are presented in **Table 1**. The distributions of the mean values of ESD for patient exposures for individual patient's exposures for the ten projections are shown as in **Table 2**.

Table 1. Mean X-ray exposure parameters for each projection.

Examination	Projection	kVp	mAs	Field Size, cm ²	FSD, cm
Skull (AP)	PA	59	20	24 × 30	85
Skull (PA)	AP	58	20	24 × 30	95
Chest (PA)	AP	62	20	24 × 30	80
Chest (AP)	PA	60	20	24 × 30	180
Cervical Spine (AP)	AP	61	10	24 × 30	85
Cervical Spine (LAT)	LAT	61	10	24 × 30	107
Lumbar Spine (AP)	AP	91	20	14 × 17	76
Lumbar Spine (LAT)	LAT	85	20	14 × 17	71
Pelvis (AP)	AP	74	10	14 × 17	74
Pelvis (LAT)	LAT	85	20	14 × 17	75

Table 2. The ESD (mGy) for adult patients and comparison with America College of Radiology, 2018 [11] (ACR, 2018), and International Atomic Energy Agency, 2001 [12] (IAEA, 2001).

Protocol	Current Study	ACR, 2018	IAEA, 2001
Skull (AP)	0.73		5
Skull (PA)	0.75		5
Chest (PA)	0.17	0.15	0.4
Chest (AP)	0.60	0.15	0.3
Cervical Spine (AP)	0.43		5
Cervical Spine LAT	0.24		10
Lumbar Spine (AP)	2.11	6	10
Cervical Spine (LAT)	2.56	15	10
Pelvis (AP)	1.50	3.4	10
Pelvis (LAT)	0.72	3.4	5

The mean entrance skin dose for the skull (AP), skull (PA), skull (LAT), cervical spine (PA), cervical spine (LAT), lumbar spine (AP), lumbar spine (LAT), pelvis (AP) and pelvis (LAT) of adult X-ray examinations were within the diagnostic reference dose level values obtained by ACR (2018). The good results given by Radiology Unit would be due to the regular monitoring that the radiology department receives except the ESD for chest (AP) which was 0.88 mGy that higher than the diagnostic reference levels.

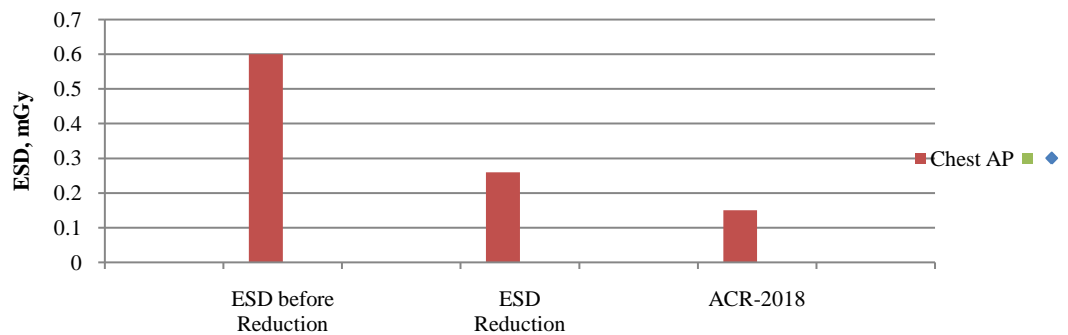
Dose minimization to chest AP (adult) compartment during X-ray imaging

Dose reduction to chest X-ray examinations was carried out via increasing kVp by 15% and decreasing mAs by 50%. The indirect entrance skin dose is measured using the mathematical model as presented in Equation (1). The ESD for the chest X-ray examinations was reduced to 58% as shown in **Table 3** and **Figure 1**. As the entrance skin dose to chest-AP decreases the effective dose the corresponding radiation risk will decrease too.

X-ray acquisition parameters for chest AP for adults were reviewed to optimize diagnostic reference dose levels. The mean dose reduction to the chest was 58% because of increasing high kVp by 15% and decreasing mAs by 50% without compromising the image quality. It is expected to enhance image quality with Digital Radiography (DR). Thus, the use of DR is associated with lower patient exposures because of very low imaging failure rates. The recommendation to avoid unnecessary radiation exposure is to apply the digital radiography to obtain image quality.

Table 3. ESD for chest and pelvic examinations before and after optimization.

Examination	Before Optimization			After Optimization			Dose Reduction
	Group A			Group B			
	kV	mAs	ESD (mGy)	kV	mAs	ESD (mGy)	
Chest (AP)	62	20	0.88	65	6	0.26	58



The ESD for Chest (AP) before and after Dose Optimization and Comparison with American College of Radiology , 2018

Figure 1. The ESD for chest (AP) before and after dose optimization.

4. Discussions

It can be seen in **Table 1** that the tube voltage used for different X-ray examinations varied with respect to the type of X-ray examination. The European Commission recommended the use of tube voltage values of 100 to 120 kVp for adults. In the current study, the tube voltage used for skull was 58 to 50 kVp and 20 mAs; for chest was ranged from 60 to 62 and 20 mAs; for cervical spine (AP) was 61 kVp and 10 mAs; for cervical spine (LAT) was 61 kVp and 10 mAs; for lumbar spine (AP) was 91 kVp and 20 mAs; for lumbar spine (LAT) was 85 kVp and 20 mAs; for pelvis (AP) was 74 kVp and 10 mAs and for pelvis (LAT) was 85 kVp and 10 mAs [13]. Most X-ray conventional radiography was within the operating conditions of the kilo-voltage settings. The selected tube voltage for chest was lower than that reported by Akhdar (2007) by 62 kVp [14]. The tube loading (mAs) used in combination with tube voltage for different X-ray examinations are presented in **Table 1**. The range of mAs used for most X-ray examinations performed on patients was from 10 to 20 mAs. Generally, it can be observed that the exposure factors used for patients in the present study comprised of high voltage (58 to 85 kVp) and low mAs (10 to 20 mAs) similar to values reported by Akhdar (2007) [14] for all protocols and they were higher than value for chest AP protocol by 55 Kvp. In case of the current Pelvic-AP radiography imaging, 85 kVp is a fact so better use where photoelectric absorption is directly proportional with cube of atomic number and inversely proportional with triple of energy. Bones absorb more radiation because they contain a high amount of calcium [3]. As mentioned by many authors who stated that the absorbed dose in skin is directly proportional to tube current, the length of exposure time, and the square of peak kilovoltage [12] Cervical Spine. **Table 2** presents the mean entrance skin dose for the skull, cervical spine (AP/LAT), lumbar spine (AP/LAT) and pelvic (AP/LAT) of adult X-ray examinations were within the diagnostic reference dose level of IAEA (2001) and ACR (2018) except the ESD for chest which was 1.44 mGy (higher than the diagnostic reference levels). The ESD (mGy) for chest (PA) was higher than (ACR, 2018) by 13.33% and lower than that reported by the IAEA (2001) by 57.5%. The ESD (mGy) for chest (AP) was higher than ACR (2018) by 75% and higher than that reported by the IAEA, (2001) by 50%. Image quality is automatically controlled because the use of X-ray machine has an option of digital imaging and reduces the dose as a function of Automatic Exposure Control (AEC). It can be seen in **Table 2** that the ESD (mGy) for the AP skull was lower than reported by IAEA (2001) [12]. The ESD (mGy) for AP pelvic half that value recorded by the American College of Radiology, 2018 [11]. The measurement of the ESD for patients in the Radiology Department of the NRC was lower than the value of the international organizations except for chest (AP). It is expected to enhance image quality with digital radiography, and DR. Thus, the use of the DR is associated with lower patient exposures because of very low imaging failure rates. The recommendations to avoid unnecessary radiation exposure are could be implemented by applying digital radiography to obtain im-

age quality.

5. Conclusion

The current research focuses on generating skin dose baselines for diagnostic X-ray machines. The indirect entrance skin dose associated with X-ray examinations does not exceed that recommended by IAEA and ACR. The mentioned method for dose estimation can predict the ESD before X-ray imaging. The study concluded that by adjusting applied tube voltage, kV, and tube current product time, mAs the radiation doses to the chest X-ray was decreased by 58% and a high image quality could be obtained using digital radiography.

Conflicts of Interest

The authors declare no conflicts of interest regarding the publication of this paper.

References

- [1] Vañó, E., Miller, D.L., Martin, C.J., Rehani, M.M., Kang, K., Rosenstein, M., Ortiz-López, P., Mattsson, S., Padovani, R. and Rogers, A. (2017) ICRP Publication 135: Diagnostic Reference Levels in Medical Imaging. *Annals of the ICRP*, **46**, 1-144. <https://doi.org/10.1177/0146645317717209>
- [2] Cameron, J.R. and Skofronick, J.G. (1978) *Medical Physics*. 2nd Edition, John Wiley & Sons, Inc., Hoboken.
- [3] Ofori, K., Gordon, S.W., Akrobortu, E., Ampene, A.A. and Darko, E.O. (2014) Estimation of Adult Patient Doses for Selected X-Ray Diagnostic Examinations. *Journal of Radiation Research and Applied Sciences*, **7**, 459-462. <https://doi.org/10.1016/j.jrras.2014.08.003>
- [4] Mor, H.B., Altinsoy, N. and Söyler, I. (2018) Estimation of Adult Patient Doses for Chest X-Ray Examination and Comparison with Diagnostic Reference Levels (DRLs). *Radiation Protection Dosimetry*, **182**, 377-385. <https://doi.org/10.1093/rpd/ncy076>
- [5] Alghoul, A., Abdalla, M.M. and Abubaker, H.M. (2017) Mathematical Evaluation of Entrance Surface Dose (ESD) for Patients Examined by Diagnostic X-Rays. *Open Access Journal of Science*, **1**, 8-11. <https://doi.org/10.15406/oajs.2017.01.00003>
- [6] Mohamadain, K.E.M. and Ibrahim, S.M. (2013) Evaluation of X-Ray Doses on Children, from Paediatric Hospitals in Sudan. *Open Journal of Radiology*, **3**, 169-173. <https://doi.org/10.4236/ojrad.2013.34028>
- [7] Komarskiy, A.A., *et al.* (2014) Reducing Radiation Dose by Using Pulse X-Ray Apparatus. *Journal of Biosciences and Medicines*, **2**, 17-21. <https://doi.org/10.4236/jbm.2014.22003>
- [8] Njiki, C.D., Ebele Yigbedeck, Y.H., Ndjaka Manyol, J.E.M. and Ndzana Ndah, T. (2019) Comparison between Predicted and Measured X-Ray Output in Some Conventional Radiography Units. *International Journal of Medical Physics, Clinical Engineering and Radiation Oncology*, **8**, 204-210. <https://doi.org/10.4236/ijmpcero.2019.84018>
- [9] Bope Kwete, M.B., Pembi, F., Ngoyi, K.N., Muanyim, B.P., Byeka, M.D., Milambo, K.P., Mbulu, B.S., Munanga, L.A. and Kafinga, L.E. (2022) Knowledge and Practices of Health Professionals on the Optimization of Radiation Protection in Diagnostic

Radiology in Children and Adults in the General Referral Hospitals of Bukavu in South Kivu, DRC. *Journal of Biosciences and Medicines*, **10**, 97-113.

<https://doi.org/10.4236/jbm.2022.107008>

- [10] Davies, M., McCallum, H., White, G., Brown, J. and Hlem, M. (1997) Patient Dose Audit in Diagnostic Radiography Using Custom-Designed Software. *Radiography*, **3**, 17-25. [https://doi.org/10.1016/S1078-8174\(97\)80021-1](https://doi.org/10.1016/S1078-8174(97)80021-1)
- [11] American College of Radiology (ACR) (2018) General Diagnostic Radiology Practice Parameter. <https://www.acr.org/>
- [12] International Atomic Energy Agency (IAEA) (2001) Radiological Protection of Patients in Diagnostic and Interventional Radiology, Nuclear Medicine and Radiotherapy. IAEA, Vienna.
- [13] European Commission (1996) European Guidelines on Quality Criteria for Diagnostic Radiographic Images. EUR 16260EN. Office for Official Publications of the European Communities, Luxembourg.
- [14] Akhdar, H.F. (2007) Assessment of Entrance Skin Dose and Effective Dose of Some Routine X-Ray Examinations Using Calculation Technique. MSc. Thesis, King Saud University, Riyadh.

A Validated Model for the Imaging Diagnosis of Cystic Lung Disease

Wallace T. Miller¹, Karen C. Patterson^{2,3}, Shweta Sood², James E. Schmitt⁴, Arshad A. Wani², Robert Borden⁵, Maya Galperin-Aisenberg⁴, Mary K. Porteus², Michelle L. Hershman⁴, Michael Hewitt⁴, Jennifer Levy⁴, Victor D. Babatunde⁴, Tetiana Glushko⁶, Timothy J. Niesen⁴, Sergey Leshchinskiy⁴, Karine Sahakyan⁷, Keyur Desai⁴, Jennifer A. Gillman⁴, Sandeep Reddy⁴, Michael Shriver⁴, Nathaniel B. Linna⁴, Abass M. Noor⁴, Aysenur Buz⁸, Matthew E. Biron⁴, Scott Simpson⁴

¹Department of Radiology, University of Botswana, Gaborone, Botswana

²Department of Medicine, Perelman School of Medicine, University of Pennsylvania, Philadelphia, USA

³Brighton and Sussex Medical School, Brighton, England

⁴Department of Radiology, Perelman School of Medicine, University of Pennsylvania, Philadelphia, USA

⁵Department of Radiologic Sciences, Drexel University College of Medicine, Philadelphia, USA

⁶Department of Radiology, Mercy Catholic Medical Center, Philadelphia, USA

⁷Department of Diagnostic Imaging, School of Alpert Medical, Brown University, Providence, USA

⁸Department of Radiology, Goztepe Research and Training Hospital, Istanbul Medeniyet University, Istanbul, Türkiye

Email: millerw@ub.ac.bw

How to cite this paper: Miller, W.T., Patterson, K.C., Sood, S., Schmitt, J.E., Wani, A.A., Borden, R., Galperin-Aisenberg, M., Porteus, M.K., Hershman, M.L., Hewitt, M., Levy, J., Babatunde, V.D., Glushko, T., Niesen, T.J., Leshchinskiy, S., Sahakyan, K., Desai, K., Gillman, J.A., Reddy, S., Shriver, M., Linna, N.B., Noor, A.M., Buz, A., Biron, M.E. and Simpson, S. (2023) A Validated Model for the Imaging Diagnosis of Cystic Lung Disease. *Open Journal of Radiology*, 13, 42-57. <https://doi.org/10.4236/ojrad.2023.131005>

Received: December 25, 2022

Accepted: March 4, 2023

Published: March 7, 2023

Copyright © 2023 by author(s) and Scientific Research Publishing Inc. This work is licensed under the Creative Commons Attribution International License (CC BY 4.0). <http://creativecommons.org/licenses/by/4.0/>



Open Access

Abstract

Rationale and Objectives: Cystic lung disease may be accurately diagnosed by imaging interpretation of specialist radiologists, without other information. We hypothesized that with minimal training non-specialists could perform similarly to specialist physicians in the diagnosis of cystic lung disease. **Methods:** 72 cystic lung disease cases and 25 cystic lung disease mimics were obtained from three sources: 1) a prospective acquired diffuse lung disease registry, 2) a retrospective search of medical records and 3) teaching files. Cases were anonymized, randomized and interpreted by 7 diffuse lung disease specialists and 15 non-specialist radiologists and pulmonologists. Clinical information other than age and sex was not provided. Prior to interpretation, non-specialists viewed a short PDF training document explaining cystic lung disease interpretation. **Results:** Correct first choice diagnosis of 85% - 88% may be achieved by high-performing specialist readers and 71% - 80% by non-specialists and lower-performing specialists, with mean accuracies in the diagnosis of LAM (91%, $p < 0.0001$), BHD (93%, $p < 0.0001$), PLCH (89%, $p < 0.0001$) and LIP (92%, $p < 0.0001$). A strategy based on cyst appearance: simple cysts (LAM), peri-septal cysts (BHD), bizarre-shaped cysts (PLCH) and vascular indented cysts (LIP) gave non-specialists accuracies of 90% ($p < 0.0001$), 94% ($p < 0.0001$),

92% ($p < 0.0001$) and 88% ($p < 0.0001$), respectively, for these diagnoses. Cystic lung abnormalities caused by diseases other than LAM, BHD, PLCH and LIP are rarely accurately diagnosed by imaging alone. **Conclusion:** With specific but limited training, non-specialist physicians can diagnose cystic lung diseases from CT appearance alone with similar accuracy to specialists, correctly identifying approximately 75% of cases.

Keywords

Lymphangiomyomatosis, Histiocytosis, Langerhans-Cell, Idiopathic Interstitial Pneumonias, Birt-Hogg-Dube Syndrome, Lung Diseases, Interstitial, Diagnoses, Differential

1. Introduction

Widespread cystic lung disease is an uncommon imaging finding that may be clinically irrelevant or cause significant morbidity and mortality. Pulmonary cysts appear as low-attenuation regions with a surrounding wall and are often round or oval in shape, but other appearances may occur [1].

The most common causes of cystic lung disease are Lymphangiomyomatosis (LAM), Langerhans Cell Histiocytosis (PLCH), Birt-Hogg-Dube (BHD) syndrome and Lymphocytic Interstitial Pneumonia (LIP) [2] [3] [4] [5] [6]. Other causes include metastases, amyloidosis, neurofibromatosis, light-chain deposition disease, pneumocystis pneumonia, hypersensitivity pneumonitis, pulmonary interstitial glycogenosis and nonspecific interstitial pneumonia [2]-[12].

Most diffuse parenchymal lung diseases require clinical information to establish a diagnosis. However, the imaging appearance of cystic lung diseases is often diagnostic, even without clinical information [3] [13] [14]. Prior studies indicate that experts may be highly accurate in the diagnosis of cystic lung disease based on imaging appearance alone [2] [13]. Previous studies have suggested that pulmonologists and trainees perform less well than chest radiologists [2]. Our hypothesis was that limited training with a simple strategy based on cyst appearance would allow non-specialists to achieve similar accuracy to experts in the diagnosis of cystic lung disease.

2. Materials and Methods

The authors have no conflict of interest, the study is IRB-approved (IRB# 820774) and HIPA compliant. Informed consent was waived by the IRB. We acquired all cases of cystic lung disease available from a single medical center, from three sources: 1) our institution prospectively acquired diffuse lung disease registry, 2) a retrospective search of medical records, and 3) teaching files.

Our institution began a diffuse lung disease registry in January 2013. To be entered into the registry, cases were evaluated jointly by two pulmonologists, a thoracic radiologist and a pulmonary pathologist and classified by cause and confi-

dence in the diagnosis. Thirty-nine cases with moderate or high confidence diagnosis of cystic lung disease were included in this study (**Figure 1**).

Our radiology information system database was searched using a commercially available search engine (MONTAGE™ Search and Analytics, Nuance mPower Clinical Analytics, Nuance Communications, Inc.) from 2012-2018 for 5 thoracic CT exam codes and the following search terms: “lymphangiomyomatosis”, “LAM”, “Langerhans cell histiocytosis”, “PLCH”, “eosinophilic granuloma”, “Birt-Hogg-Dube”, “Birt Hogg Dube”, “lymphocytic interstitial pneumonia”, “LIP” and “cystic PCP”. The time frame was chosen to match that of the ILD registry resulting in 270 cases.

CT reports and a limited evaluation of medical records separated cases into those likely or unlikely to meet criteria for a diagnosis of cystic lung disease. Causes for exclusion at this stage included, 1) no evaluation by a pulmonologist (n = 118), 2) duplicate cases (n = 27), 3) other lung disease diagnosed (n = 18), 4) a history of disease without imaging findings (n = 9), 5) superimposed lung disease (n = 6). Cases without a pulmonologist evaluation were excluded because analysis showed these cases were unlikely to have sufficient documentation to prove a diagnosis. Each “likely case” received an extensive review of medical records by two individuals independently, a chest radiologist and pulmonologist specializing in diffuse lung disease to determine if the case met criteria for a diagnosis of a cystic lung disease (LAM and LIP: American Thoracic Society guidelines [14] [15], PLCH: guidelines by Girschikofsky [16], BHD: guidelines by Menko [17]). Both reviewers had to agree on a diagnosis for study inclusion, adding 31 cases to the study. Teaching file case diagnoses were also confirmed by agreement following independent review of the medical record by both reviewers, adding 27 cases to the study (**Figure 1**).

The database was augmented with cases of emphysema, cystic bronchiectasis and honeycombing that might be confused with cystic lung disease. Proof of diagnosis followed the same protocol as the cystic lung diseases, but cases were selected for a high likelihood of confusion with cystic lung disease.

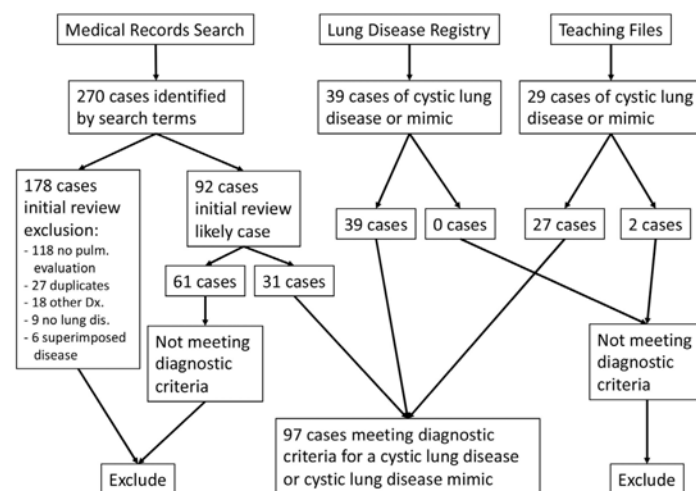


Figure 1. Source of cases for the cystic lung disease database.

Searches yielded a total of 72 cystic lung disease cases and 25 cystic mimics.

2.1. Reviewers

Cases were anonymized, randomized and blindly reviewed by 22 individuals of varying experience for the diagnosis of cystic lung disease. Reviewers were recruited from several medical centers in our metropolitan area. Seven reviewers were specialists in thoracic imaging or pulmonologists specializing in diffuse lung diseases. The remaining reviewers were non-specialist radiologists or pulmonologists. The reviewers had not previously been exposed to the any cases used in the study.

2.2. Training Algorithm

Two separate training documents were created and tested. A PDF document of 12 PowerPoint slides, which is a synopsis of the experience of the first author, a radiologist with 24 years of subspecialty experience, outlined a method with imaging examples, for distinguishing cystic lung diseases. The algorithm is similar to one independently proposed by another group [3] and is follows a pattern typically used by chest radiologists. The critical points of the document are as follows:

- 1) True cysts must be distinguished from honeycombing, emphysema, and cystic bronchiectasis.
- 2) Most common cystic lung diseases are: LAM, PLCH, BHD and LIP.
- 3) Simple cysts have round or oval shape and a thin wall.
- 4) Number of cysts may be helpful in the diagnosis. High profusion simple cysts (defined as ≥ 100) (**Figure 2**) is usually LAM. A low profusion of simple cysts (defined as < 50) is usually BHD or LIP.
- 5) Appearance of BHD cysts may be peri-septal or peri-pleural and lenticular in shape (**Figure 3**).



Figure 2. Simple cysts. This 29-year-old woman had a history of tuberous sclerosis and multiple spontaneous pneumothoraxes. The CT exam shows a high profusion of round or oval, thin walled (simple) cysts.

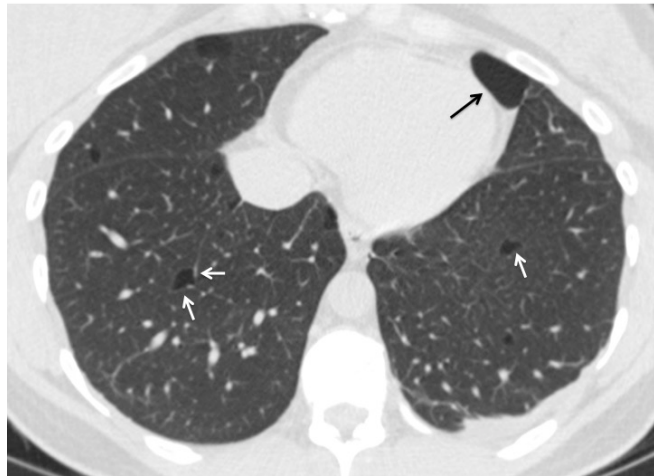


Figure 3. Birt-Hogg-Dube (BHD) type cysts. This 33-year-old woman presented with a spontaneous pneumothorax. Two lower lobe cysts have a vague lenticular shape. This is because sides of the cysts are created by borders of secondary pulmonary lobules (white arrows). These peri-septal cysts are typical of BHD. There is also a larger cyst adjacent to the pleura (peri-pleural) (black arrow). Evaluation of performance after Round 1, suggested that this feature introduced diagnostic error in the diagnosis of BHD and was excluded as a criterion in the second teaching document.

6) Appearance of PLCH cyst may be irregularly or bizarrely shaped and/or thick walled (**Figure 4**).

Analysis of results of the first round of cases showed deficiencies in the training document and a second training document was created, with five principal changes: 1) Cyst counting was discarded and LAM was recommended as first choice diagnosis of all simple cysts in women and PLCH as first diagnosis in men, 2) BHD-type cysts were defined as peri-septal (removing peri-pleural from the criteria), 3) PLCH-type cysts were defined as irregularly or bizarrely shaped (removing thick walled as a criterion), 4) cheerio-type cysts (small thick walled cysts) were explained to be caused by a variety of diseases, usually PLCH and metastasis in approximately equal frequency (**Figure 5**), 5) LIP-type cysts were defined as those containing vascular indentations or septations (**Figure 6**).

2.3. Image Review

Images were viewed using a DICOM imaging database (Horus, 2019 Horus project, <https://horosproject.org/>) on each reader's personal computer. Horus allows for scrollable images, window/level conversion and coronal and axial reconstructions. Reviewers were blinded to clinical information, except age and sex. Reviewers were aware that the database contained a variety of cystic lung diseases and cystic mimics but were unaware of the relative frequencies within the database.

Specialists reviewed the cases without other input. In Round 1, 8 non-specialist

reviewers were given the first training document prior to case interpretation. In Round 2, non-specialists numbers 2 and 5 reviewed the second training document and re-evaluated cases for the diagnosis of disease an average of 4 months after the previous interpretation session. An additional 7 new non-specialists were given the second training document prior to evaluation of cases.

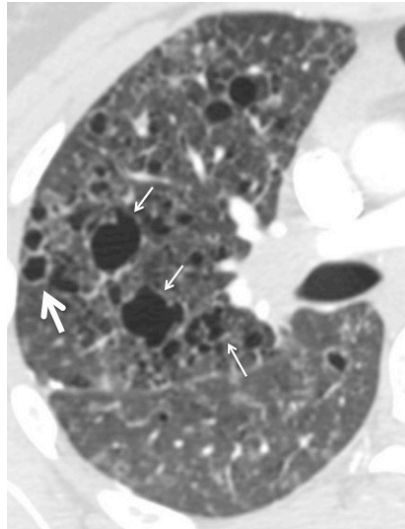


Figure 4. Langerhans Cell Histiocytosis (PLCH) type cysts. This 23-year-old woman had a 10-pack year smoking history. Small arrows demonstrate irregularly, bizarrely shaped cysts, these are characteristic of PLCH and usually indicate a diagnosis of PLCH. The large arrow shows a thick-walled cyst that can be seen in PLCH but is not specific.

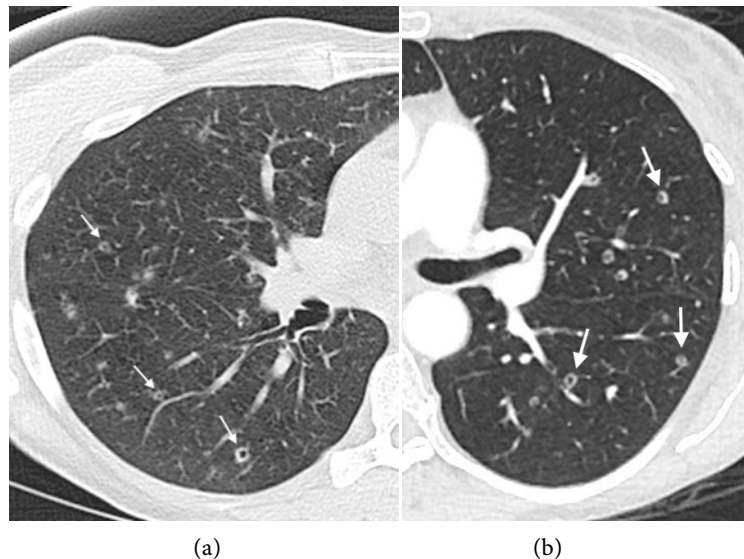


Figure 5. Cheerio type cysts in LCH and metastasis. (a) This 54-year-old woman had a chronic cough. The CT image shows several small thick-walled cysts proven to be due to LCH. (b) This 54-year-old woman had a history of colon cancer. The CT image shows several thick-walled cysts due to metastasis.



Figure 6. Lymphocytic Interstitial Pneumonia (LIP) type cysts. This 56-year-old woman had a history of Sjogren syndrome. There are three cysts where the wall is indented by blood vessels (small arrows). One also has a thin septation (large arrow). These features often indicate a diagnosis of LIP.

Reviewers were asked to provide the 1st, 2nd and 3rd most likely diagnoses for each case to simulate a typical differential diagnosis given in radiology reports. Answers were selected from a drop-down menu: LAM, PLCH, BHD, LIP, honeycombing, bronchiectasis, emphysema and other diagnosis. If “other diagnosis” was selected, an additional free text box was supplied. Non-specialist reviewers in Round 1 were asked to provide the cyst character and cyst number from specified lists. Cyst character choices were: 1) true cyst: thin wall round or oval, 2) true cyst: thick wall and/or bizarre shape, 3) true cyst: lenticular, subpleural and/or peri-septal, 4) true cyst: other, 5) honeycombing, 6) emphysema, 7) cystic bronchiectasis. Cyst number choices: 1) ≥ 100 , 2) < 50 , 3) 51 - 99, 4) < 5 , and 5) Not applicable. Reviewers in Round 2 were asked to evaluate for cyst character with choices: 1) Simple-type, 2) BHD-type, 3) PLCH-type, 4) LIP type, 5) cheerio-type, 6) other.

2.4. Statistical Evaluation

Data were imported into the R statistical environment for analyses [18]. Basic statistical tabulations were made to count the number of correct diagnoses for each rater. Diagnostic performance was assessed for each rater by calculating sensitivity, specificity Positive Predictive Value (PPV), Negative Predictive Value (NPV), and accuracy for each diagnosis separately (*i.e.* LAM, LCH, LIP, BHD, Mimics). Total accuracy (*i.e.* irrespective of specific diagnoses) was also assessed. For each rater, Receiver Operating Characteristic (ROC) curves were generated for each diagnosis, and the Area under the Curve (AUC) was estimated. In addition to individual measures, group estimates (e.g. pulmonary specialists as a whole) were estimated based on group means. 95% confidence intervals for proportions were estimated based on the formula:

$$\hat{p} \pm z^* \sqrt{\frac{\hat{p} * (1 - \hat{p})}{N}}$$

where \hat{p} represents the proportion, N the sample size, and $z = 1.96$. Categorical variables were also evaluated for statistical significance with two-tailed Fisher's exact tests.

3. Results

3.1. Characteristics of the Database

The patients' age ranged from 20 to 86 years with both mean and median ages of 48 years. Women accounted for 71/97, 73% of patients. The causes, frequency and source of cases are listed in **Table 1**.

3.2. Reader Performance

Table 2 lists the clinical experience of the reviewers and the fraction of correct 1st choice and 1st and 2nd choice diagnoses. Rad-specialists 1 and 2 performed better than all other readers with 1st diagnosis true positive rates of 87% and 82%, respectively. Utilizing the first teaching tool, two non-specialist readers, a 3rd year radiology resident and a general pulmonologist were able to outperform rad-specialists 3 and 4 and the two pulmonary specialists. Four additional non-specialists: a body imaging fellow, interventional radiologist, body imaging radiologist and a 2nd year radiology resident performed similarly to rad-specialists 4 and 5 and the two pulmonary specialists.

Using the second teaching tool, two non-specialists (general pulmonologist, body imaging radiologist) outperformed rad-specialists 3 and 4 and the two pulmonary specialists. Five other non-specialists (two 4th year radiology residents, one 3rd year radiology resident, and two 2nd year radiology residents) performed similarly to rad-specialists 4 and 5 and the two pulmonary specialists.

Table 3 shows the performance of readers for the correct first choice diagnosis of LAM, BHD, LIP, LCH and non-cystic lung disease respectively. Rad-specialists 1 and 2 achieved accuracies of greater than 94% for each of the five specific diagnoses. The accuracy of diagnosis was high, usually >80% for all readers individually. Of the 115 diagnostic accuracies measured (23 readers \times 5 categories), 86 (75%) were $\geq 90\%$ among both specialists and non-specialists. In general, across both rounds, the lowest performance measures for all diseases were the sensitivity and PPV.

Figure 7 shows the mean and standard deviation of the area under the ROC curve for each of the reader groups for each of the diseases, showing overlap in the performance of all readers. However, two rad-specialists, 1 and 2, did generally better than all other readers for all diseases. The performance of rad-specialists 3 and 4, the pulmonary specialists and the non-specialists for each diagnosis is nearly indistinguishable. LIP was the most problematic diagnosis with the lowest average area under the ROC curve and the greatest variance among all readers. The training algorithms in Round 1 and Round 2 performed similarly, with the exception of the diagnosis of LIP, where the second algorithm resulted in substantial improvement in diagnosis.

Table 1. Causes of cystic lung disease and cystic mimics.

Cystic Disease	DLD Registry*	MR Search^	Teaching File	Total
LAM	19	1	10	30
PLCH	4	5	4	13
BHD	2	13	1	16
LIP	2	5	0	7
Cystic Metastasis	0	0	3	3
Amyloidosis	0	0	1	1
Neurofibromatosis	0	1	0	1
Sarcoidosis	1	0	0	1
IPF	0	1	0	1
Total Cystic Disease	28	26	19	73
Cystic Mimics				
Emphysema	1	4	4	9
Honeycombing				
IPF	2	0	0	2
CTD	3	0	0	3
HP	1	0	1	2
Sarcoidosis	4	1	0	5
Cystic Bronchiectasis	0	0	3	3
Total Mimics	11	5	8	24
Grand Total	39	31	27	97

*Diffuse lung disease registry; ^Medical records search.

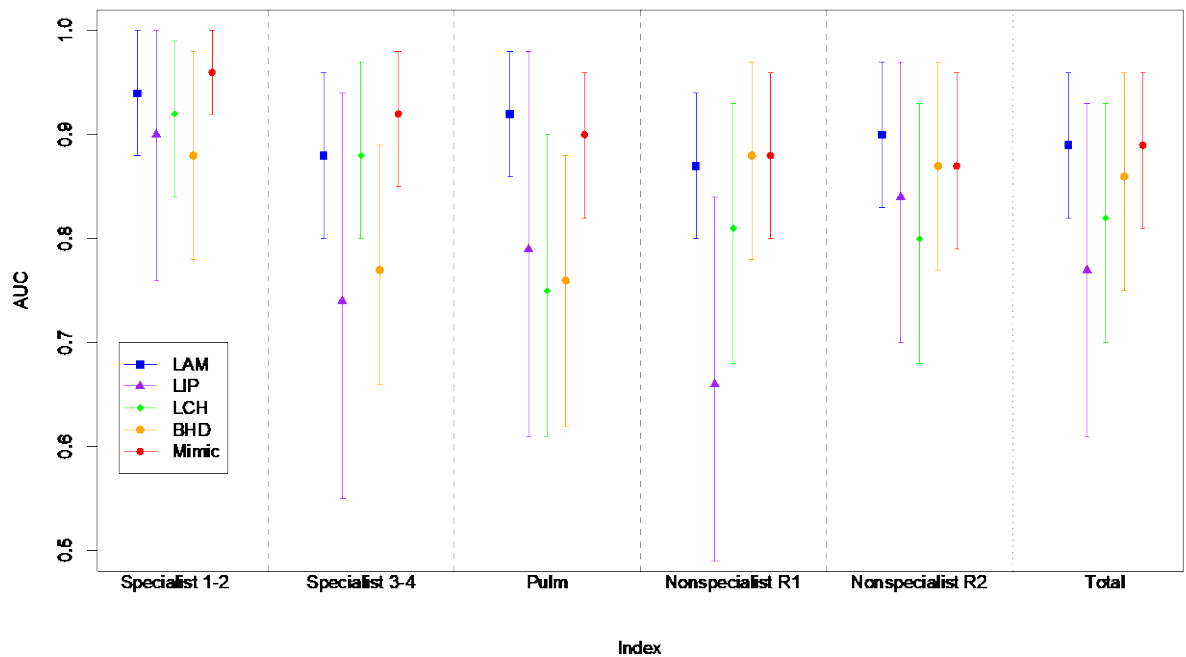


Figure 7. Areas under the ROC curve for reader type and clinical diagnosis. The figure shows the mean and standard deviation of the area under the ROC curve for each reader group and each diagnosis.

Table 2. Diagnostic accuracy of cystic lung disease diagnosis as a function of training.

Reader	Specialty	Years Practice	Pulm ILD+	Dx1 TP*	Dx1-2 TP^
Rad-specialist 1	Radiology (Thoracic)	5	5 yr	83 (86)	87 (91)
Rad-specialist 2	Radiology (Thoracic)	5	5 yr	79 (82)	81 (84)
Rad-specialist 3	Radiology (Thoracic)	8	4 yr	73 (75)	81 (84)
Rad-specialist 4	Radiology (Thoracic)	1	1 yr	67 (70)	78 (81)
Pulm-specialist 1	Pulmonology (DLD specialist)	7	7 yr	66 (69)	71 (74)
Pulm-specialist 2	Pulmonology (DLD specialist)	5	5 yr	68 (71)	74 (77)
<u>Round 1</u>					
Non-specialist 1	Radiology (3 rd Year Resident)	3	2 mo	78 (81)	80 (83)
Non-specialist 2	Pulmonology (General)	14	6 mo	73(76)	76 (79)
Non-specialist 3	Radiology (Body Imaging Fellow)	6	6 mo	69 (72)	77 (80)
Non-specialist 4	Radiology (Interventional)	6	4 mo	71 (74)	77 (79)
Non-specialist 5	Radiology (Body Imaging)	13	4 mo	69 (72)	74 (77)
Non-specialist 6	Radiology (2 nd Year Resident)	1.8	2 mo	67 (70)	75 (78)
Non-specialist 7	Radiology (1 st Year Resident)	0.8	1 mo	55 (58)	69 (72)
Non-specialist 8	Radiology (2 nd Year Resident)	1.8	3 mo	54 (57)	69 (72)
<u>Round 2</u>					
Non-specialist 2	Pulmonology (General)	14	6 mo	77 (80)	83 (87)
Non-specialist 5	Radiology (Body Imaging)	13	4 mo	79 (82)	86 (90)
Non-specialist 9	Radiology (4 th Year Resident)	3.3	3 mo	75 (78)	87 (91)
Non-specialist 10	Radiology (4 th Year Resident)	3.3	3 mo	72 (75)	76 (79)
Non-specialist 11	Radiology (3 rd Year Resident)	2.3	3 mo	72 (75)	73 (76)
Non-specialist 12	Radiology (2 nd Year Resident)	1.3	1 mo	73 (76)	87 (91)
Non-specialist 13	Radiology (2 nd Year Resident)	1.3	2 mo	69 (72)	82 (86)
Non-specialist 14	Radiology (2 nd Year Resident)	1.3	2 mo	64 (66)	75 (78)
Non-specialist 15	Radiology (1 st Year Resident)	0.3	1 mo	64 (67)	71 (74)

+Years of specialization in thoracic radiology (radiologists) or pulmonary diffuse infiltrative lung disease (pulmonologists) or months of specific training in thoracic radiology or diffuse infiltrative lung disease. *Frequency of 1st choice correct diagnosis (% correct in parentheses). ^Frequency that correct diagnosis was in the top 2 diagnoses (% correct in parentheses).

3.3. Rare Causes of Cystic Lung Disease

There were 7 cases of cystic disease (9.6%) that were not one of the four common causes: 3 cases of cystic metastases and one each of amyloidosis, neurofibromatosis, sarcoidosis and idiopathic pulmonary fibrosis. None of these, except for cystic metastasis, were correctly diagnosed by any reader. Correct diagnosis of cystic metastasis was made in 2/12 (17%) instances by rad-specialists. Non-specialists correctly diagnosed cystic metastasis in 0/24 instances in Round 1 and in 15/27 (55%) instances in Round 2 after specific training regarding cheerio type cysts was given in the second training document.

Table 3. Reader performance in the diagnosis of LAM, BHD, PLCH, LIP and cystic mimics.

Reader	Sensitivity	Specificity	PPV	NPV	Accuracy
Lymphangioleiomyomatosis (N = 30)					
Rad-specialists 1-2	90 (84 - 96)	99 (96 - 99)	97 (93 - 99)	96 (92 - 99)	96 (92 - 99)
Rad-specialists 3-4	80 (72 - 88)	96 (91 - 99)	89 (83 - 95)	91 (86 - 97)	91 (85 - 96)
Pulmonary Specialists	92 (86 - 97)	92 (86 - 97)	84 (77 - 91)	96 (92 - 99)	92 (86 - 97)
Round 1 Non-specialists	81 (73 - 89)	94 (89 - 99)	86 (79 - 93)	92 (86 - 97)	90 (84 - 96)
Round 2 Non-specialists	86 (79 - 93)	94 (89 - 98)	86 (79 - 93)	94 (89 - 99)	91 (86 - 97)
All Readers	84 (77 - 92)	94 (89 - 99)	87 (80 - 94)	93 (88 - 98)	91 (85 - 97)
Birt Hogg Dube Syndrome (N = 16)					
Rad-specialists 1-2	78 (70 - 86)	99 (97 - 99)	94 (89 - 99)	96 (92 - 99)	95 (91 - 99)
Rad-specialists 3-4	56 (46 - 66)	98 (95 - 99)	90 (84 - 96)	92 (87 - 97)	91 (86 - 97)
Pulmonary Specialists	56 (46 - 66)	94 (90 - 99)	68 (58 - 77)	92 (86 - 97)	88 (82 - 95)
Round 1 Non-specialists	81 (73 - 89)	94 (89 - 99)	73 (64 - 82)	96 (92 - 99)	92 (86 - 97)
Round 2 Non-specialists	77 (69 - 85)	97 (94 - 99)	86 (79 - 93)	96 (91 - 99)	94 (89 - 99)
All Readers	75 (66 - 84)	96 (92 - 99)	81 (73 - 89)	95 (91 - 99)	93 (87 - 98)
Langerhans Cell Histiocytosis (N = 13)					
Rad-specialists 1-2	88 (82 - 95)	95 (91 - 99)	76 (67 - 84)	98 (96 - 99)	94 (90 - 99)
Rad-specialists 3-4	85 (77 - 92)	92 (87 - 98)	68 (59 - 77)	98 (95 - 99)	91 (86 - 97)
Pulmonary Specialists	58 (48 - 68)	92 (87 - 98)	54 (44 - 64)	93 (88 - 98)	88 (81 - 94)
Round 1 Non-specialists	75 (66 - 84)	86 (79 - 93)	47 (37 - 57)	96 (92 - 99)	85 (78 - 92)
Round 2 Non-specialists	68 (59 - 78)	92 (87 - 97)	59 (49 - 69)	95 (91 - 99)	89 (83 - 95)
All Readers	73 (64 - 82)	90 (85 - 96)	57 (47 - 67)	96 (92 - 99)	88 (82 - 94)
Lymphocytic Interstitial Pneumonia (N = 7)					
Rad-specialists 1 - 2	86 (79 - 93)	95 (91 - 99)	61 (51 - 70)	99 (97 - 99)	94 (90 - 99)
Rad-specialists 3 - 4	57 (47 - 67)	92 (87 - 98)	51 (41 - 61)	97 (93 - 99)	90 (84 - 96)
Pulmonary Specialists	64 (55 - 74)	96 (91 - 99)	56 (46 - 66)	97 (94 - 99)	93 (88 - 98)
Round 1 Non-specialists	36 (26 - 45)	97 (94 - 99)	56 (46 - 65)	95 (91 - 99)	93 (88 - 98)
Round 2 Non-specialists	76 (68 - 85)	93 (88 - 98)	47 (37 - 57)	98 (95 - 99)	92 (86 - 97)
All Readers	60 (51 - 70)	95 (90 - 99)	52 (42 - 62)	97 (93 - 99)	92 (87 - 98)
Cystic Lung Disease Mimics (N = 24)					
Rad-specialists 1 - 2	96 (92 - 99)	97 (93 - 99)	91 (85 - 97)	99 (96 - 99)	96 (93 - 99)
Rad-specialists 3 - 4	90 (84 - 96)	94 (89 - 99)	83 (76 - 92)	96 (93 - 99)	93 (88 - 98)
Pulmonary Specialists	84 (77 - 91)	94 (90 - 99)	85 (78 - 92)	95 (90 - 99)	92 (86 - 97)
Round 1 Non-specialists	80 (71 - 88)	96 (92 - 99)	88 (81 - 94)	93 (88 - 98)	92 (86 - 97)
Round 2 Non-specialists	77 (69 - 86)	97 (94 - 99)	92 (86 - 97)	93 (87 - 98)	92 (87 - 98)
All Readers	81 (74 - 89)	96 (92 - 99)	89 (83 - 95)	94 (89 - 99)	92 (87 - 98)

Table 4. Performance of cyst characteristics in diagnosing cystic lung diseases by non-specialists.

Cyst Type	Sensitivity	Specificity	PPV	NPV	Accuracy
Simple Cyst (LAM)					
Non-specialists	88 (83 - 91)	91 (89 - 93)	83 (78 - 96)	94 (92 - 96)	90 (88 - 92)
Simple Cyst + Female* (LAM)					
Non-specialists	91 (86 - 94)	94 (91 - 95)	86 (82 - 89)	96 (94 - 97)	92 (91 - 94)
BHD-type					
Non-specialists	76 (68 - 82)	98 (96 - 99)	86 (80 - 91)	95 (94 - 96)	94 (92 - 96)
LIP-type					
Non-specialists	73 (60 - 83)	93 (91 - 95)	45 (38 - 52)	98 (97 - 99)	92 (89 - 93)
PLCH-type					
Non-specialists	38 (30 - 48)	96 (94 - 97)	59 (49 - 69)	91 (90 - 92)	88 (86 - 90)

*If both simple cyst and female as criteria for Dx of LAM

3.4. Causes of Misdiagnosis

There was a subset of cases that accounted for the majority of the remaining diagnostic errors. For 22 cases (23%) in Round 1, $\leq 50\%$ of observers (0 - 7/14 observers) correctly diagnosed disease. For 22 cases (23%) in Round 2, $\leq 55\%$ of observers (0 - 5/9 observers) correctly diagnosed disease. Seven cases were the uncommon cystic diseases discussed previously and two were cases where superimposed emphysema confused the case. The majority of misdiagnosed cases were confined to a small number of the common causes of cystic lung disease: LAM, PLCH, BHD and LIP (5 LIP, 3 LAM, 2 BHD and 2 PLCH in Round 1 and 4 BHD, 3 LAM, 3 PLCH, 1 LIP and 4 cystic mimics in Round 2).

3.5. Evaluation of Diagnostic Strategies

We employed two different teaching strategies. Round 1 used a combination of cyst characteristics and cyst number to inform a diagnosis similar to current conventional teaching strategies. Round 2 relied exclusively on the recognition of five cyst types: 1) simple-type, 2) BHD-type, 3) PLCH-type, 4) LIP-type and 5) cheerio-type. Strategy 2 slightly outperformed strategy 1, predominantly because of improved diagnosis of LIP. Two individuals, non-specialists 2 and 5 were involved in both rounds of testing and both improved with the second strategy.

The performance characteristics of the various cyst types for their respective diseases are listed in **Table 4**. In general, the cyst types are moderately to highly specific for the disease with specificities from 91% - 100%. However, with the exception of simple cysts for the diagnosis of LAM, the sensitivity of cyst types was moderate to low.

4. Discussion

Our study and others [2] [3] [13] [19] indicate that cystic lung diseases can be accurately diagnosed based solely on imaging characteristics, with a correct first-choice

diagnosis of as high as 86% by the best-performing specialists. This accuracy is principally due to the diagnosis of the most common cystic lung diseases: LAM (combined accuracy 91%), BHD (combined accuracy of 93%), LIP (combined accuracy of 92%) and PLCH (combined accuracy of 88%). Previous reports have shown similar accuracy in the diagnosis of LAM and LIP but lesser accuracy in the diagnosis of PLCH [2].

Previous studies have suggested that pulmonologists and trainees perform less well than chest radiologists [2], a finding we also showed when comparing non-specialists with our highest-performing chest radiologists. However, we have demonstrated that with minimal training, non-specialist radiologists and pulmonologists can also have high performance with the correct first choice diagnosis of as high as 82% which is similar to some specialists.

We devised two training strategies, both of which helped non-specialist readers achieve moderate to high accuracy in the diagnosis of common cystic lung diseases. The second training strategy performed slightly better than the first. This second strategy is simpler and is based on the recognition of 4 cyst types: Simple-type, BHD-type, PLCH-type and LIP-type cysts that are moderate to highly predictive of LAM, BHD, PLCH and LIP respectively.

Misdiagnosis related to the cheerio sign, small thick-walled cysts, was an important cause of reduced accuracy, a finding that has not been noted by prior studies. This sign, which is commonly associated with PLCH, was therefore interpreted as PLCH by nearly all reviewers in Round 1. However, in our database, metastasis, another known cause of the cheerio sign [7] [15], accounted for half of the cases. In Round 2, the training document specifically noted that the cheerio sign could be caused by both metastasis and PLCH and suggested that lower predominant cheerio signs are likely metastasis and upper predominant cheerio signs are likely PLCH. This strategy reduced, by half, diagnostic errors of cheerio-type cysts. Other reported causes of the cheerio sign include, amyloidosis (present in our database) adenocarcinoma spectrum lesions, primary lung carcinoma, granulomatosis with polyangiitis, rheumatoid nodules and pulmonary meningotheelial-like nodules [20] [21]. If our database is representative of the general population, cheerio-type cysts are caused by metastasis and PLCH in approximately equal frequency.

To simulate clinical practice, we included lung diseases such as emphysema, cystic bronchiectasis and severe honeycombing that might be confused with cystic lung disease, a confounding factor that previous studies have not included [2] [3] [13] [19]. We have shown that readers can usually distinguish cystic lung diseases from mimics with a combined accuracy of 92%.

In our database, a significant fraction of diagnostic errors were due to rare causes of cystic lung disease including cystic metastases, amyloidosis, neurofibromatosis, sarcoidosis, and idiopathic pulmonary fibrosis. With the exception of cystic metastasis, none of these diagnoses were correctly diagnosed. Imaging alone is usually not adequate to diagnose these cases.

The majority of the remainder of diagnostic errors occurred in a small subset

of cases, 13 - 15 of 97 cases, or 13% - 15% in our database. This finding suggests that in most cases, approximately 85% - 87%, of LAM, BHD, PLCH and LIP produce cysts with the characteristic cyst features outlined in this report and can be identified by trained non-specialists. However, there are small subsets of LAM, BHD, PLCH and LIP that produce cysts that are not characteristic of the disease or for other reasons are easily misclassified.

Our study has strengths related to a large number of cases and large number and varied experiences of readers. In addition, our training algorithm is a teaching tool that can be readily and widely utilized in clinical practice. The principal limitation of the study is the source of the cases. Sixty percent of cases were obtained by retrospective review of the medical records or from teaching files. There is a possibility that biases regarding cyst appearance were introduced in this process. There were no normal exams and the relative frequency of cystic disease and cystic mimics was not controlled. This may have increased reader performance compared with the daily practice where cystic diseases are rarely seen and cystic mimics are more common. The low number of pulmonologists participating in the study is another limitation such that little can be deduced about differences in performance between radiologists and pulmonologists.

5. Conclusion

In conclusion, most cases of cystic lung diseases can be accurately diagnosed from their appearance on thin-section CT utilizing a novel strategy based on 5 cyst appearances: 1) Simple-type, 2) BHD-type, 3) PLCH-type, 4) LIP-type and 5) Cheerio-type. With limited training, non-specialist radiologists and non-specialist pulmonologists can perform as well or better than some diffuse lung disease specialists, although not as well as the highest-performing specialists.

Conflicts of Interest

The authors declare no conflicts of interest regarding the publication of this paper.

References

- [1] Hansell, D.M., Bankier, A.A., MacMahon, H., McLoud, T.C., Müller, N.L. and Remy, J. (2008) Fleischner Society: Glossary of Terms for Thoracic Imaging. *Radiology*, **246**, 697-722. <https://doi.org/10.1148/radiol.2462070712>
- [2] Gupta, N., Meraj, R., Tanase, D., *et al.* (2015) Accuracy of Chest High-Resolution Computed Tomography in Diagnosing Diffuse Cystic Lung Diseases. *European Respiratory Journal*, **46**, 1196-1199. <https://doi.org/10.1183/13993003.00570-2015>
- [3] Gupta, N., Vassallo, R., Wikenheiser-Brokamp, K.A. and McCormack, F.X. (2015) Diffuse Cystic Lung Disease. Part II. *American Journal of Respiratory and Critical Care Medicine*, **192**, 17-29. <https://doi.org/10.1164/rccm.201411-2096CI>
- [4] Trotman-Dickenson, B. (2014) Cystic Lung Disease: Achieving a Radiologic Diagnosis. *European Journal of Radiology*, **83**, 39-46. <https://doi.org/10.1016/j.ejrad.2013.11.027>

- [5] Xu, K.-F., Feng, R., Cui, H., *et al.* (2016) Diffuse Cystic Lung Diseases: Diagnostic Considerations. *Seminars in Respiratory and Critical Care Medicine*, **37**, 457-467. <https://doi.org/10.1055/s-0036-1580690>
- [6] Lee, J.E., Cha, Y.K., Kim, J.S. and Choi, J.H. (2017) Birt-Hogg-Dubé Syndrome: Characteristic CT Findings Differentiating It from Other Diffuse Cystic Lung Diseases. *Diagnostic and Interventional Radiology*, **23**, 354-359. <https://doi.org/10.5152/dir.2017.16606>
- [7] Zhang, J., Zhao, Y.-L., Ye, M.-X., *et al.* (2012) Rapidly Progressive Diffuse Cystic Lesions as a Radiological Hallmark of Lung Adenocarcinoma. *Journal of Thoracic Oncology*, **7**, 457-458. <https://doi.org/10.1097/JTO.0b013e31823c5a39>
- [8] Dumlu, T., Karapolat, B.S., Yıldırım, Ü., Güngör, A. and Aydın, L.Y. (2011) Medical Image. Bilateral Diffuse Cystic, Cavitory Lung Metastasis of Adenocarcinoma. *The New Zealand Medical Journal*, **124**, 93-95
- [9] Zamora, A.C., Collard, H.R., Wolters, P.J., Webb, W.R. and King, T.E. (2006) Neurofibromatosis-Associated Lung Disease: A Case Series and Literature Review. *European Respiratory Journal*, **29**, 210-214. <https://doi.org/10.1183/09031936.06.00044006>
- [10] Madhyastha, S.P., Gopalswamy, V., Reddy, C.T. and Acharya, R.V. (2017) Interesting Association of Neurofibroma with Diffuse Cystic Lung Disease (NF-DLD). *BMJ Case Reports*, **2017**, bcr2016217774. <https://doi.org/10.1136/bcr-2016-217774>
- [11] Alves Júnior, S.F., Zanetti, G., Alves de Melo, A.S., *et al.* (2019) Neurofibromatosis Type 1: State-of-the-Art Review with Emphasis on Pulmonary Involvement. *Respiratory Medicine*, **149**, 9-15. <https://doi.org/10.1016/j.rmed.2019.01.002>
- [12] Weinman, J.P., White, C.J., Liptzin, D.R., Deterding, R.R., Galambos, C. and Browne, L.P. (2018) High-Resolution CT Findings of Pulmonary Interstitial Glycogenosis. *Pediatric Radiology*, **48**, 1066-1072. <https://doi.org/10.1007/s00247-018-4138-4>
- [13] Raoof, S., Bondalapati, P., Vydyla, R., *et al.* (2016) Cystic Lung Diseases: Algorithmic Approach. *CHEST*, **150**, 945-965. <https://doi.org/10.1016/j.chest.2016.04.026>
- [14] Gupta, N., Finlay, G.A., Kotloff, R.M., *et al.* (2017) Lymphangiomyomatosis Diagnosis and Management: High-Resolution Chest Computed Tomography, Transbronchial Lung Biopsy, and Pleural Disease Management. An Official American Thoracic Society/Japanese Respiratory Society Clinical Practice Guideline. *American Journal of Respiratory and Critical Care Medicine*, **196**, 1337-1348. <https://doi.org/10.1164/rccm.201709-1965ST>
- [15] Kokosi, M.A., Nicholson, A.G., Hansell, D.M. and Wells, A.U. (2016) Rare Idiopathic Interstitial Pneumonias: LIP and PPFE and Rare Histologic Patterns of Interstitial Pneumonias: AFOP and BPIP. *Respirology*, **21**, 600-614. <https://doi.org/10.1111/resp.12693>
- [16] Girschikofsky, M., Arico, M., Castillo, D., *et al.* (2013) Management of Adult Patients with Langerhans Cell Histiocytosis: Recommendations from an Expert Panel on Behalf of Euro-Histio-Net. *Orphanet Journal of Rare Diseases*, **8**, Article No. 72. <https://doi.org/10.1186/1750-1172-8-72>
- [17] Menko, F.H., van Steensel, M.A., Giraud, S., *et al.* (2009) Birt-Hogg-Dubé Syndrome: Diagnosis and Management. *The Lancet Oncology*, **10**, 1199-206. [https://doi.org/10.1016/S1470-2045\(09\)70188-3](https://doi.org/10.1016/S1470-2045(09)70188-3)
- [18] R Core Team (2020). R: A Language and Environment for Statistical Computing. R Foundation for Statistical Computing, Vienna. <https://www.R-project.org/>
- [19] Escalon, J.G., Richards, J.C., Koelsch, T., Downey, G.P. and Lynch, D.A. (2019) Isolated Cystic Lung Disease: An Algorithmic Approach to Distinguishing Birt-Hogg-Dubé


Syndrome, Lymphangioliomyomatosis, and Lymphocytic Interstitial Pneumonia. *American Journal of Roentgenology*, **212**, 1260-1264. <https://doi.org/10.2214/AJR.18.20920>

- [20] Abbott, G.F., Rosado-de-Christenson, M.L., Franks, T.J., Frazier, A.A. and Galvin, J.R. (2004) From the Archives of the AFIP: Pulmonary Langerhans Cell Histiocytosis. *Radiographics*, **24**, 821-841. <https://doi.org/10.1148/rg.243045005>
- [21] Chou, S.-H., Kicska, G., Kanne, J.P. and Pipavath, S. (2013) Cheerio Sign. *Journal of Thoracic Imaging*, **28**, W4. <https://doi.org/10.1097/RTI.0b013e31827944d2>

Abbreviations

LAM: Lymphangioliomyomatosis;
PLCH: Langerhans Cell Histiocytosis;
LIP: Lymphocytic Interstitial Pneumonia;
BHD: Birt-Hogg-Dubé Syndrome;
IPF: Idiopathic Pulmonary Fibrosis;
CTD: Connective Tissue Disease Related Interstitial Lung Disease;
PPV: Positive Predictive Value;
NPV: Negative Predictive Value;
ILD: Interstitial Lung Disease.

Compliance of Magnetic Resonance Imaging Examination Requests at the Diagnostic Center of the National Social Security Fund of Conakry

Ousmane Aminata Bah^{1,2,3*} , Aminata Sakho², Alpha Abdoulaye Balde², Alpha Issiaga Barry³, Kaba Mohamed Douty¹, Aboubacar Toure²

¹Armed Forces Reference Imaging Center (CIRA), Conakry, Guinea

²Faculty of Health Sciences and Techniques, Gamal Abdel Nasser University of Conakry, Conakry, Guinea

³Diagnostic Center of the National Social Security Fund (CNSS), Conakry, Guinea

Email: *oabah81@gmail.com

How to cite this paper: Bah, O.A., Sakho, A., Balde, A.A., Barry, A.I., Douty, K.M. and Toure, A. (2023) Compliance of Magnetic Resonance Imaging Examination Requests at the Diagnostic Center of the National Social Security Fund of Conakry. *Open Journal of Radiology*, 13, 58-66.

<https://doi.org/10.4236/ojrad.2023.131006>

Received: December 21, 2022

Accepted: March 5, 2023

Published: March 8, 2023

Copyright © 2023 by author(s) and Scientific Research Publishing Inc. This work is licensed under the Creative Commons Attribution International License (CC BY 4.0).

<http://creativecommons.org/licenses/by/4.0/>



Open Access

Abstract

Introduction: MRI is a rapidly growing technique with more and more indications and requests in the Republic of Guinea. Its correct prescription is a guarantee for the satisfaction of the actors, both prescribers, radiologists and patients. The main objective of this study was to evaluate the compliance of MRI examination requests at the Diagnostic Center of the National Social Security Fund (CNSS) in Conakry. **Material and Methods:** This was a descriptive cross-sectional study of MRI prescription forms sent to the MRI unit of the CNSS Diagnostic Center from February 1 to May 1, 2021. The 8 compliance criteria established by the French High Authority for Health were used to evaluate the compliance of the examination requests. **Results:** A total of 7003 examination forms were sent to the facility, including 7% (n = 468) of MRIs. 56.2% of MRI requests were performed by specialists. We observed an overall compliance of 10%. Administrative and clinical compliance were missing in 24% and 38%, respectively. More specifically, the purpose of the examination was not mentioned in 60%, followed by the requesting department in 48.1% and the patient's age in 35.1%. **Conclusion:** This study allowed us to highlight the gaps in establishing MRI requests. It would be important to organize an awareness campaign for prescribers on the usefulness of correctly filling an MRI request and to design templates to be filled out by prescribers.

Keywords

CNSS, Compliance, Conakry Exams, MRI

1. Introduction

The request for a radiological examination is a prescription addressed to a radiologist by a healthcare professional authorized by law [1]. It must enable the radiologist to understand the problem posed by the patient and the circumstances for which the examination is requested. It constitutes the basis of the contract between the prescriber, the patient and the radiologist [1] [2].

The accuracy of information in prescriptions is of great interest in the care process and in imaging [3]. In this regard, several studies have assessed the quality of information on prescriptions for imaging examinations. In particular, the study conducted by Cohen *et al.* [4] on the evaluation of the quality of requests for radiology examinations for patients in the intensive care unit at the Riley paediatric hospital of the Indianapolis University Hospital reported that the clinical information was incomplete or inadequate in 24% of cases.

Incorrect prescribing has a significant impact on the radiological workup and can lead to technical protocol errors in the radiologist's performance of the examinations, wasting time and money for the patient and the hospital [5] [6].

Medical imaging examinations require a good prescription to better orient the radiologist, especially for Magnetic Resonance Imaging (MRI). MRI is one of the medical imaging modalities based on the use of electromagnetic fields to obtain images of the human body [7]. It is a rapidly expanding technique, with an increasing number of indications, requests and long waiting times [8].

In France, the Haute Autorité de Santé (HAS) has established a guide of good recommendations, recommending the use of eight compliance criteria for the request of imaging examinations in order to improve patient management:

Administrative information, *i.e.* the date of the request, the requesting department, the name of the requesting physician, the patient's identity and the patient's date of birth or age.

Clinical information, *i.e.* the anatomical region, the reason for the examination (clinical history) and the purpose of the examination (question asked) [9] [10].

In Cameroon, Moifo *et al.* [11] reported in 2014 in their study on the evaluation of compliance of medical imaging examination requests that only 1.1% of requests were compliant.

Napon *et al.* [12] in Burkina Faso in 2020 collected 97/421 MRIs *i.e.* 24.25% overall compliance of MRI requests.

Gbazi *et al.* [13] in Côte d'Ivoire in 2006 reported that 82% of requests for radiology examinations at the CHU of Cocody did not comply with the criteria established by the HAS in France.

The aim of this study was to evaluate the conformity of requests for magnetic resonance imaging examinations at the Diagnostic Center of the National Social Security Fund (CNSS) in Conakry.

2. Materials and Methods

This was a cross-sectional study with a descriptive aim lasting three months from

February 1st to May 1st, 2021 at the CNSS diagnostic center in Conakry.

We included in this study all the MRI examination request forms sent to and performed at the CNSS diagnostic center in Conakry, regardless of the site to be explored, the age, sex and origin of the patients.

Our study variables were the frequency of MRI examinations at the CNSS diagnostic center and the 8 criteria established by the HAS in France.

The compliance or non-compliance of the examination forms was based on the criteria established by the HAS of France. These criteria are eight, divided into two orders (5 administrative and 2 clinical).

The administrative order, includes: date of the request, requesting department, patient's identity, patient's age, identification of the requestor

The clinical order includes: the anatomical region, the reason for the examination and the purpose of the examination

An examination report is considered compliant if the eight criteria established by the HAS of France are present on the report and it is considered non-compliant if one of the criteria is absent.

Data were collected from an established survey form.

SPSS version 21 software was used for data analysis.

3. Results

3.1. Overall Results

3.1.1. Frequency of MRI Examinations

During the study period, 7003 requests for medical imaging examinations (MRI, ultrasound, CT and X-ray) were sent to and performed at the CNSS diagnostic center in Conakry, including 468 (7%) requests for MRI examinations (**Figure 1**).

3.1.2. Overall Compliance

In this study, we observed an overall compliance of 10% (n = 47) of MRI examination requests and a 90% (421) of non-compliance (**Figure 2**).

3.1.3. Overall Administrative

For overall administrative compliance, it was represented in our series in 24% (n = 112). Thus at least one administrative criterion was missing in 76% (n = 356) (**Figure 3**).

3.1.4. Clinical Compliance

Overall clinical compliance represented 38% (n = 178) of all MRI request. Thus at least one clinical criterion was missing in 62% (n = 290) (**Figure 4**).

3.2. Specific Results

3.2.1. Administrative Criteria (Table 1)

Among the administrative criteria, the requesting service was the parameter with the least information in 48.1% (n = 225) followed by the patient's age in 35.5% (n = 166).

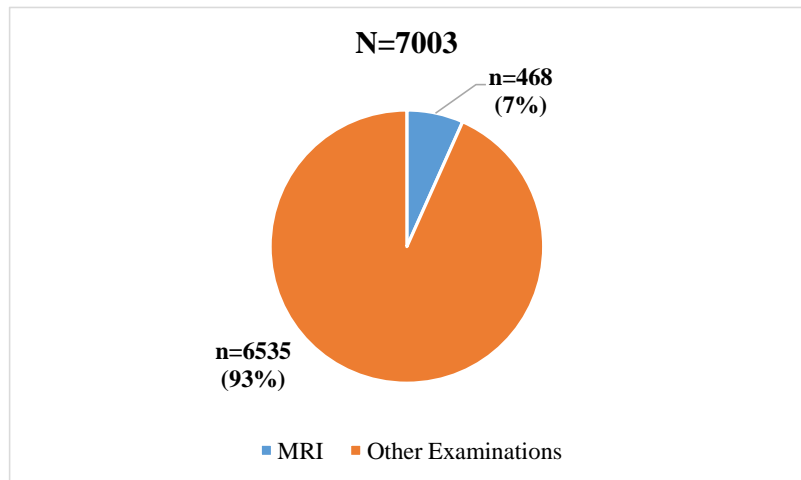


Figure 1. Frequency of MRI examinations.

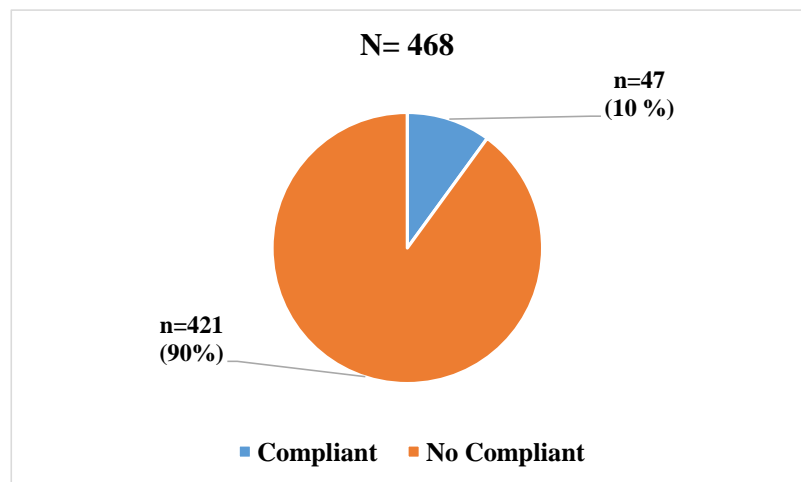


Figure 2. Distribution of reports according to overall compliance of MRI examination requests.

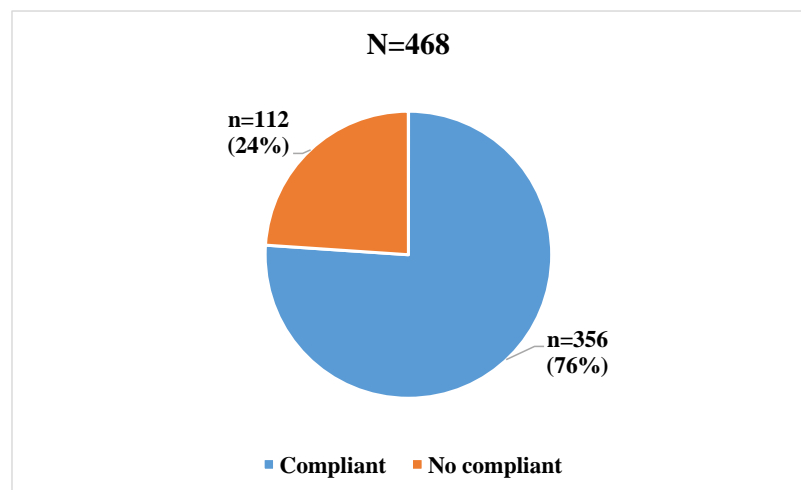


Figure 3. Distribution of reports according to overall administrative compliance of MRI examination requests.

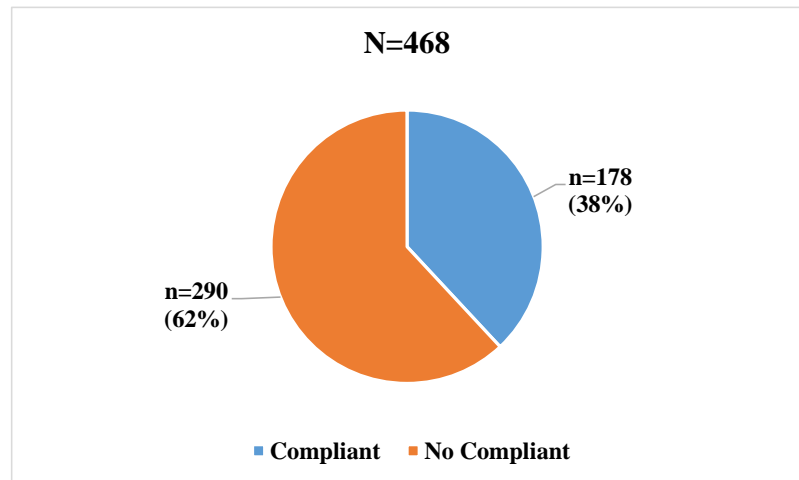


Figure 4. Distribution of reports according to overall clinical compliance of MRI examination requests.

Table 1. Distribution of MRI examination requests according to administrative criteria.

Administrative Criteria	Number (N = 468)	Percentage (%)
Request Date		
No	45	9.6
Yes	423	90.4
Requesting Department		
No	225	48.1
Yes	243	51.9
Patient's Name and Surname		
No	7	1.5
Yes	461	98.5
Patient's Age		
No	166	35.5
Yes	302	64.5
Identification of the Prescriber		
No	36	7.7
Yes	432	92.3

3.2.2. Clinical Criteria (Table 2)

Among the clinical criteria, the purpose of the examination was not specified in 60% (n = 281).

3.2.3. Qualification of the Prescriber (Table 3)

One hundred and forty-nine MRI forms, *i.e.* 31.8%, did not include the qualification of the prescriber. In addition, the healthcare professionals who prescribed the most MRI were specialists in 56.2% (n = 263).

3.2.4. Requesting Department (Table 4)

In our series, 48% of the MRI reports (n = 225) did not include the requesting department. Among these requesting departments, the Neurology department represented 32% (n = 150) of the requests followed by Neurosurgery in 7.26% (n = 34).

Table 2. Distribution of MRI reports according to clinical criteria.

Clinical Criteria	Number (N = 468)	Percentage (%)
Anatomical Region		
No	26	5.6
Yes	442	94.4
Reason for Examination		
No	39	8.3
Yes	429	91.7
Purpose of the Examination		
No	281	60.0
Yes	187	40.0

Table 3. Distribution of MRI reports according to the applicant's qualification.

Qualification of the Prescriber	Number	Percentage (%)
Doctor (Registrars)	34	7.3
General Practitioner	22	4.7
Specialist	263	56.2
Not Know	149	31.8
Total	468	100.0

Table 4. Distribution of reports according to the requesting department.

Requesting Department	Numbers (N = 468)	Percentage (%)
Not Known	225	48.1
Neurology	150	32.1
Neurosurgery	34	7.3
Orthopaedics and Traumatology	16	3.4
Ophtalmology	12	2.6
Surgical Oncology	8	1.7
Gynaeco-obstetrics	7	1.5
General Médecine	4	0.9
General Surgery	3	0.6
Cardiology	2	0.4
ENT	2	0.4
Paediatrics	2	0.4
Gynaecological Surgery	1	0.2
Endocrinology	1	0.2
ICU	1	0.2

4. Discussion

We carried out a cross-sectional study with a descriptive aim over a period of four months from 1st February to 1st May at the CNSS in Conakry.

This study represents the first study carried out in our context to assess the compliance of requests for MRI examinations.

It allowed us to provide data on the quality of MRI prescriptions by the health-care professionals.

During our study, the number of MRI examination forms sent to the CNSS imaging department was very low compared to all other examination forms (ultrasound, CT scan and X-ray).

This result shows that MRI remains a relatively inaccessible examination in Guinea because of its cost, which is about seven times the minimum wage.

On the other hand, the frequency of MRI examination requests in our study was higher than that reported by Napon *et al.* [12] in Burkina Faso in 2020, who in a study of 468 MRI prescriptions, reported an MRI examination frequency of 3.97%. This difference can be explained by the size of our sample and the duration of our study.

More than the majority of the MRI requests in our study did not comply with the French HAS recommendations on Indicators of conformity of requests for imaging examinations.

Our result is lower than that of Napon *et al.* [12] in Burkina Faso in 2020 who reported an overall MRI compliance of 24.25%. This result could be explained by our prescribers' lack of knowledge of the compliance criteria and their importance on one hand, and by the absence of a standardized form mentioning all these compliance criteria on the other.

While non-compliance of examination requests could have an impact on the quality of the examination, as mentioned by Alkasab *et al.* [5] and Smith *et al.* [6] "an incorrect prescription has a considerable impact on the radiological assessment and can lead to technical protocol errors in the performance of examinations by the radiologist, a loss of time and money for the patient and the hospital and overall the healthcare system".

During this study, administrative compliance (date of request, requesting department, patient identity, patient age, identification of the requestor) and clinical compliance (anatomical region, reason for the examination and purpose of the examination) were inadequate in less than half of the cases.

Our clinical compliance result is lower than that of the HAS in France in 2014, which found a clinical compliance rate of 69% for all requests for imaging examinations [9].

Among the administrative criteria, the requesting department and the patient's age were the least specified in almost half of the cases. This result is different from that of Togola in his 2014 Ph.D. thesis in Mali [14] who reported that the requesting department and age were missing in 3% and 75.05% respectively. The fact that their study included all radiological examinations could explain this difference.

However, the presence of the requesting service facilitates the identification of the patient and the orientation of the radiologist in his explorations.

Regarding the clinical criteria, the purpose of the examination was the least frequently mentioned in more than half of the examination requests. This reflects the low proportion of the diagnostic hypothesis mentioned in the examination requests. This result is similar to that found by Moifo *et al.* [11] in Cameroon where a high proportion of requests without any purpose in 76.3% of cases.

The purpose of the examination is as important as the reason, as it allows the radiologist's observation to be compared with that of the clinician.

The majority of those requesting the examinations were specialists. This finding is similar to that reported by Napon *et al.* [12] who found that specialists prescribed in 71.25% of cases.

This predominance of specialists could be explained by their higher level of education, reflecting the objectivity of their diagnosis.

5. Conclusions

This study shows that the majority of requests for MRI examinations sent to the CNSS diagnostic centre in Conakry were not compliant.

Half of the examination forms had poor administrative and clinical compliance.

Among the administrative criteria, the requesting department and the patient's age were the least specified while for the clinical criteria, the purpose of the examination was the least specified.

Dissemination of the compliance elements and raising prescribers' awareness of the usefulness of correctly filling an MRI examination request and the design and printed use of the form could improve the quality of these requests.

Conflicts of Interest

The authors declare no conflicts of interest regarding the publication of this paper.

References

- [1] Colleges of Physicians of Quebec (2005) Prescriptions Made by a Physician. Colleges of Physicians of Quebec, Montreal, 36 p.
<https://www.cmq.org/.../MedecinsMembres/.../>
- [2] Kouamé, Y.N. (2006) Evaluation of the Demand for Radiological Examination in the Medical Imaging Department of the CHU of Cocody. Thesis of Medicine, University of Abidjan, Abidjan.
- [3] Troudea, P., Dozola, A., Soyerb, P., Girarda, D., Martinez, F., Montagne, B., *et al.* (2014) Improvement of the Imaging Request Process. *Journal de Radiologie Diagnostique et Interventionnelle*, **95**, 74-80.
- [4] Cohen, M.D., Curtin, S. and Lee, R. (2006) Evaluation of the Quality of Radiology Requisitions for Intensive Care Unit Patients. *Academic Radiology*, **13**, 236-240.
<https://doi.org/10.1016/j.acra.2005.10.017>
- [5] Alkasab, T.K., Alkasab, J.R. and Abujudeh, H.H. (2009) Effects of a Computerized

- Provider Order Entry System on Clinical Histories Provided in Emergency Department Radiology Requisitions. *Journal of the American College of Radiology*, **6**, 194-200. <https://doi.org/10.1016/j.jacr.2008.11.013>
- [6] Smith, P.C., Araya-Guerra, R., Bublitz, C., Parnes, B., Dickinson, L.M., Van Vorst, R., et al. (2005) Missing Clinical Information during Primary Care Visits. *JAMA*, **293**, 565-571. <https://doi.org/10.1001/jama.293.5.565>
- [7] Delmas, A. (2017) Definition, Validation and Implementation of a Monitoring of the Exposure to Static Magnetic Field of MRI Workers. Thesis of Medicine, University of Lorraine, Nancy, 194 p.
- [8] Diaferia, D. (2015) Installation of an MRI. *Medical Imaging and Radiotherapy Manipulator*, 20-26.
- [9] HAS (2011) Indicator Compliance of Requests for Imaging Examinations.
- [10] Indicateur Conformité des demandes d'examens d'imagerie, Campagne 2011: Analyse descriptive des résultats agrégés 2010 et analyse des facteurs associés à la variabilité des résultats—Juillet 2012. Haute Autorité de Santé. http://www.has-sante.fr/jcms/c_1277960/fr/indicateur-conformite-des-demandes-d-examens-d-imagerie-campagne-2011-analyse-descriptive-des-resultats-agreges-2010-et-analyse-des-facteurs-associes-a-la-variabilite-des-resultats-juillet-2012
- [11] Moifo, B., Ndeh, K.M., Fuh, F.N., Tamba, J., Tebere, H. and Gonsu, F.J. (2014) Compliance Assessment of Medical Imaging Requests: An Experiment in Sub-Saharan Africa. *Médecine et Santé Tropicales*, **24**, 392-396. <https://doi.org/10.1684/mst.2014.0382>
- [12] Napon, M., Nde/Ouedraogo, N.-A., Nama, B., Kambou/Tiemtore, B.M.A., Ouattara, B., Zanga, M., et al. (2020) Compliance of Magnetic Resonance Imaging Requests in Ouagadougou (Burkina Faso). *Journal Africain d'Imagerie Médicale*, **12**, 8-12.
- [13] Gbazi, G.C. and Kouassi, B. (2006) Analysis of Radiology Examination Request Forms at the CHU of Cocody: Initial Results of 1446 Requests. *Journal de Radiologie*, **87**, 1425-1426. [https://doi.org/10.1016/S0221-0363\(06\)87467-6](https://doi.org/10.1016/S0221-0363(06)87467-6)
- [14] Togola, K. (2014) Indicators of Compliance of Requests for Imaging Examinations in the Radiology and Nuclear Medicine Department of the CHU du Point G. Ph.D. Thesis, University of Sciences, Techniques and Technologies of Bamako, Bamako.

Burden of Congenital Defects Diagnosed through Ultrasonography in Soba Fetomaternal Unit, Khartoum, Sudan

Mona Awadallah Mohammed Ali Osman¹, Isam Ahmed Ali Elhassan¹, Fareeda Nikhat Khan², Abdulmutallab Alimam³, Mounkaila Noma¹, Atif Fazari^{1,2*}

¹Faculty of Medicine, University of Medical Sciences and Technology, Khartoum, Sudan

²Department of Obstetrics & Gynecology, Latifa Hospital, DHA, Dubai, UAE

³Department of Obstetrics and Gynecology, Faculty of Medicine, University of Khartoum, Khartoum, Sudan

Email: *atiffazari@hotmail.co.uk

How to cite this paper: Osman, M.A.M.A., Elhassan, I.A.A., Khan, F.N., Alimam, A., Noma, M. and Fazari, A. (2023) Burden of Congenital Defects Diagnosed through Ultrasonography in Soba Fetomaternal Unit, Khartoum, Sudan. *Open Journal of Radiology*, 13, 67-76.

<https://doi.org/10.4236/ojrad.2023.131007>

Received: January 20, 2023

Accepted: March 24, 2023

Published: March 27, 2023

Copyright © 2023 by author(s) and Scientific Research Publishing Inc. This work is licensed under the Creative Commons Attribution International License (CC BY 4.0).

<http://creativecommons.org/licenses/by/4.0/>



Open Access

Abstract

Background: Congenital anomalies are among the leading causes of fetal loss, despite it can be identified prior to birth through advanced technology in expert hands. Our research aimed at estimating the prevalence of congenital anomalies in Sudan. **Methods:** A facility-based retrospective cross-sectional study combined with a community-based survey through a telephone interview was implemented on a purposive convenient sample of 138 participants. The data were computerized in Epi Info 7. Google Earth Pro enabled to collect the geographical coordinates for the residence of the participants. Descriptive statistics were performed through SPSS 23 and ArcGIS 10.3 was used to generate the geographical distribution map of congenital defects to visualize the catchment areas of Soba Ultrasonography Unit. **Results:** Of the 138 participants, the estimated prevalence of congenital defects was 2.2/10,000 live births. The ultrasonography screening revealed that neural tube defects were the most prevalent anomalies with 13.0% (18/138), which represented 47.4% (18/38) of all defects. Concerning children, a mortality rate of 23.2% (32/138) was reported. **Conclusions:** The child mortality rate post ultrasound screening of 23.2%, and the neural tube defects being the most common anomalies appealed to Sudan health authorities for focusing on more preventive antenatal practices to strengthen and promote maternal and child health.

Keywords

Prevalence, Congenital Defects, Ultrasound, Spatial Distribution

1. Introduction

Congenital anomalies are conditions of prenatal origin that can be identified prenatally, at birth, or may only be detected later in infancy. They include structural and functional abnormalities that impact fetal or infant health, development and/or survival. Congenital anomalies have a significant impact on individuals, families and healthcare systems as they contribute to perinatal mortality and morbidity. These anomalies can occur in isolation (single defect) or as a group of defects (multiple defects), and have different names such as congenital abnormalities, malformations, disorders or defects. An estimated 240,000 newborns die worldwide within 28 days of birth every year due to birth defects. Birth defects cause a further 170,000 deaths of children between the ages of 1 month and 5 years. Moreover, low- and middle-income nations are disproportionately impacted by congenital abnormalities, which are one of the primary causes of the global disease burden [1] [2].

Ultrasound Scanning (USS) is an ideal imaging procedure for a primary diagnostic and screening method during pregnancy. The detection of anomalies could be hampered by factors that intervene with visualization like maternal obesity, oligo/anhydramnios, fetal position and reverberation caused by bone. This would indicate another screening modality like magnetic resonance imaging. The types of fetal anomalies, which can be detected by ultrasonic diagnosis in different gestational ages, include: central nervous system, genitourinary, cardiovascular, respiratory, gastrointestinal, musculoskeletal, facial deformity, ascites and pleural effusion, cystic hygroma, teratoma and multiple malformations [1] [3].

Second-trimester scan, between 18 and 22 weeks, remains the standard for fetal anatomical assessment worldwide. However, significant improvement in detecting fetal abnormalities in the first trimester of pregnancy is also recognized [4].

The European Surveillance of Congenital Anomalies (EUROCAT) was set up for detecting any epidemic of congenital anomalies. The prevalence and trend of 61 congenital anomaly subgroups (excluding chromosomal) in 25 population-based EUROCAT registries (1980-2012) indicated a significant increase in Congenital Heart Disease (CHD) which was attributed to the increase in the number of diabetics as well as overweight mothers; while the decrease of the prevalence of limb reduction could not be explained. The increase in renal anomalies was due to rigorous screening; the reported birth prevalence of congenital heart disease had reached an estimate of 9/1000 live births in the last 15 years; the birth prevalence of congenital heart disease varies according to the geographical location of the patient and the severity of the heart defect [5].

The Netherlands National Screening Program on prenatal detection of severe congenital heart anomalies was evaluated. It was found that the detection rate of all CHD increased significantly from 35.8% before to 59.7% after the introduction of the National Screening Program ($p < 0.001$). It was concluded that pre-

natal detection of CHD remains challenging, especially for ultrasonographers who were minimally exposed to these anomalies [6]. It cannot be denied that computerized birth registries and new software applications play a significant role in analyzing and identifying trends; consequently, the current study attempted to apply similar technologies in spatially distributing the types of defects for visualization and easy capture of regions that require more attention in terms of antenatal health services. The identification of multiple congenital defects was made more accurate by combining population-based birth defect data such as EUROCAT with epidemiological data in a computer-based algorithm [7].

A household survey was conducted in Nepal villages on a sample of 21,111 women and 27,201 children with congenital defects. The prevalence of congenital defects was 52.0/10,000 children (95% CI: 44.0 - 61.0), and the majority were born to mothers with poor health. One of the most severe forms of congenital defects was Neural Tube Defects (NTDs) which can be prevented through proper nutrition and folic acid supplements [8]. The province of Shanxi in China had the highest reported worldwide incidence of congenital heart defects which was partially attributed to the presence of coal mines and many other minerals in the soil. Various strategies were applied in order to reduce the incidence. A spatial and temporal analysis of a live and stillbirths was conducted in two Chinese localities between the years 1998-2012. The findings indicated that the interventions implemented by the government, such as food fortification by adding five micro-nutrients, might have a positive impact on reducing the overall incidence of NTDs. The results also revealed the existence of significant spatial heterogeneity. NTD clusters were identified in areas close to coal sites and main roads even after intervention [9].

Food fortification with folic acid is a proven strategy to reduce neonatal and under-five mortality in general and those associated with spina bifida in particular, and it is recommended that countries implement mandatory folic acid fortification of staple foods without further delay [10].

This study aimed to estimate the prevalence of congenital defects, their types and geographical distribution in pregnant women who had ultrasonography examinations at the Fetomaternal Unit of Soba University Hospital, Sudan.

2. Methodology

A facility-based retrospective record-based study combined with a community-based survey was implemented. The research was conducted in the Fetomaternal Unit of Soba University Hospital in Al Khartoum (Sudan), where a purposive convenient sample of 138 ultrasonography records was extracted, in March-May 2018, from the electronic database of a total of 2500 patients examined during the period of January 2016 to December 2017. Hence, the sample examined represented 5.5% of the women who had ultrasonography screening during the period of January 2016 to December 2017. A standardized data tool

was used to extract the data needed to address the research objective. The research tool had two parts; Part 1 for recording maternal characteristics and part 2 for fetal characteristics. A community survey was conducted through a telephone interview to collect the missing data on the residence of participants, mother and child's current health status (at the time of interview) and the outcome of the pregnancy.

The data collected were computerized using a template elaborated in Epi Info™ 7.1.5.2, free software developed by the Center for Disease Control, Atlanta, USA. The Statistical Package for Social Sciences (SPSS version 23) was used to summarize the data numerically (mean, standard deviation and median) and graphically (frequency tables for estimating prevalence and graphics). Google Earth Pro 7.1.8.3036 (32bit) was used to obtain the geographical coordinates (latitudes and longitudes) of the residence of the participants. The Geographical Information System (ArcGIS 10.3 for Desktop version 10.3.043322) was used to elaborate the spatial distribution map of congenital defects.

Ethical Approval and Consent to Participate

The research was reviewed by the Institutional Review Committee of the University of Medical Sciences and Technology (UMST) and was authorized by the General Director of Soba University Hospital. The community-survey obtained a verbal well informed consent from all the participants.

3. Results

3.1. Characteristics of Participants

The age of the 138 females, who went through ultrasonography screening, ranged from 17 to 40 years with an average age (median) of 29 years. 40.6% (56/138) were highly educated whereas 5.8% (8/138) had never attended a formal schooling. Their gynecological and obstetrical backgrounds revealed that their gravidity ranged from 1 to 8 pregnancies with an average of 3 pregnancies; their average parity of 2 varied from 0 to 8. They had between 0 to 8 miscarriages as revealed in **Table 1**. **Figure 1** displayed the geographical distribution of the participants according to their respective state of residence.

3.2. Types and Prevalence of Congenital Defects

Types of Congenital Defects

Congenital defects were present in 38 of 138 pregnant women who went through ultrasonography screening. This represented a proportion of 27.5% (38/138) congenital defects of all types. **Table 2** revealed the details of the ultrasonography screening results and **Figure 2** displayed the distribution of congenital anomalies in the involved states. The ultrasonography screening revealed that neural tube defects were the most prevalent anomalies with 13.0% (18/138), which represented 47.3% (18/38) of all defects. The ultrasonography examination also revealed cardiac (10.5%, 4/38), renal (7.9%, 3/38), musculoskeletal (5.3%, 2/38) and abdominal wall (2.6%, 1/38) anomalies. Multiple defects (more than one system

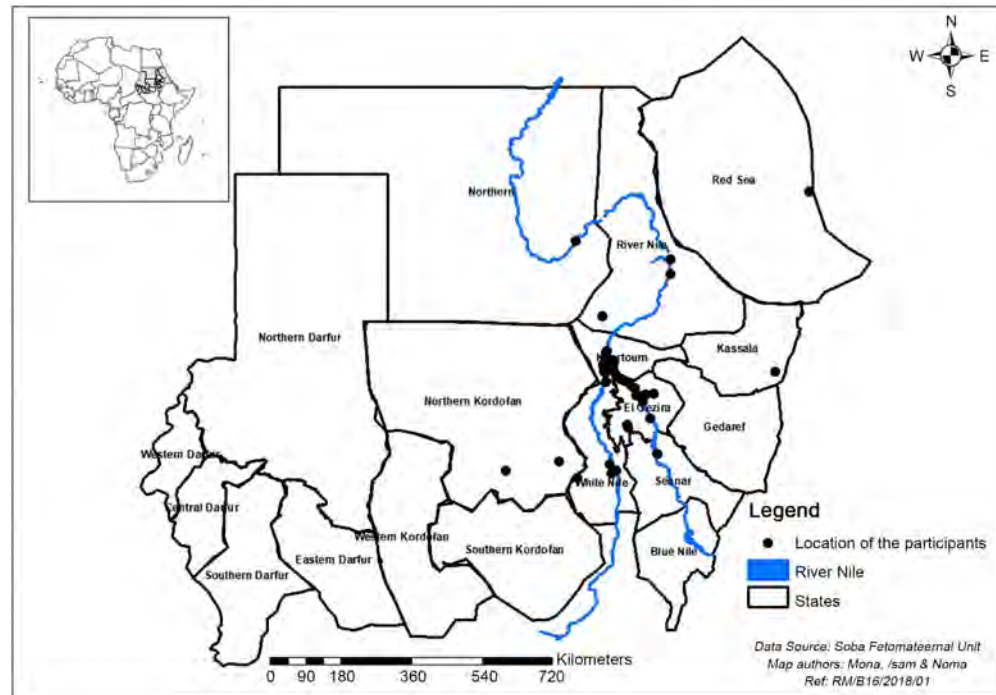


Figure 1. Geographical distribution of the study participants based on their state of origin (n = 138).

Table 1. Characteristics of the study participants (n = 138).

Variable	Number	%
Study setting (n = 138)		
Soba University Hospital (SUH)	138	100
Education levels (n = 138)		
University or higher	56	40.6
Secondary	46	33.3
Primary	28	20.3
Never been to school	8	5.8
Age in years (n = 138)		
Median	29	
Min-Max	17 - 40	
Gravidity (n = 138)		
Median	3	
Min-Max	1 - 11	
Parity (n = 138)		
Median	2	
Min-Max	0 - 8	
Miscarriage (n = 137)		
Median	0	
Min-Max	0 - 8	

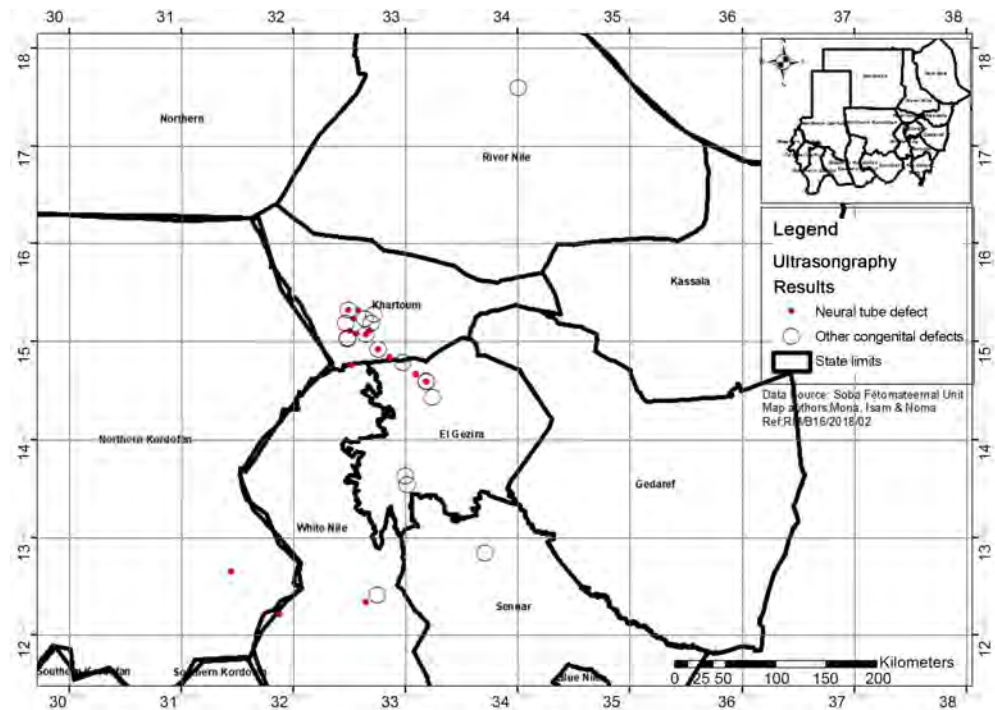


Figure 2. Geographical distribution of the congenital defects (n = 38) diagnosed through ultrasonography in Soba Fetomaternal Unit.

Table 2. Results of 138 women who went through ultrasonography screening in Soba Fetomaternal Unit.

Type of congenital defect	Number	%
No structural abnormality	100	72.5
Neural tube defect	18	13.0
Multiple defects	5	3.6
Others	5	3.6
Cardiac defect	4	2.9
Renal defect	3	2.2
Musculoskeletal defect	2	1.4
Abdominal wall defect	1	0.8

affected) represented 13.2% (5/38) of the total anomalies detected (n = 38) whereas hydrops, cystic hygroma and down syndrome categorized as “others” were 13.2% (5/38).

The *neural tube defect* was diagnosed in young adult women aged on the average (median) 29 years (range: 21 - 39 years). These women had a history of 4 pregnancies (range: 1 - 11) which lasted on an average delivery of 2.5 ranging from 0 to 8. Unfortunately, they presented late for ultrasound screening with an average (median) gestational age of 31 weeks.

The *other types of congenital defects* (n = 20), except neural tube anomaly, were diagnosed in women aged 28 years ranging from 17 to 40 years, they had

an average of 3 pregnancies (range: 1 - 6) and delivered between 0 and 5 newborns with an average of 2 newborns. They presented to ultrasound examination earlier than those with neural tube defects with an average of 29 weeks ranging from 14 to 36 weeks; 85.0% (17/20) who presented at a gestational age \geq 25 weeks, one participant (1/20) was examined at a gestational age of 14 weeks and 10.0% (2/20) at the period between 18 and 24 weeks.

Maternal and Child Health Status

Telephone interviews enabled to collect the data which were missed from the ultrasound reports. These data were the pregnancy outcome, the mothers and children health status at the time of the interview. Except one participant whose husband verbally consented to provide the above information, all the participants freely provided the data related to their pregnancy outcome, their health status and the child condition.

Regarding the outcome of the pregnancy, 79.7% (110/138) of the participants delivered live newborns without disability and 1.4% (2/138) of the newborns presented anomalies at the delivery. Stillbirth was recorded in 4.4% (6/138) of the participants. A perinatal mortality rate of 14.5% (20/138) was reported with respectively 6.5% fetal and 8.0% neonatal deaths (**Table 3**).

Table 3. Pregnancy outcomes, mother and children health status at time of interview and ultrasound screening results (n = 138).

Variable	Ultrasonography results				Total	Total %
	Neural tube	Other congenital	No congenital	Total defects		
Pregnancy outcome						
Alive without apparent disability	12	7	91	19	110	79.7
Alive with a disability	0	0	2	0	2	1.4
Fetal death	3	5	1	8	9	6.5
Neonatal death	3	4	4	7	11	8.0
Stillbirth	0	4	2	4	6	4.3
Total	18	20	100	38	138	
Maternal health status						
Unwell	0	1	2	1	3	2.2
Well	18	19	98	37	135	97.8
Total	18	20	100	38	138	
Child health status						
Alive and well	5	5	86	10	96	69.6
Alive with complication	4	2	4	6	10	7.2
Deceased	9	13	10	22	32	23.2
Total	18	20	100	38	138	

At the time of the interview, 97.8% (135/138) of the participants were in good health; of the three participants who reported not being healthy, their ultrasonography screening had not detected any congenital defect in two and one was diagnosed with a congenital defect other than NTDs. Concerning the children, a mortality rate of 23.2% (32/138) was reported; the ultrasonography screening was normal for 31.3% (10/32) and congenital defects were diagnosed in 68.8% (22/32). 7.2% (10/138) of the children lived with complications. Overall, only 69.6% (96/138) of the children were living healthily at the time of interview.

4. Discussion

Of the 138 cases that underwent ultrasound examination in our study, the prevalence of congenital structural defects was estimated at 2.2/10,000 live births (range: 0.3 - 7.4/10,000). This prevalence was comparable with the 7.2% and 2.5% reported in the literature [3] [11]. Neural tube defects were the most prevalent congenital defects (13.0%); this was in line with published data [10] and contradicted those publications [8] [9] where the most prevalent anomalies were congenital heart defects. As it is known that folic acid treatment in the first trimester can prevent neural tube defects, our findings indicated that the antenatal care provided in primary health care settings should be enhanced by a health promotion message emphasizing the importance of taking folic acid supplements.

It has been suggested that congenital malformations may emerge in the first trimester of pregnancy as a result of genetic aberrations or gene-environment interaction. The etiology is predominantly multifactorial, arising from complex gene-environment interactions that impair normal embryo-fetal development. Environmental factors (such as chemical toxins, infectious agents, maternal sickness, and exogenous factors) can have pre-conceptional mutagenic, post-conceptional teratogenic, peri-conceptional endocrine disruption and epigenetic effects [11]. Unfortunately, our research did not investigate the impact of environmental factors in our country where irrigated farming using pesticides is widely practiced. Another limitation of our research was the convenient sampling technique used due to the inaccessibility of the entire database of ultrasound records available. However, as an explorative study, the findings revealed that neural tube defects, preventable through supplementation, were the predominant anomaly. The use of spatial distribution software for mapping health conditions facilitated the visualization of locations with the highest concentration of affected population, hence enhancing relevant stake-holders ability to respond promptly. Healthcare providers are urged to promote maternal health, incorporate ultrasonography screening into routine antenatal care and support pregnant women with abnormal fetal outcomes.

Availability of Data and Materials

The data are available upon request at any time needed from the corresponding

author.

Funding

The research was fully funded by the researcher Osman, M.A.M.A. and Elhassan, I.A.A. in the course of their field research related to their thesis for the diploma in Research Methodology and Biostatistics.

Authors' Contribution

- 1) Osman, M.A.M.A.: Designed and implemented the research as well as the data management and drafting of the manuscript.
- 2) Elhassan, I.A.A.: Contributed to the implementation of the research and the data management, and reviewed the draft manuscript.
- 3) Alimmam A.: Facilitated access to the ultrasound reports.
- 4) Noma, M.: Supervised the data management, orientated the GIS analysis and edited the final manuscript.
- 5) Fazari, A.: Designed and contributed to drafting, and edited the final manuscript.
- 6) Khan, F.N.: Designed and contributed to drafting, and edited the final manuscript.

All the authors read and approved the final manuscript prior to submission.

Acknowledgements

We acknowledge Dr. Durreya Alrayah, and her staff of the Habib Fetomaternal Unit of Soba University Hospital, with special thanks to the nurses for their support. The University of Medical Sciences and Technology for guidance in the framework of the Diploma in Research Methodology and Biostatistics, in particular Prof. Humeida and Dr. Hanan Tahir. We are also greatly in debt to our Batch Diploma colleagues in particular Dr. Al Nazeer and Ms. Maria for their assistance.

Conflicts of Interest

The authors declare no conflicts of interest regarding the publication of this paper.

References

- [1] Jarvis, D., Mooney, C., Cohen, J., Papaioannou, D., Bradburn, M., Sutton, A., *et al.* (2017) A Systematic Review and Meta-Analysis to Determine the Contribution of Mr Imaging to the Diagnosis of Foetal Brain Abnormalities *in Utero*. *European Radiology*, **27**, 2367-2380. <https://doi.org/10.1007/s00330-016-4563-4>
- [2] World Health Organization (2022) Birth Defects Fact Sheet. <https://www.who.int/news-room/fact-sheets/detail/birth-defects>
- [3] Han, N., Cheng, C., Wang, Y., Zhou, M. and Xia, B. (2017) Perinatal and Follow-Up Outcome Study of Fetal Anomalies with Multidisciplinary Consultation. *Therapeutics and Clinical Risk Management*, **13**, 1303-1307.

<https://doi.org/10.2147/TCRM.S138808>

- [4] Tomasz, G., Krzyanowski, A., Stupak, A., Kwasniewska, A., Pikula, T., *et al.* (2014) Complementary Role of Magnetic Resonance Imaging after Ultrasound Examination in Assessing Fetal Renal Agenesis: A Case Report. *Journal of Medical Case Reports*, **8**, Article No. 96. <https://doi.org/10.1186/1752-1947-8-96>
- [5] Dolk, H., *et al.* (2015) Detection and Investigation of Temporal Clusters of Congenital Anomaly in Europe: Seven Years of Experience of the EUROCAT Surveillance System. *European Journal of Epidemiology*, **30**, 1153-1164. <https://doi.org/10.1007/s10654-015-0012-y>
- [6] Van Velzen, C.L., Clur, S.A., Rijlaarsdam, M.E.B., Bax, C.J., Pajkrt, E., Heymans, M.W., Bekker, M.N., Hruda, J., De Groot, C.J.M., Blom, N.A. and Haak, M.C. (2016) Prenatal Detection of Congenital Heart Disease—Results of a National Screening Programme. *BJOG: An International Journal of Obstetrics & Gynaecology*, **123**, 400-407. <https://doi.org/10.1111/1471-0528.13274>
- [7] Calzolari, E., Barisic, I., Loane, M., Morris, J., Wellesley, D., Dolk, H., Addor, M.C., Arriola, L., Bianchi, F., Neville, A.J. and Budd, J.L. (2014) Epidemiology of Multiple Congenital Anomalies in Europe: A EUROCAT Population-Based Registry Study. *Birth Defects Research Part A: Clinical and Molecular Teratology*, **100**, 270-276. <https://doi.org/10.1002/bdra.23240>
- [8] Bhandari, S., *et al.* (2015) Prevalence of Congenital Defects Including Selected Neural Tube Defects in Nepal: Results from a Health Survey. *BMC Pediatrics*, **15**, Article No. 133. <https://doi.org/10.1186/s12887-015-0453-1>
- [9] Liao, Y., Zhang, Y., He, L., Wang, J., Liu, X., Zhang, N., *et al.* (2016) Temporal and Spatial Analysis of Neural Tube Defects and Detection of Geographical Factors in Shanxi Province, China. *PLOS ONE*, **11**, e0150332. <https://doi.org/10.1371/journal.pone.0150332>
- [10] Kancherla, V., Wagh, K., Pachón, H. and Oakley Jr., G.P. (2021) A 2019 Global Update on Folic Acid-Preventable Spina Bifida and Anencephaly. *Birth Defects Research*, **113**, 77-89. <https://doi.org/10.1002/bdr2.1835>
- [11] Baldacci, S., Gorini, F., Santoro, M., Pierini, A., Minichilli, F. and Bianchi, F. (2018) Environmental and Individual Exposure and the Risk of Congenital Anomalies: A Review of Recent Epidemiological Evidence. *Epidemiologia e Prevenzione*, **42**, 1-34.

Place of Selective Tubal Catheterization in the Management of Female Infertility in Togo

Komlanvi Etteh Victor Adjénou^{1,2,3*}, Hassiatou Sabi Couscous², Ndouandju Saha², Kwokwo Kafupi², Etsri Wallace², Sonhaye Lantam^{1,3}, Amadou Abdoulatif³, Adambounou Kokou^{1,3}, Lama Kegdigoma Agoda-Koussema³

¹Department of Radiology and Medical Imaging, CHU Campus, Lomé, Togo

²Center for Radiology and Medical Imaging, Clinique Autel d'Elie, Lomé, Togo

³Faculty of Health Sciences, University of Lomé, Lomé, Togo

Email: *kadjenou@yahoo.fr

How to cite this paper: Adjénou, K.E.V., Sabi Couscous, H., Saha, N., Kafupi, K., Wallace, E., Lantam, S., Abdoulatif, A., Kokou, A. and Agoda-Koussema, L.K. (2023) Place of Selective Tubal Catheterization in the Management of Female Infertility in Togo. *Open Journal of Radiology*, 13, 77-85. <https://doi.org/10.4236/ojrad.2023.131008>

Received: February 14, 2023

Accepted: March 27, 2023

Published: March 30, 2023

Copyright © 2023 by author(s) and Scientific Research Publishing Inc. This work is licensed under the Creative Commons Attribution International License (CC BY 4.0).

<http://creativecommons.org/licenses/by/4.0/>



Open Access

Abstract

Objective: To determine the effectiveness of selective tubal catheterization in the management of female infertility due to proximal tubal obstruction. **Method:** This was a longitudinal descriptive study, conducted over a period of 24 months, which included 73 patients presenting with objectified bilateral proximal tubal obstruction after standard HSG. The intervention was performed on an outpatient basis, during the follicular phase with negative β -hCG assay the day before, in the interventional radiology room and under antibiotic coverage. Confirmatory hysterosalpingography was performed as the first step followed by selective tubal catheterization after the failure of spontaneous tubal opacification. The parameters studied related to socio-epidemiological, clinical and radiological data. **Results:** The age of our patients was between 24 and 42 years with an average of 33.97 years. The average duration of infertility was 3.95 years, with a predominance of primary infertility in 83.56% of cases. Voluntary termination of pregnancy (38.89%) and fibromyomas (33.33%) were the most represented gynecological-obstetrical antecedents. Selective tubal catheterization was successful in 92.14% of cases (129/140 tubes). It was possible bilaterally in 93.02% of cases and unilaterally in 6.98% of cases. The confirmatory HSG allowed a spontaneous opacification of 4.10% of the fallopian tubes. At the end of the procedure, all the recanalized tubes were opacified; 62.01% of them were normal, against 37.99% pathological with a preponderance of inflammatory tubes 26.61% followed by hydrosalpinx in 5.03% of cases. No major complications were encountered. The fertility rate was 23.29%. **Conclusion:** Selective tubal catheterization is a simple technique, without major complications with an efficiency close to natural fertility. It should be proposed as the first intention before any other procedure in the treatment of infertility by proximal tubal obstruction.

Keywords

Female Infertility, Selective Tubal Catheterization, Togo

1. Introduction

Infertility is the inability to achieve pregnancy in a woman with normal sexual activity, without any notion of contraception, for a period of one year [1]. It represents a real public health problem and spares no country in the world. In Africa, although underestimated due to the refusal of consultation for many patients who suffer from it, its prevalence seems to be increasingly high. In Togo, female infertility represents 12% of consultations [2]. Its consequences on the viability of the couple are enormous and women are the most indexed in most African societies. The causes of female infertility are dominated by tubal pathologies [3]. In 10% to 25% of cases, it is a proximal tubal obstruction, the management of which depends on the etiology [4]. In Africa south of the Sahara, selective salpingography has been proposed by some authors as the first-line therapeutic method [5]. It may or may not be followed by tubal catheterization, which is a now well-codified interventional radiology technique, aimed at evaluating proximal tubal obstructions revealed by conventional hysterosalpingography, and if necessary, attempting to repermeabilize the uninjected tubes. Tubal catheterization is therefore both a diagnostic and a therapeutic act, and is an effective part of the therapeutic regimen for tubal infertility [6] [7]. In the literature, reversal rates between 40% and 87% have been reported [8]. In France, 75% clearance was achieved in a study of 100 cases of proximal tubal obstruction. A similar study in Mali recorded a 92.7% success rate for tubal reversal [9]. No publication has been found on selective tubal catheterization to date in Togo. However, since 2019 an interventional radiology table has been introduced there with the aim of contributing to the improvement of the management of this condition. The need for the present study was therefore necessary in order to determine the effectiveness of selective tubal catheterization in the management of female infertility by proximal tubal obstruction.

2. Methodology

Our longitudinal descriptive study was conducted over a period of 24 months, from June 2019 to May 2021. The study included 73 patients aged 42 years or less, presenting bilateral proximal tubal obstruction with a uterine cavity of normal morphology or partially deformed by uterine lesions (partial synechia or fibroid) observed on a standard HSG previously performed and dating from less than 06 months. It took place at the interventional radiology center of the “AUTEL d’ELIE” clinic, the only structure for the whole country. This center began its activities in Lomé in the Togolese capital in June 2019. It has a SHIMADZU brand CATH LAB interventional radiology device (**Figure 1(a)**), a

remote-controlled interventional table (**Figure 1(a)**), a scope, a control room (**Figure 1(b)**), an interpretation station with an Internet connection and a printer. The examination was scheduled between day 6 and day 12 of the last menstrual period with a negative β -hCG assay the day before. Diagnostic HSG was required to study uterine position and anatomy. Broad-spectrum antibiotic prophylaxis, such as cyclins, was started 48 hours before the procedure and continued 72 hours later. A vaginal toilet with Betadine was also prescribed 48 hours before the examination. The procedure, performed on an outpatient basis, did not require sedation.

Taking an antispasmodic was proposed just before the procedure, for analgesic purposes. The intervention took place in two stages: the first consisted in the realization of a HSG of confirmation which made it possible to confirm the PTO (proximal tubal obstruction) and to avoid unnecessary gestures; the second consisted of the actual catheterization. The specific equipment consisted of a 9F caliber carrier catheter, a 5F caliber pre-curved probe, a 3F caliber flexible mini probe and a flexible, ultra-thin 0.03-inch caliber micro-guide. The data were collected after a minimum follow-up of 3 months from the interrogation of the patients, reports of HSG and tubal unblocking carried out remotely from the preliminary HSG. The parameters studied related to socio-epidemiological, clinical and radiological data.

3. Results

The average age of our patients was 33.97% with extremes of 24 and 42 years. The age group of 26 to 30 years was the most represented (**Table 1**). The majority of patients (86.30%) were married women, the rest of the sample (13.70%) being single people living together. The average duration of infertility was 3.95 years, with a predominance of primary infertility in 83.56% of cases. Voluntary termination of pregnancy (38.89%) and myomas (33.33%) were the most represented gynecological-obstetrical antecedents (**Table 2**).

Standard hysterosalpingography was indicated in 98.63% of cases ($n = 72$) as part of an infertility assessment. It had objectified a homogeneous uterine cavity in 84.93% of cases ($n = 62$), fibroids and partial synechiae respectively in 12.33% and 2.73% of cases. The uterine contours were regular in 95.89% of cases ($n = 70$) and deformed in 4.11% of cases ($n = 3$). The tubal obstruction was bilateral in all cases. The HSG confirmation allowed a spontaneous opacification of 4.10% of the tubes. Selective tubal catheterization was successful in 92.14% of cases (129/140 tubes). It was possible bilaterally in 93.02% of cases and unilaterally in 6.98% of cases (**Table 3**). At the end of the procedure, all recanalized tubes were opacified (**Figure 2**); 62.01% of them were normal, against 37.99% pathological with a preponderance of inflammatory tubes (26.61%) followed by hydrosalpinx in 5.03% of cases (**Table 4**). Overall the intervention lasted an average of 38.31 min \pm 6.06 min with extremes of 15 min and 56 min. The average radiation dose of the pelvis in our patients was estimated at 3.2 mGy.

No major complications were encountered (**Table 5**). Pregnancies were ob-

tained by 23.29% of our patients (n = 17). In 70.59% of them (n = 12), they occurred between 6 and 10 months after the unblocking, against 29.41% of cases between 1 and 5 months. The mean time to onset of pregnancy was 6.64 months \pm 1.9 months with extremes of 3 and 10 months.



Figure 1. (a) & (b) CATH LAB 2 interventional radiology device, control room.

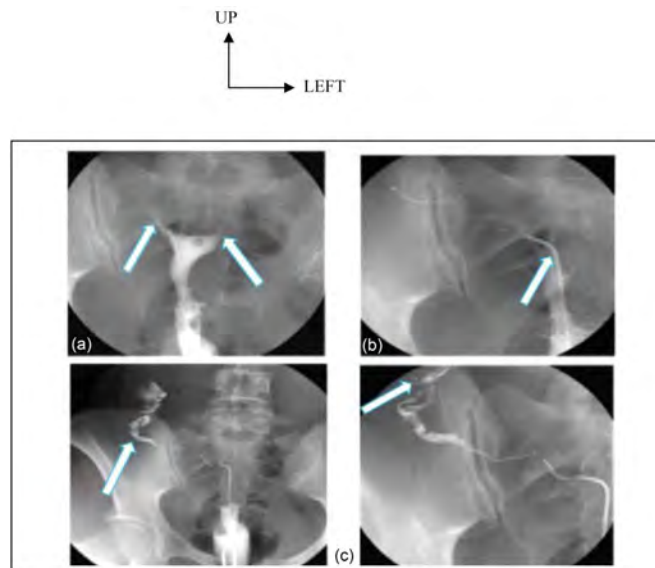


Figure 2. Right proximal tubal obstacle recanalized by tubal catheterization. (a) Bilateral PTO with confirmatory HSG; (b) Right tubal catheterization; (c) Right effective tubal opacification.

Table 1. Distribution of patients according to age groups.

	Effective	%
21 - 25	3	4.11
26 - 30	24	32.88
31 - 35	20	27.40
36 - 40	15	20.55
41 - 45	11	15.07
Total	73	100

Mean age = 33.97 years \pm 5.23 years; Extremes: 24 and 42.

Table 2. Distribution of patients according to gynecological and surgical history.

	Effective	%
Gynecological history	18	100
Abortion	7	38.89
Fibroids	6	33.33
Spontaneous abortion	4	22.22
Salpingitis	1	5.56
Surgical history	7	100
Myomectomy	6	85.71
C-sections	1	14.29

Table 3. Distribution of tubes according to results of tubal catheterization (n = 140 tubes).

	Pass		Fail	
	Effective	%	Effective	%
Bilateral	120	93.02	2	18.18
Right	6	4.66	3	27.27
Left	3	2.32	6	54.55
Total	129	100	11	100

Table 4. Distribution of the tubes according to their appearance after tubal catheterization.

	Effective	%
Normal tubes	80	62.01
Inflammatory tubes	37	28.70
Hydrosalpinx	7	5.42
Phimosi	5	3.87
Total	129	100

Table 5. Distribution of patients according to complications after catheterization.

	Effective	%
Complications (N = 69)		
Abdomino-pelvic pain	55	75.34
Vascular invasion	13	17.81
Post procedure bleeding	1	1.73

4. Discussion

Our study took place in a context marked by the recent start (less than 3 years) of the activities of the interventional radiology center of the "Autel d'Elie" clinic equipped with an adapted interventional table, the skills and the equipment ne-

cessary to the realization of a tubal unblocking. This justifies the choice of the study framework and allows our results to be representative of data from the general population. She was interested in tubal infertility, which is the main cause of sterility in Africa south of the Sahara [10] with all its known repercussions on marital stability. Given the small size of our sample, linked to the relatively short duration of recruitment in a practically nascent center, this study, which aims to be a pioneer in the field, has the merit of bringing new results to the scientific community on a practice less common in our black African context.

The patients concerned by our study were mostly married and on average in the third decade of life, as in most African series dealing with female infertility [11] [12]. The duration of infertility was long and approached 10 years in some patients. The primary type of infertility found in a dominant way seems to present a contrast with this previous result, insofar as the conception of a childless marriage remains unclear in African societies. At the same time, these data highlight, on the one hand, the endogenous beliefs that tend to victimize women in the absence of conception in our societies [13] and on the other hand, the use of traditional therapists due to the low purchasing power of patients faced with the high cost of laboratory tests and drugs in pharmacies, which lead to late consultations.

The antecedents of our patients were dominated by abortions, salpingitis and a notion of pelvic surgery. A set of phenomena could have been responsible for the obstruction of the tubes in some of them. Indeed, these past health conditions are identified as contributing to the installation of inflammatory processes in the pelvis, which have been reported as risk factors for infertility by tubal obstruction [14]. Gandji *et al.* reported that 46.4% of patients with secondary couple infertility had declared having voluntarily terminated their pregnancy at least once [12].

Our patients had in all cases, a hysterosalpingography performed mainly in the context of an initial consultation for the desire to conceive. In only one, hysterosalpingography had been performed for post-surgical control of hydrosalpinx previously diagnosed as well, in a follow-up process for the desire to conceive. This brings all of the indications for this examination in our study to female infertility as mentioned in the literature. Indeed, hysterosalpingography remains the main indication for exploring tubal pathology and permeability as part of the assessment of primary or secondary infertility [15]. However, it remains of interest during the exploration of certain uterine pathologies and also plays a role in the event of repeated miscarriages (isthmic open bite, malformation). Its formal contraindications in the face of the notion of genital infection and the possibility of early pregnancy, justifies the specific measures for the preparation of patients and the systematization of the dosage of b-HCG before tubal catheterization.

Confirmatory hysterosalpingography was the first step in tubal catheterization as conventionally reported in the technique. It revealed bilateral tubal obstruc-

tion in all our patients, irregular uterine contours with lesions dominated by synechiae and fibroids. The pressure of the contrast product allowed a spontaneous unblocking of 6 tubes, which revives the debate on the limits of hysterosalpingography in terms of detection of proximal tubal obstructions. False positives are attributed to it in proportions ranging from 15% to 32% in relation to the existence of mucous plugs but also cornual spasms caused by pain on injection of the contrast product [16] [17] [18].

The selective tubal catheterization itself constituted the second stage of the unblocking in our patients. It focused on the tubes not cleared spontaneously during the previous step and allowed a successful recanalization of 94.17% of the tubes. All the unobstructed tubes were opacified, thus making it possible to attest to the effective proximal unobstructing, to study the ampulla and to assess the quality of the peritoneal circulation. The entire procedure took an average of less than 39 minutes with an average radiation dose of 3.1 mGy.

The post-catheterization follow-up made it possible to record an occurrence of pregnancy in 23.29% of our patients within an average period of 6.64 months after the intervention. 70.59% of them became pregnant within a period of between 6 and 10 months after the unblocking against 29.41% of cases in which the pregnancy occurred between the first and the 5th month. In the literature, the pregnancy rate varies between 6% and 55% depending on the series with an average of 25%. This rate is close to that of natural fertility for a normal couple and also close to that obtained by medically assisted procreation (25%). It varies according to the patient selection criteria, the salpingographic aspects (pathological tubes or not), and the duration of patient follow-up after tubal recanalization.

Our data allow us to conclude that selective tubal catheterization has an objective and satisfactory therapeutic value. In a context where its indications are only shared with other techniques with subjective results such as hydrotubation, it remains the first-line treatment of infertility by proximal tubal obstruction. Admittedly, laparoscopy remains the “gold standard” in this area because of its therapeutic interest and the advantage it has of directly visualizing the tubes and adhesions [19] [20]. Although minimally invasive, the complications described to him [21] have led some authors to believe that selective tubal catheterization can be offered as first-line therapy after hysterosalpingography [22].

5. Conclusion

Selective tubal catheterization has improved fertility in patients with the onset of pregnancy in proportions close to natural fertility for a normal couple. This technique could therefore be popularized in Togo in order to improve female fertility.

Conflicts of Interest

The authors declare no conflicts of interest regarding the publication of this paper.

References

- [1] Collège National des Gynécologues et Obstétriciens Français (CNGOF) (2015) Item 37-UE 2: Stérilité du couple: Conduite de la 1ere consultation. 49 p.
- [2] Sonhaye, L., Tchaou, M., Agoda-Koussema, L.K., Adjénou, K., Amadou, A., Adam-bounou, K., Ahonsou-Toussa, S. and N'dakena, K. (2011) Exploration de la stérilité tubaire par l'hystérosalpingographie à Lomé (Togo). *Journal de la Recherche Scientifique de l'Université de Lomé*, **13**, 75-80.
- [3] Allahbadia, G. and Merchant, R. (2010) Fallopian Tube Recanalization: Lessons learnt and Future Challenges. *Women's Health*, **6**, 531-549.
<https://doi.org/10.2217/WHE.10.34>
- [4] Billet, P. and Ardaens, Y. (2017) Chapitre 12—Hystérosalpingographie et cathétérisme tubaire selectif. In: Ardaens, Y., et al., Eds., *Echographie et imagerie pelvienne en pratique gynécologique*, Elsevier, Masson, 381-412.
- [5] Ba, S.D., Badiane, M., Ba, A.A., Niang, E.H., Ba, A.L., Ba, A. and Agaïcha, A. (1999) La salpingographie sélective dans le traitement des infertilités par obstacle tubaire proximal: À propos de 122 cas traités à Dakar. *Cahiers d'Études et de Recherches Francophones/Santé*, **9**, 81-84.
- [6] IRIS (2018) Cathétérisme tubaire: Principe de l'examen. Radiologie interventionnelle.
- [7] Ajavon, Y., Seror, O., Amrane, H., Haddar, D., Poittevin, X., Dordea, M., Ghenassia, C., Coderc, E. and Sellier, N. (2004) Cathétérisme tubaire sélectif: Indications, Fiabilité et Précautions. *Journal de Radiologie*, **85**, 1338.
[https://doi.org/10.1016/S0221-0363\(04\)77096-1](https://doi.org/10.1016/S0221-0363(04)77096-1)
- [8] Garbin, O. and Faller, E. (2013) Chapitre 19—Catheterisme tubaire retrograde: Niveau de difficulté. In: Fernandez, H., Garbin, O. and Gervaise, A., Eds., *Hystérocopie et Fertiscopie*, Elsevier, Masson, 159-164.
<https://doi.org/10.1016/B978-2-294-71521-1.00019-8>
- [9] Bakayoko, C.O. (2009) Place du cathétérisme tubaire sélectif dans le traitement des stérilités par obstruction tubaire proximale. Thèse de Médecine, Université de Bamako, Bamako, 65-66.
- [10] Fiadjoe, M.K., Adjénou, V., Kolani, J.C. and Egah, K.K. (2012) Les recommandations pour la pratique clinique du CNGOF. Infertilité tubaire en Afrique. CNGOF, 641-656.
- [11] Nana, P.N., Wandji, J.C., Fumulu, J.N., Mbure, L., Leke, R.J.I. and Woubinwou, M.J. (2011) Aspects psycho-sociaux des patients infertiles à la maternité principale de l'Hôpital Central de Yaoundé, Cameroun. *Clinics in Mother and Child Health*, **8**, 1-5.
- [12] Gandji, S., Adisso, S., Atrevi, N., Dougnon, T.V., Bankole, H.S., Hontonnou, F., Bi-aou, O. and Loko, F. (2013) Diagnostic des lésions étiologiques de l'infertilité secondaire à Cotonou: Rôle de l'hystérosalpingographie et de l'échographie pelvienne. *Journal of Applied Biosciences*, **68**, 5349-5355.
<https://doi.org/10.4314/jab.v68i0.95059>
- [13] Priso, E.B., Nguefack, C.T., Nguemgne, C., Njamen, T.N., Taila, W. and Banag, E. (2015) L'infertilité féminine à l'Hôpital Général de Douala: Aspects épidémiologiques et radiologiques (à propos de 658 cas). *Journal Africain d'Imagerie Médicale*, **2**, 16-23.
- [14] He, X., Hou, G. and Jiang, H. (2009) A Case-Control Study on the Risk Factors of Female Infertility. *Chinese Journal of Epidemiology*, **30**, 352-355.
- [15] Kehila, M., Hmid, R.B., Khedher, S.B., Mahjoub, S. and Channoufi, M.B. (2014) Con-

- cordance et apports de l'hystérosalpingographie et de la coelioscopie dans l'exploration tubaire et pelvienne en cas d'infertilité. *Pan African Medical Journal*, **17**, Article 126. <https://doi.org/10.11604/pamj.2014.17.126.3567>
- [16] Maubon, A., Pouquet, M., Piver, P., Mazet, N., Viala-Trentini, M. and Rouanet, J.P. (2008) Imagerie de l'infertilité féminine. *Journal de Radiologie*, **89**, 172-183. [https://doi.org/10.1016/S0221-0363\(08\)70391-3](https://doi.org/10.1016/S0221-0363(08)70391-3)
- [17] Canis, M., Mage, G., Pouly, J.L., Manhes, H., Wattiez, A. and Bruhat, M.A. (1991) Laparoscopic Distal Tuboplasty: Report of 87 Cases and a 4-Year Experience. *Fertility and Sterility*, **56**, 616-621. [https://doi.org/10.1016/S0015-0282\(16\)54589-0](https://doi.org/10.1016/S0015-0282(16)54589-0)
- [18] Kalume, M.A.J. (2014) Techniques modernes d'exploration de l'infertilité tubo-pelvienne. *Kisangani Médical*, **5**, 59-65.
- [19] Yazbeck, C., Le Tohic, A., Koskas, M. and Madelenat, P. (2010) Pour la pratique systématique d'une coelioscopie dans le bilan d'une infertilité. *Gynécologie Obstétrique & Fertilité*, **38**, 424-427. <https://doi.org/10.1016/j.gyobfe.2010.04.015>
- [20] Diouf, A., Diallo, M., Ndiaye, M., Niass, A., Guèye, M., Tchindebe, G., Dia, A., Mbaye, M. and Diouf, A. (2021) Is Laparoscopy Still Necessary in the Management of Tubal Infertility? *Open Journal of Obstetrics and Gynecology*, **11**, 63-69. <https://doi.org/10.4236/ojog.2021.112008>
- [21] Chapron, C., Pierre, F., Querleu, D. and Dubuisson, J.B. (2001) Complications of Gynecology Laparoscopy. *Gynécologie Obstétrique & Fertilité*, **29**, 605-612. [https://doi.org/10.1016/S1297-9589\(01\)00193-X](https://doi.org/10.1016/S1297-9589(01)00193-X)
- [22] De Graef, M., Juhan, V., Kassem, Z., Guillon, R., Villeval, J., Maubon, A. and Rouanet, J.P. (2005) Hystérosalpingographie et cathétérisme sélectif des trompes. *EMC-Radiologie*, **2**, 43-75. <https://doi.org/10.1016/j.emcrad.2004.07.002>



Open Journal of Radiology

ISSN Print: 2164-3024 ISSN Online: 2164-3032

<https://www.scirp.org/journal/ojrad>

Open Journal of Radiology (OJRad) is an international peer-reviewed, open-access journal dedicated to presenting the latest advancement in medical imaging. The Journal is interested in presenting a wide range of imaging topics of interest to the medical community. These would include imaging developments: 1) for diagnosis of disease and 2) for guiding and/or evaluating a therapeutic treatment. The journal is also interested in presenting research articles of general interest to the imaging community, for example: image acquisition, processing, multimodality image registration and segmentation. The goal of this journal is to provide a platform for scientists and academicians all over the world to promote, share, and discuss various new issues and developments in different areas of radiology.

Subject Coverage

The journal publishes original papers including, but not limited to the following subfields of radiology:

- ◆ Acquisition of Radiological Images
- ◆ Computed Tomography (CT)
- ◆ Fluoroscopy
- ◆ Interventional Radiology
- ◆ MRI (Magnetic Resonance Imaging)
- ◆ Nuclear Medicine
- ◆ Projection (Plain) Radiography
- ◆ Radiologist Training
- ◆ Teleradiology
- ◆ Ultrasound

We are also interested in: 1) Short Reports—2-5 page papers where an author can either present an idea with theoretical background but has not yet completed the research needed for a complete paper or preliminary data; 2) Book Reviews—Comments and critiques.

Notes for Intending Authors

Submitted papers should not have been previously published nor be currently under consideration for publication elsewhere. Paper submission will be handled electronically from the website. All papers are refereed through a peer review process. For more details about the submissions, please access the website.

Website and E-Mail

<https://www.scirp.org/journal/ojrad>

E-mail: ojrad@scirp.org

What is SCIRP?

Scientific Research Publishing (SCIRP) is one of the largest Open Access journal publishers. It is currently publishing more than 200 open access, online, peer-reviewed journals covering a wide range of academic disciplines. SCIRP serves the worldwide academic communities and contributes to the progress and application of science with its publication.

What is Open Access?

All original research papers published by SCIRP are made freely and permanently accessible online immediately upon publication. To be able to provide open access journals, SCIRP defrays operation costs from authors and subscription charges only for its printed version. Open access publishing allows an immediate, worldwide, barrier-free, open access to the full text of research papers, which is in the best interests of the scientific community.

- High visibility for maximum global exposure with open access publishing model
- Rigorous peer review of research papers
- Prompt faster publication with less cost
- Guaranteed targeted, multidisciplinary audience



**Scientific
Research
Publishing**

Website: <https://www.scirp.org>

Subscription: sub@scirp.org

Advertisement: service@scirp.org